

Dipolar quantum electrodynamics of the two-dimensional electron gas

Yanko Todorov*

Université Paris Diderot, Sorbonne Paris Cité, Paris France and Laboratoire Matériaux et Phénomènes Quantiques, UMR7162, F-75013 Paris, France

(Received 20 October 2014; revised manuscript received 21 February 2015; published 6 March 2015)

Similarly to a previous work on the homogeneous electron gas [Y. Todorov, *Phys. Rev. B* **89**, 075115 (2014)], we apply the Power-Zienau-Wooley (PZW) formulation of the quantum electrodynamics to the case of an electron gas quantum confined by one-dimensional potential. We provide a microscopic description of all collective plasmon modes of the gas, oscillating both along and perpendicular to the direction of quantum confinement. Furthermore, we study the interaction of the collective modes with a photonic structure, planar metallic waveguide, by using the full expansion of the electromagnetic field into normal modes. We show how the boundary conditions for the electromagnetic field influence both the transverse light-matter coupling and the longitudinal particle-particle interactions. The PZW descriptions appear thus as a convenient tool to study semiconductor quantum optics in geometries where quantum-confined particles interact with strongly confined electromagnetic fields in microresonators, such as the ones used to achieve the ultrastrong light-matter coupling regime.

DOI: [10.1103/PhysRevB.91.125409](https://doi.org/10.1103/PhysRevB.91.125409)

PACS number(s): 42.50.-p, 73.21.Fg, 71.45.-d, 77.22.Ch

I. INTRODUCTION

The Power-Zienau-Wooley (PZW) representation of the quantum electrodynamics [1,2] provides an alternative description of the light-matter interaction problem, that relies on field intensities rather than potentials. The main feature of this approach is that the matter and field degrees of freedom are independent dynamical variables [1,2]. In this representation, aside from the kinetic energy of the particles, the matter is characterized by a polarization vector field \mathbf{P} that is a function only on the particle positions. The polarization field \mathbf{P} not only describes the light-matter interaction through a linear coupling term, but is also connected to the particle-particle interactions inherent to a many-body system. For instance, the part of the PZW Hamiltonian that is quadratic in \mathbf{P} allows us to derive the collective excitations of a dense electron gas [3,4]. The PZW Hamiltonian thus provides a general framework that fully captures both the many-body and quantum-optical aspects in a solid-state system in interaction with the electromagnetic radiation. In particular, this formalism was proven useful in describing the ultrastrong light-matter coupling regime [5] between the intersubband plasmons of a two-dimensional electron gas and a single mode of planar waveguides or microresonators [4,6–9].

In a previous work [3], we provided a formulation of the quantum electrodynamics of a homogeneous solid-state system, in the presence of interactions, in the general framework of the PZW representation. This approach was then applied to the three-dimensional (3D) electron gas interacting with the free-space modes of the electromagnetic field. This work can be considered as a sequel to Ref. [3], with the additional constraint that both the electronic movement and the electromagnetic field are quantized in one direction of space. We explore the collective modes of the electron gas, driven by the \mathbf{P} -quadratic term of the quantum Hamiltonian as well as the polariton modes of the system, arising from the coupling with the spatially confined electromagnetic modes. Contrary to previous works [4,6,8], we now consider all possible col-

lective plasmonic modes, where electrons vibrate both along and perpendicular to the direction of quantum confinement. Furthermore, we use a full modal decomposition of the electromagnetic field. Beyond the problematic of quantum-confined plasmon polaritons, we believe that such complete treatment can be useful as a physical example of a matter-assisted quantum electrodynamics theory where light propagates in a medium with resonances. The quantization of a media with dispersion and absorption has been recently considered from a very general, yet formal, framework [10,11]. In the system described here, boundary conditions together with electron-electron interactions play an important role, and are taken into account into the quadratic terms of the full electrodynamic Hamiltonian. As such, this system could be also a useful example in the context of the ongoing debate on the possibility to realize superradiant quantum-phase transitions [12–14].

The advantage of the PZW description in the context of condensed matter problems is twofold. First, the electromagnetic field is described by two purely transverse fields: the displacement vector \mathbf{D} and the magnetic field \mathbf{H} . They can be deduced solely from the boundary conditions of the problem and are independent from the matter contained in the bulk of the system. This simplifies considerably the quantization of the field degrees of freedom even in the presence of material resonances, as it was shown in the quantization of surface plasmon modes in Ref. [3]. Such an approach is of particular interest for solid-state systems operating in the ultrastrong coupling regime, that are characterized by both high-particle density and very strong electromagnetic confinement [6,7,9,15–17].

The second advantage of our approach is that the matter polarization density \mathbf{P} , that is a central quantity in this description, can be obtained from a minimal knowledge about the system. Indeed, we showed in previous works on the electron gas [3,4] that the relevant dynamic part of the polarization field can be derived solely from the one-particle kinetic energy Hamiltonian. Then, the PZW representation provides a general prescription for expressing the interparticle interactions in the system, by using an hypothesis such as random phase approximation (RPA), that are common in condensed matter physics [18,19]. The collective many-body modes are then

*yanko.todorov@univ-paris-diderot.fr

automatically deduced from the square-polarization part of the PZW Hamiltonian.

In this work, we show that the collective plasmon modes obtained in such way are actually more general than those derived from the longitudinal Coulomb interactions in free space [20,21]. Since the matter part of the PZW Hamiltonian is canonically independent from the electromagnetic part, the collective excitations resulting from the diagonalization of the \mathbf{P}^2 term are actually independent from the electromagnetic environment of the system. With this respect these modes can be considered as “universal” and independent from the particular geometry of the problem. The interaction of these collective excitations with the electromagnetic field can then be conveniently formulated in terms of the transverse longitudinal projections their polarization vector, once the full modal decomposition of the field is known in a particular geometry defined by boundary conditions. The “universal” plasmon collective modes derived here can thus be adapted to any experimental geometry, where two-dimensional gas is coupled with resonant nanostructures, for instance, metamaterial resonators [9,16,17,22–24].

These concepts are illustrated in the trend of this work, which is organized as follows. In Sec. II, we formulate the general PZW Hamiltonian of the two-dimensional electron gas. Following an approach similar to Ref. [3], we explicit the polarization field operator \mathbf{P} in terms of bosonized electron-hole excitations, but now we take into account the quantum confinement of the gas. By diagonalizing the matter part of the PZW Hamiltonian, we obtain the corresponding intersubband and intrasubband “universal” excitations of the gas that appear to be dispersionless in the long-wavelength limit. In particular, we show how the well-known \sqrt{q} dispersion of the intrasubband plasmon [25–27] appears through the longitudinal projections of the polarization operator.

In Sec. III, we study the transverse interaction of the collective electronic excitations with the guided modes of a planar metallic waveguide and we describe the corresponding coupled polariton modes. In particular, we discuss the possibility to assign a local dielectric function that describes the propagation of polaritons, a problem that has been discussed so far in semiclassical approaches [27–32]. In the final part of Sec. III, we examine the image of our Hamiltonian in the minimal-coupling representation. This is achieved by employing an inverse unitary PZW transform that takes into account the full set of guided modes. This will allow us to recover, in particular, the longitudinal Coulomb potential of the system. It turns out that this potential results not only from the direct interaction between electrons, but also includes an infinite number of image contributions from the cavity walls. We thereby find another advantage of the PZW description, which is to account automatically for the boundary conditions, both for the transverse and longitudinal degrees of freedom of the electromagnetic field.

II. DIPOLAR DESCRIPTION OF THE TWO-DIMENSIONAL ELECTRON GAS

A. General Hamiltonian and bosonization

In the absence of magnetic interactions, the general form of the electrodynamic Hamiltonian for the electron gas in the

PZW representation is written as [1–3]

$$\mathcal{H} = \mathcal{H}_{\text{ph}} + \mathcal{H}_e - \frac{1}{\varepsilon\varepsilon_0} \int \hat{\mathbf{D}}\hat{\mathbf{P}} d^3\mathbf{r} + \frac{1}{2\varepsilon\varepsilon_0} \int \hat{\mathbf{P}}^2 d^3\mathbf{r}. \quad (1)$$

Here, \mathcal{H}_{ph} is the photon Hamiltonian and \mathcal{H}_e is the Hamiltonian of the noninteracting (single-particle) electron gas. The operator $\hat{\mathbf{P}}$ is the polarization density operator of the gas. The photonic Hamiltonian is written as

$$\mathcal{H}_{\text{ph}} = \int \frac{\hat{\mathbf{D}}^2}{2\varepsilon\varepsilon_0} d^3\mathbf{r} + \int \frac{\mu_0 \hat{\mathbf{H}}^2}{2} d^3\mathbf{r}. \quad (2)$$

Here, $\hat{\mathbf{D}}$ and $\hat{\mathbf{H}}$ are, respectively, the displacement field operator and the magnetic field operator, and ε is the dielectric constant of the media hosting the gas. The latter is supposed to be homogeneous and isotropic. The expressions of $\hat{\mathbf{D}}$ and $\hat{\mathbf{H}}$ will be specified from the particular geometry of the problem. At this point, it is important to note that the operators $\hat{\mathbf{D}}$ and $\hat{\mathbf{H}}$ describe a free photon field evolving in the medium ε . Indeed, in the PZW representation the electromagnetic field operators are canonical variables that are independent from the matter degrees of freedom contained in the polarization field $\hat{\mathbf{P}}$ [1,2]. Respectively, ε does not contain the contribution of the electron gas, as this contribution arises only after the diagonalization of the full Hamiltonian (1).

Our aim is now to define the polarization field operator of the gas $\hat{\mathbf{P}}$. For this we adopt the same approach as for the three-dimensional electron gas, as described in Ref. [3], where we derived $\hat{\mathbf{P}}$ from the noninteracting electronic Hamiltonian and the bosonization of the single-particle (noninteracting) excitations. Therefore, for completeness, in the following we recall the bosonization of the quasi-two-dimensional gas.

The electronic Hamiltonian \mathcal{H}_e now contains not only the kinetic energy of the electrons, but also the external static one-dimensional potential $V(z)$ that is responsible for the quantum confinement along the z direction:

$$\mathcal{H}_e = \sum_{\alpha} \left(-\frac{\hbar^2 \nabla_{\alpha}^2}{2m^*} + V(z_{\alpha}) \right). \quad (3)$$

The electrons move freely in the plane (x, y) . The archetype of such system is a semiconductor heterostructure, such as an inversion layer or a quantum well [26,33,34]; respectively, m^* is the effective electron mass in the heterostructure. The corresponding one-particle wave functions of Eq. (3) are

$$\langle \mathbf{r} | i, \mathbf{k} \rangle = \phi_i(z) \frac{e^{i\mathbf{k}\mathbf{r}_{\parallel}}}{\sqrt{S}}. \quad (4)$$

Here, S is the in-plane quantization surface, $\mathbf{r}_{\parallel} = (x, y)$ is the in-plane coordinate, and \mathbf{k} is the electronic wave vector for the free-electronic movement in the plane. We consider that each \mathbf{k} state is twice degenerate because of the spin. The function $\phi_i(z)$ is a solution of the one-dimensional Schrödinger equation [35]

$$-\frac{\hbar^2}{2m^*} \partial_z^2 \phi_i(z) + V(z) \phi_i(z) = \hbar\omega_i \phi_i(z) \quad (5)$$

with an eigenvalue $\hbar\omega_i$ where the Latin index i refers to a particular confined state. The total energies of the one-particle states (4) then appear as two-dimensional parabolic subbands

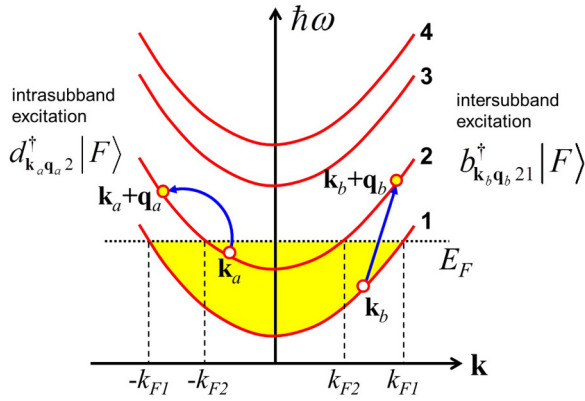


FIG. 1. (Color online) Examples of intersubband and intrasubband single-particle excitations in a general multisubband system, with two filled subbands.

(we have assumed constant effective mass [34])

$$\hbar\omega_{i\mathbf{k}} = \hbar\omega_i + \frac{\hbar^2 \mathbf{k}^2}{2m^*}. \quad (6)$$

These subband states are illustrated in Fig. 1. The above definitions allow us to write the electronic Hamiltonian in a second-quantized form

$$\mathcal{H}_e = \sum_{i\mathbf{k}} \hbar\omega_{i\mathbf{k}} c_{i\mathbf{k}}^\dagger c_{i\mathbf{k}} \quad (7)$$

with $c_{i\mathbf{k}}^\dagger$ and $c_{i\mathbf{k}}$ the fermionic creation and annihilation operators for the state (4).

Following Ref. [3], our aim is now to identify the bosonized excited states that will help us construct the polarization field of the gas $\hat{\mathbf{P}}(\mathbf{r})$. We shall consider a closed system at equilibrium at $T = 0$ K, with a total number of N_e electrons. The electrons fill all the subband states below the Fermi energy E_F which satisfy $\hbar\omega_{i\mathbf{k}} \leq E_F$. For each subband, the corresponding Fermi wave vector is noted k_{Fi} and we have $k_{Fi} = 0$ for the empty subbands. The ground state $|F\rangle$ of the noninteracting Hamiltonian (7) is

$$|F\rangle = \prod_{\hbar\omega_{i\mathbf{k}} \leq E_F} c_{i\mathbf{k}}^\dagger |0\rangle. \quad (8)$$

Respectively, all possible one-particle excitations are $c_{i\mathbf{k}+\mathbf{q}}^\dagger c_{j\mathbf{k}} |F\rangle$, and they are characterized with an excitation wave vector \mathbf{q} in the plane of the confining potential. The corresponding excitation energies $\Delta\omega_{\mathbf{k}\mathbf{q}ij}$ are provided by the commutator of the excitation operator $c_{i\mathbf{k}+\mathbf{q}}^\dagger c_{j\mathbf{k}}$ with the electronic Hamiltonian (7):

$$[\mathcal{H}_e, c_{i\mathbf{k}+\mathbf{q}}^\dagger c_{j\mathbf{k}}] = \hbar\Delta\omega_{\mathbf{k}\mathbf{q}ij} c_{i\mathbf{k}+\mathbf{q}}^\dagger c_{j\mathbf{k}}, \quad (9)$$

$$\Delta\omega_{\mathbf{k}\mathbf{q}ij} = \omega_i - \omega_j + \frac{\hbar}{2m^*} \mathbf{q}(2\mathbf{k} + \mathbf{q}). \quad (10)$$

We now construct the bosonized excitation subspace of the two-dimensional electron gas as the subspace where the excitation operators $c_{i\mathbf{k}+\mathbf{q}}^\dagger c_{j\mathbf{k}}$ obey bosonic commutation

relations. Their exact commutator is

$$[c_{j\mathbf{k}}^\dagger c_{i\mathbf{k}+\mathbf{q}}, c_{i'\mathbf{k}'+\mathbf{q}}^\dagger c_{j'\mathbf{k}'}] = \delta_{ii'} \delta_{\mathbf{k}+\mathbf{q}, \mathbf{k}'+\mathbf{q}} c_{j'\mathbf{k}'}^\dagger c_{j\mathbf{k}} - \delta_{jj'} \delta_{\mathbf{k}, \mathbf{k}'} c_{i\mathbf{k}+\mathbf{q}}^\dagger c_{i'\mathbf{k}'+\mathbf{q}}. \quad (11)$$

Its mean value on the fundamental state is

$$\langle F | [c_{j\mathbf{k}}^\dagger c_{i\mathbf{k}+\mathbf{q}}, c_{i'\mathbf{k}'+\mathbf{q}}^\dagger c_{j'\mathbf{k}'}] | F \rangle = \delta_{ii'} \delta_{\mathbf{k}, \mathbf{k}'} \delta_{\mathbf{q}, \mathbf{q}'} (f_{j\mathbf{k}} - f_{i\mathbf{k}+\mathbf{q}}). \quad (12)$$

Here, $f_{j\mathbf{k}} = \langle F | c_{j\mathbf{k}}^\dagger c_{j\mathbf{k}} | F \rangle$ and accordingly $f_{i\mathbf{k}+\mathbf{q}} = \langle F | c_{i\mathbf{k}+\mathbf{q}}^\dagger c_{i\mathbf{k}+\mathbf{q}} | F \rangle$ are the occupation numbers in the ground state. Since we have $f_{j\mathbf{k}}, f_{i\mathbf{k}+\mathbf{q}} \leq 1$ from Eq. (12), we obtain the following conditions which render the commutator (11) bosonlike:

$$\begin{aligned} f_{j\mathbf{k}} &= 1, & |\mathbf{k}| &\leq k_{Fj} \\ f_{i\mathbf{k}+\mathbf{q}} &= 0, & |\mathbf{k} + \mathbf{q}| &> k_{Fi}. \end{aligned} \quad (13)$$

These conditions basically express the Pauli exclusion principle, that is, an electron excited from the ground state can only transit into the empty states outside the Fermi surface. Such bosonlike excitations are divided into intersubband ($i > j$) or intrasubband ($i = j$), depending on whether the electron switches or not the confined state. Examples of such intrasubband and intersubband excitations are provided in Fig. 1. All these excitations satisfy $\Delta\omega_{\mathbf{k}\mathbf{q}ij} > 0$. Clearly, the intrasubband subspace is very similar to the subspace of RPA states for the three-dimensional electron gas [3]. The intersubband excitations arise from the electronic confinement, and they do not have any analogy with the excitations of the three-dimensional gas. For instance, these excitations can be realized with strictly vertical transitions $\mathbf{q} = \mathbf{0}$.

We now introduce specific notations for the intersubband and intrasubband excitation operators. Since for intersubband excitations we have always $i > j$, the pair of Latin indexes “ i, j ” will be noted as a single Greek index. With this remark, we introduce the following definitions:

$$b_{\mathbf{k}\mathbf{q}\alpha}^\dagger = c_{i\mathbf{k}+\mathbf{q}}^\dagger c_{j\mathbf{k}}, \quad \text{intersubband excitation} \quad (14)$$

$$\text{with } \alpha \equiv i > j$$

$$d_{\mathbf{k}\mathbf{q}i}^\dagger = c_{i\mathbf{k}+\mathbf{q}}^\dagger c_{i\mathbf{k}}, \quad \text{intrasubband excitation.} \quad (15)$$

The action of these operators is restricted only on the excitations described in Eq. (13). Therefore, if we consider the subspace spanned by the states $\{|F\rangle, b_{\mathbf{k}\mathbf{q}\alpha}^\dagger |F\rangle, d_{\mathbf{k}\mathbf{q}i}^\dagger |F\rangle\}$ the above operators satisfy bosonic commutation relations

$$[b_{\mathbf{k}\mathbf{q}\alpha}, b_{\mathbf{k}'\mathbf{q}'\beta}^\dagger] = \delta_{\mathbf{k}\mathbf{k}'} \delta_{\mathbf{q}\mathbf{q}'} \delta_{\alpha, \beta}, \quad (16)$$

$$[d_{\mathbf{k}\mathbf{q}i}, d_{\mathbf{k}'\mathbf{q}'j}^\dagger] = \delta_{\mathbf{k}\mathbf{k}'} \delta_{\mathbf{q}\mathbf{q}'} \delta_{i, j}, \quad (17)$$

and all the commutators involving one intersubband and one intrasubband operator vanish. Using these operators, we can replace the fermionic Hamiltonian \mathcal{H}_e with an equivalent effective bosonized form

$$\mathcal{H}_e = \sum_{\mathbf{k}\mathbf{q}\alpha} \hbar\Delta\omega_{\mathbf{k}\mathbf{q}\alpha} b_{\mathbf{k}\mathbf{q}\alpha}^\dagger b_{\mathbf{k}\mathbf{q}\alpha} + \sum_{\mathbf{k}\mathbf{q}i} \hbar\Delta\omega_{\mathbf{k}\mathbf{q}i} d_{\mathbf{k}\mathbf{q}i}^\dagger d_{\mathbf{k}\mathbf{q}i}. \quad (18)$$

In the case of intrasubband excitations, since we assumed parabolic bands, the energy difference $\Delta\omega_{\mathbf{k}qii} = \Delta\omega_{\mathbf{k}q}$ is independent from the subband index i , therefore we shall drop it in the notations. The quantity $\Delta\omega_{\mathbf{k}q}$ describes a momentum exchange process that is very similar to the elementary excitations in a homogeneous electron gas, except that now the wave vectors \mathbf{k} and \mathbf{q} are restricted to evolve in the plane (x, y) .

We defined the bosonization of the two-dimensional electron gas (2DEG) rigorously in the case $T = 0$ K, however, it can be also extended at a finite temperature, assuming that the number of excitations is low as compared to the ground-state occupancy [21,36].

In the next section, we express the polarization field operator $\hat{\mathbf{P}}$ of the 2DEG as a function of the bosonized excitation operators $b_{\mathbf{k}q\alpha}^\dagger$ and $d_{\mathbf{k}q}^\dagger$, and their Hermitian conjugates. Furthermore, for the rest of this part we will focus only on the matter part of the Hamiltonian (1):

$$\mathcal{H}_e + \frac{1}{2\epsilon\epsilon_0} \int \hat{\mathbf{P}}^2 d^3\mathbf{r}. \quad (19)$$

In particular, we will be concerned by the collective excitations driven by the square-polarization part of Eq. (19). Let us recall that in the PZW representation the square-polarization part contains the Coulomb interaction between electrons, as well as retarded interactions, that in the minimal-coupling representation can be related to the square-vector potential term of the standard Hamiltonian [2,3]. The two contributions can be separated by splitting the polarization field into longitudinal and transverse parts with respect to a three-dimensional Fourier transform [2], and then the longitudinal part of $(1/2\epsilon\epsilon_0) \int \hat{\mathbf{P}}^2 d^3\mathbf{r}$ is exactly the Coulomb potential of the system. In the current work, the collective electronic excitations of the electron gas are approached from a more general point of view, as besides the instantaneous Coulomb interaction between electrons we also include a retarded interaction that is contained in the transverse part of the Hamiltonian of Eq. (19). This fact is further discussed in Sec. IID.

B. Polarization field operator of the two-dimensional electron gas

Following Refs. [3,4,8] we use the following relation between the polarization operator $\hat{\mathbf{P}}$ and the current operator $\hat{\mathbf{j}}$ in a system of charged particles:

$$\hat{\mathbf{j}} = \frac{d\hat{\mathbf{P}}}{dt} = \frac{i}{\hbar} [\mathcal{H}, \hat{\mathbf{P}}] = \frac{i}{\hbar} [\mathcal{H}_e, \hat{\mathbf{P}}]. \quad (20)$$

According to Eq. (20), the dynamic polarization field operator $\hat{\mathbf{P}}$ of the two-dimensional gas is constructed in such a way that its time derivative coincides with the current operator $\hat{\mathbf{j}}$ of the gas [3]. A key point is that, since dynamic magnetic interactions are absent, only the electronic Hamiltonian \mathcal{H}_e contributes to the evolution of the polarization field. The current operator $\hat{\mathbf{j}}$ can be expressed on the basis of the eigenstates of \mathcal{H}_e using the following expression:

$$\hat{\mathbf{j}}(\mathbf{r}) = \frac{ie\hbar}{2m^*} [\hat{\Psi}^\dagger \nabla \hat{\Psi} - \nabla \hat{\Psi}^\dagger \hat{\Psi}]. \quad (21)$$

Indeed, in the PZW representation the current is expressed only from the matter degrees of freedom, as the momentum of the particles is expressed only through their velocities and the vector potential contribution is absent [2]. Here, the field operator $\hat{\Psi}(\mathbf{r})$ is expressed through the single-particle wave functions of \mathcal{H}_e from Eq. (4):

$$\Psi(z, \mathbf{r}_\parallel) = \sum_{\lambda\mathbf{k}} \phi_\lambda(z) \frac{e^{i\mathbf{k}\mathbf{r}_\parallel}}{\sqrt{S}} c_{\lambda\mathbf{k}}. \quad (22)$$

Equations (21) and (22) lead to the following expressions for the in-plane $\hat{\mathbf{j}}_\parallel$ and perpendicular \hat{j}_z components of the current:

$$\hat{j}_z = \frac{i\hbar e}{2m^*S} \sum_{\mathbf{k}qij} \xi_{ij}(z) e^{-i\mathbf{q}\mathbf{r}_\parallel} c_{i\mathbf{k}+\mathbf{q}}^\dagger c_{j\mathbf{k}}, \quad (23)$$

$$\xi_{ij}(z) = \phi_i^*(z) \partial_z \phi_j(z) - \partial_z \phi_i^*(z) \phi_j(z), \quad (24)$$

$$\hat{\mathbf{j}}_\parallel = \frac{-\hbar e}{2m^*S} \sum_{\mathbf{k}qij} (2\mathbf{k} + \mathbf{q}) \eta_{ij}(z) e^{-i\mathbf{q}\mathbf{r}_\parallel} c_{i\mathbf{k}+\mathbf{q}}^\dagger c_{j\mathbf{k}}, \quad (25)$$

$$\eta_{ij}(z) = \phi_i^*(z) \phi_j(z). \quad (26)$$

The contributions with $i = j$ and $\mathbf{q} = \mathbf{0}$ correspond to the center-of-mass motion of the electron gas with $\Delta\omega_{\mathbf{k}qij} = 0$. These terms must be excluded from the definition of the dynamic polarization. Using Eq. (9) we arrive at the following formal definitions:

$$\hat{P}_z = -\frac{\hbar e}{2m^*S} \sum_{\mathbf{k}qij} \frac{c_{i\mathbf{k}+\mathbf{q}}^\dagger c_{j\mathbf{k}}}{\Delta\omega_{\mathbf{k}qij}} \xi_{ij}(z) e^{-i\mathbf{q}\mathbf{r}_\parallel}, \quad (27)$$

$$\hat{\mathbf{P}}_\parallel = \frac{-i\hbar e}{2m^*S} \sum_{\mathbf{k}qij} \frac{c_{i\mathbf{k}+\mathbf{q}}^\dagger c_{j\mathbf{k}} (2\mathbf{k} + \mathbf{q})}{\Delta\omega_{\mathbf{k}qij}} \eta_{ij}(z) e^{-i\mathbf{q}\mathbf{r}_\parallel}. \quad (28)$$

The quantities $\xi_{ij}(z)$ and $\eta_{ij}(z)$ describe, respectively, the polarization and the density matrix elements associated to the transition $j \rightarrow i$. We have the following properties, which ensure the Hermiticity of the current density and polarization density operators defined above:

$$\xi_{ij}^*(z) = -\xi_{ji}(z), \quad \eta_{ij}^*(z) = \eta_{ji}(z). \quad (29)$$

In the following, we will also make use of the relation

$$\partial_z \xi_{ij}(z) = \frac{2m^*(\omega_i - \omega_j)}{\hbar} \eta_{ij}(z), \quad (30)$$

which is an immediate consequence of the Schrödinger equation (5). This equation can also be related to the charge conservation of the system. Let us introduce the charge density operator $\hat{\rho}(\mathbf{r})$ for the electron gas:

$$\hat{\rho}(\mathbf{r}) = e\hat{\Psi}^\dagger \hat{\Psi} = \frac{e}{S} \sum_{\mathbf{k}qij} \eta_{ij}(z) e^{-i\mathbf{q}\mathbf{r}_\parallel} c_{i\mathbf{k}+\mathbf{q}}^\dagger c_{j\mathbf{k}}. \quad (31)$$

Then, the continuity equation that expresses the charge conservation is

$$\frac{d\hat{\rho}}{dt} = \frac{i}{\hbar} [\mathcal{H}, \hat{\rho}] = \text{div} \hat{\mathbf{j}}. \quad (32)$$

In the case where \mathcal{H} is the single-particle electronic Hamiltonian \mathcal{H}_e it can be readily shown with the help of Eq. (30) that this equation is satisfied term by term with respect to the sum over all possible electronic transitions in Eq. (31), each term oscillating at the frequency of the transition $\Delta\omega_{\mathbf{k}\mathbf{q}i}$. When we consider the subspace of bosonized excitation, this equation is also valid for the total Hamiltonian from Eq. (19), as then it can be shown that the density operator $\hat{\rho}$ commutes with the square-polarization part of \mathcal{H} .

In order to obtain a self-consistent bosonic model in the PZW representation, we must restrict the definitions of the polarization field only to the bosonized states defined in the previous section [3]. For this, we isolate the appropriate terms in Eqs. (27) and (28) and then replace the excitation operators with their bosonized versions $b_{\mathbf{k}\mathbf{q}\alpha}^\dagger$ and $d_{\mathbf{k}\mathbf{q}i}^\dagger$. Let us consider first the case of the z component from Eq. (27). We split the sum over the subband indexes into intersubband and intrasubband contributions:

$$\sum_{\mathbf{q}\mathbf{k}i} = \left(\sum_{\mathbf{q}\mathbf{k}, i>j} + \sum_{\mathbf{q}\mathbf{k}, i<j} \right) \Big|_{\text{inter}} + \sum_{\mathbf{q}\mathbf{k}, i=j} \Big|_{\text{intra}}.$$

In the first term of the intersubband contribution, we restrict the sum over the electronic wave vector which satisfies Eq. (13). In the second term, we relabel the indexes (i, j) as (j, i) and make the substitution $\mathbf{k} = -\mathbf{k}' - \mathbf{q}$. Using the property (29) and the definition of the excitation operators, we obtain the following expression for the intersubband polarization along z :

$$\hat{P}_z|_{\text{inter}} = -\frac{\hbar e}{2m^*S} \sum_{\mathbf{q}, \alpha, \mathbf{k} \in I_{n_\alpha}} \frac{e^{-i\mathbf{q}\mathbf{r}_\parallel}}{\Delta\omega_{\mathbf{k}\mathbf{q}\alpha}} \times [\xi_\alpha(z)b_{\mathbf{k}\mathbf{q}\alpha}^\dagger + \xi_\alpha^*(z)b_{-\mathbf{k}-\mathbf{q}\alpha}]. \quad (33)$$

This sum runs over all pairs of subband states with $i > j$, and each such pair is labeled with a single Greek index α as indicated in the previous section. The notation “ $\mathbf{k} \in I_{n_\alpha}$ ” means that the wave vector satisfies the restriction imposed by Eq. (13). The intrasubband contribution is obtained in the same way as the polarization operator of the homogeneous electron gas [3], by splitting the sum over the wave vectors in contributions greater and smaller than the Fermi wave vector in each subband k_{Fi} . As a result, we obtain

$$\hat{P}_z|_{\text{intra}} = -\frac{\hbar e}{2m^*S} \sum_{\substack{\mathbf{q}, i \\ |\mathbf{k}| \leq k_{Fi} \\ |\mathbf{k} + \mathbf{q}| > k_{Fi}}} \frac{e^{-i\mathbf{q}\mathbf{r}_\parallel}}{\Delta\omega_{\mathbf{k}\mathbf{q}}} \xi_{ii}(z)[d_{\mathbf{k}\mathbf{q}i}^\dagger - d_{-\mathbf{k}-\mathbf{q}i}]. \quad (34)$$

It is very convenient to rewrite the above expressions with the help of the occupation numbers, which will automatically take into account the constraints from Eq. (13). We introduce the following notations:

$$\Delta n_{\mathbf{k}\mathbf{q}\alpha} = f_{j\mathbf{k}} - f_{i\mathbf{k}+\mathbf{q}} > 0, \quad \alpha = [i > j] \quad (35)$$

$$\Delta n_{\mathbf{k}\mathbf{q}i} = f_{i\mathbf{k}}(1 - f_{i\mathbf{k}+\mathbf{q}}). \quad (36)$$

The polarization operator now sums over all possible wave vectors:

$$\hat{P}_z|_{\text{inter}} = -\frac{\hbar e}{2m^*S} \sum_{\mathbf{q}\mathbf{k}\alpha} \frac{e^{-i\mathbf{q}\mathbf{r}_\parallel}}{\Delta\omega_{\mathbf{k}\mathbf{q}\alpha}} \Delta n_{\mathbf{k}\mathbf{q}\alpha} \times [\xi_\alpha(z)b_{\mathbf{k}\mathbf{q}\alpha}^\dagger + \xi_\alpha^*(z)b_{-\mathbf{k}-\mathbf{q}\alpha}], \quad (37)$$

$$\hat{P}_z|_{\text{intra}} = -\frac{\hbar e}{2m^*S} \sum_{\mathbf{q}\mathbf{k}i} \frac{e^{-i\mathbf{q}\mathbf{r}_\parallel}}{\Delta\omega_{\mathbf{k}\mathbf{q}}} \Delta n_{\mathbf{k}\mathbf{q}i} \xi_{ii}(z)[d_{\mathbf{k}\mathbf{q}i}^\dagger - d_{-\mathbf{k}-\mathbf{q}i}]. \quad (38)$$

The advantage of this representation is that it can be easily generalized for the case of a finite temperature; however, in this case we must bear in mind that the bosonization is an approximation valid in the limit where the number of excitations in the system is low as compared to the total number of particles.

The expressions for the parallel component of the polarization field are established in a similar way:

$$\hat{\mathbf{P}}_{\parallel}|_{\text{inter}} = \frac{-i\hbar e}{2m^*S} \sum_{\mathbf{q}\mathbf{k}\alpha} \frac{e^{-i\mathbf{q}\mathbf{r}_\parallel}(2\mathbf{k} + \mathbf{q})}{\Delta\omega_{\mathbf{k}\mathbf{q}\alpha}} \Delta n_{\mathbf{k}\mathbf{q}\alpha} \times [\eta_\alpha(z)b_{\mathbf{k}\mathbf{q}\alpha}^\dagger + \eta_\alpha^*(z)b_{-\mathbf{k}-\mathbf{q}\alpha}], \quad (39)$$

$$\hat{\mathbf{P}}_{\parallel}|_{\text{intra}} = \frac{-ie}{S} \sum_{\mathbf{q}\mathbf{k}i} e^{-i\mathbf{q}\mathbf{r}_\parallel} \beta_{\mathbf{q}\mathbf{k}} \Delta n_{\mathbf{k}\mathbf{q}i} \eta_{ii}(z)[d_{\mathbf{k}\mathbf{q}i}^\dagger + d_{-\mathbf{k}-\mathbf{q}i}], \quad (40)$$

$$\beta_{\mathbf{q}\mathbf{k}} = \frac{2\mathbf{k} + \mathbf{q}}{\mathbf{q}(2\mathbf{k} + \mathbf{q})}. \quad (41)$$

As expected, the intrasubband contribution (40) which arises from the free in-plane electronic movement is formally identical to the polarization field of the 3D electron gas [3].

The expressions (37)–(40) are the most general expressions for the polarization field of a 2DEG, in the bosonization approach. Using these expressions, we can expand the square-polarization part of the PZW Hamiltonian from Eq. (19):

$$\frac{1}{2\varepsilon\varepsilon_0} \int \hat{\mathbf{P}}^2 d^3\mathbf{r} = \mathcal{H}_{\text{P}2}^{\text{inter}} + \mathcal{H}_{\text{P}2}^{\text{intra}} + \mathcal{H}_{\text{P}2}^{\text{inter-intra}}, \quad (42)$$

$$\mathcal{H}_{\text{P}2}^{\text{inter}} = \frac{1}{2\varepsilon\varepsilon_0} \left(\int \hat{P}_z^2|_{\text{inter}} d^3\mathbf{r} + \int \hat{\mathbf{P}}_{\parallel}^2|_{\text{inter}} d^3\mathbf{r} \right), \quad (43)$$

$$\mathcal{H}_{\text{P}2}^{\text{intra}} = \frac{1}{2\varepsilon\varepsilon_0} \left(\int \hat{P}_z^2|_{\text{intra}} d^3\mathbf{r} + \int \hat{\mathbf{P}}_{\parallel}^2|_{\text{intra}} d^3\mathbf{r} \right), \quad (44)$$

$$\mathcal{H}_{\text{P}2}^{\text{inter-intra}} = \frac{1}{\varepsilon\varepsilon_0} \left(\int \hat{P}_z|_{\text{inter}} \hat{P}_z|_{\text{intra}} d^3\mathbf{r} \right) + \frac{1}{\varepsilon\varepsilon_0} \left(\int \hat{\mathbf{P}}_{\parallel}|_{\text{inter}} \hat{\mathbf{P}}_{\parallel}|_{\text{intra}} d^3\mathbf{r} \right). \quad (45)$$

This Hamiltonian, that is quadratic in the operators $b_{\mathbf{k}\mathbf{q}\alpha}^\dagger, b_{\mathbf{k}\mathbf{q}\alpha}$, $d_{\mathbf{k}\mathbf{q}i}^\dagger$, and $d_{\mathbf{k}\mathbf{q}i}$ couples the intersubband and intrasubband excitations with different wave vectors, as well as the intersubband or intrasubband excitation from different subbands among each other. In the subsequent sections, we will see

that the apparent complexity of this Hamiltonian can be greatly reduced by separating the excitations of the gas into single-particle-like and collective excitations. The single-particle-like solutions are very similar to free-electronic excitations that ignore the quadratic interaction term of the Hamiltonian [3]. Therefore, their contribution to the polarization field of the gas is vanishing [3,8,15]. On the contrary, the collective excitations are obtained as a result of the self-polarization interaction, and their energies strongly differ from the initial electronic energies of the single-particle Hamiltonian \mathcal{H}_c . These collective excitations appear as coherent sums of elementary excitations over the electronic wave vectors, and can be interpreted as a set of quantum-confined plasmons. As a result, these plasmon modes will have a dominant contribution to the polarization field of the gas. The problem described in Eq. (42) can be further reduced to the interaction of a discrete set of plasmon modes with each other. In the following sections, we will provide closed expressions for the collective plasmonic operators and the plasmon-plasmon coupling in the long-wavelength limit $\mathbf{q} \rightarrow \mathbf{0}$.

We can simplify considerably the expressions in Eqs. (43)–(45) by considering a closed system with hard-wall boundary conditions. Indeed, an arbitrary one-dimensional finite potential $V(z)$ leads in general to two sets of eigenstates: bound states with discrete energy eigenvalues, described by wave functions $\phi_i(z)$ which are real and localized in a finite region of space, and a high-energy continuum of unbound states, described by propagating plane waves $\phi_k(z) \sim \exp(ik_z z)$. Clearly, if we restrict the description of the system only to the first few bound states, according to Eq. (29) we have $\xi_{ii}(z) = 0$ and the intrasubband part of the polarization field $\hat{P}_z|_{\text{intra}}$ [Eq. (38)] becomes identically zero for all states. As a consequence, the first terms in Eqs. (44) and (45) vanish. This approximation is excellent for systems where the Fermi level E_F lies within the ensemble of bound states (Fig. 2). Further, if we model our system with hard-wall boundary conditions, that are situated sufficiently far from the region where the potential $V(z)$ varies appreciably, we can describe the unbound states in the continuum as electronic standing waves described by real wave functions $\phi_k(z) \sim \cos(ik_z z)$ (Fig. 2), which also allows simplifying Eqs. (43)–(45). In the following, for simplicity we shall assume that our system is well described within that approximation. Nevertheless, it is interesting to note that the set of equations (43)–(45) also hint at the possibility to describe the interaction between confined plasmons that arises from the bound states of the potential $V(z)$ with “transport” single-particle states within the continuum with nonvanishing perpendicular current $\xi_{ii} = 2 \text{Im}[\phi_i^*(z)\partial_z \phi_i(z)] \neq 0$.

For the following, it is very useful to introduce the overlap integrals

$$I_{\alpha,\beta} = \int \xi_\alpha(z)\xi_\beta(z)dz, \quad (46)$$

$$J_{\alpha,\beta} = \int \eta_\alpha(z)\eta_\beta(z)dz, \quad (47)$$

$$J_{i,j} = \int \eta_{ii}(z)\eta_{jj}(z)dz, \quad (48)$$

$$J_{\alpha,j} = \int \eta_\alpha(z)\eta_{jj}(z)dz. \quad (49)$$

These integrals appear naturally while expressing the square-polarization Hamiltonian by the use of Eqs. (37), (39), and (40).

In the next section, we take a particular case of a two-subband system and we identify the collective modes in the long-wavelength approximation. These modes will be then generalized for the case of a system with any finite number of occupied subbands.

To conclude this section, let us note that we can reexpress similarly the current density operator $\hat{\mathbf{j}}$ [Eqs. (23) and (25)] and the charge density operator $\hat{\rho}$ [Eq. (31)] in terms of bosonized operators $b_{\mathbf{k}q\alpha}^\dagger$, $b_{\mathbf{k}q\alpha}$, $d_{\mathbf{k}qi}^\dagger$, and $d_{\mathbf{k}qi}$. Using this form of the charge density operator, it can be readily shown that it commutes with the square-polarization interaction terms from Eq. (42), which ensure the validity of the continuity equation (32). This fact is an important confirmation for the self-consistency of our approach [3].

C. Collective modes in a two-subband system

We now consider the collective excitations which arise in a two-subband system, where the Fermi level E_F lies between the first and the second subbands, as described in Fig. 3. Our aim is to diagonalize the electronic Hamiltonian (19), as provided by Eqs. (18) and (43)–(45). This will allow us to identify the intersubband and intrasubband plasmon modes linked to the bound states of the system, which will subsequently be generalized for the multisubband case. We will provide the polarization operators for each collective excitation, with the corresponding spatial dependence, which will permit us to discuss the physical characteristics of the collective modes.

Using the polarization operators from the previous section, and restraining them to the case of two bound states, the

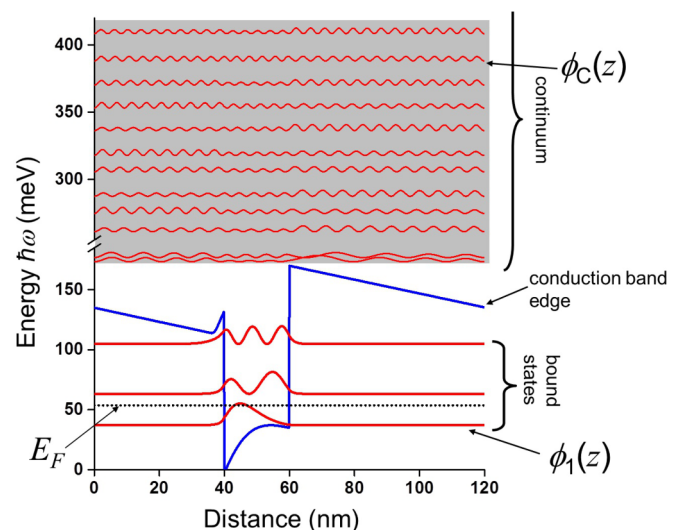


FIG. 2. (Color online) Illustration of a finite one-dimensional binding potential $V(z)$, inserted in a larger box with hard-wall boundary conditions. The bound states are not affected by the hard walls, as the corresponding wave functions $\phi_i(z)$ vanish on the boundary. The unbound states in the continuum are modeled as real standing waves $\phi_C(z) = \phi_{k_z}(z)$.

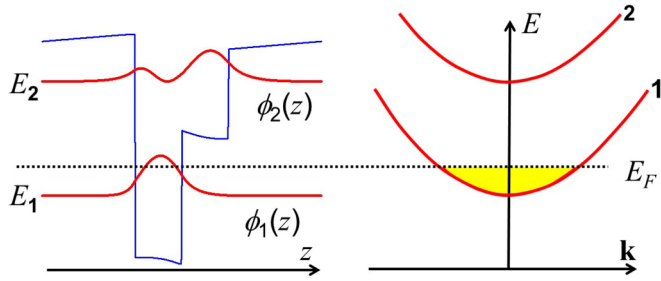


FIG. 3. (Color online) A two-subband system, with only the fundamental (first) subband occupied.

electronic Hamiltonian is written explicitly as follows:

$$\mathcal{H}_e = \sum_{\mathbf{k}\mathbf{q}} \hbar\Delta\omega_{\mathbf{k}\mathbf{q}21} b_{\mathbf{k}\mathbf{q}}^\dagger b_{\mathbf{k}\mathbf{q}} + \sum_{\mathbf{k}\mathbf{q}} \hbar\Delta\omega_{\mathbf{k}\mathbf{q}} d_{\mathbf{k}\mathbf{q}}^\dagger d_{\mathbf{k}\mathbf{q}}, \quad (50)$$

$$\begin{aligned} \mathcal{H}_{P2}^{\text{inter}} &= \frac{\hbar^2 e^2}{8m^* \epsilon_0 S} \sum_{\mathbf{k}\mathbf{k}'\mathbf{q}} (\mathbf{V}_{\mathbf{k}\mathbf{q}} \cdot \mathbf{V}_{\mathbf{k}'\mathbf{q}}) \\ &\times (b_{\mathbf{k}\mathbf{q}}^\dagger + b_{-\mathbf{k}-\mathbf{q}})(b_{\mathbf{k}'\mathbf{q}} + b_{-\mathbf{k}'-\mathbf{q}}), \end{aligned} \quad (51)$$

$$\mathbf{V}_{\mathbf{k}\mathbf{q}} = \frac{\Delta n_{\mathbf{k}\mathbf{q}21}}{\Delta\omega_{\mathbf{k}\mathbf{q}21}} [\sqrt{I_{21,21}} \mathbf{e}_z + \sqrt{J_{21,21}} (2\mathbf{k} + \mathbf{q})], \quad (52)$$

$$\begin{aligned} \mathcal{H}_{P2}^{\text{intra}} &= \frac{e^2 J_{1,1}}{2S\epsilon\epsilon_0} \sum_{\mathbf{k}\mathbf{k}'\mathbf{q}} \Delta n_{\mathbf{k}\mathbf{q}1} \Delta n_{\mathbf{k}'\mathbf{q}1} (\boldsymbol{\beta}_{\mathbf{q}\mathbf{k}} \boldsymbol{\beta}_{\mathbf{q}\mathbf{k}'}) \\ &\times (d_{\mathbf{k}\mathbf{q}}^\dagger + d_{-\mathbf{k}-\mathbf{q}})(d_{\mathbf{k}'\mathbf{q}} + d_{-\mathbf{k}'-\mathbf{q}}), \end{aligned} \quad (53)$$

$$\mathcal{H}_{P2}^{\text{inter-intra}} = \frac{1}{\epsilon\epsilon_0} \left(\int \hat{\mathbf{P}}_{\parallel} |_{\text{inter}} \hat{\mathbf{P}}_{\parallel} |_{\text{intra}} d^3\mathbf{r} \right). \quad (54)$$

Since the distinction between intersubband and intrasubband operators is clear for this case, we drop the subband indexes for the operators. All terms except the last coupling term from Eq. (54) split naturally into intersubband and intrasubband contributions. Each of these contributions is formally equivalent to the general PZW bosonic Hamiltonian considered in Ref. [3], which can be resolved within the characteristic function approach recalled in Appendix A. Once we have worked out the intrasubband and intersubband contributions separately, we will be able to provide the coupled modes induced by the interaction term in Eq. (54). In the end of this section (Sec. II C 3), we will also consider numerical examples with two different heterostructure potentials.

1. Intrasubband plasmon

The intrasubband parts of Eqs. (50) and (53) provide the following quadratic bosonic form:

$$\sum_{\mathbf{k}\mathbf{q}} \hbar\Delta\omega_{\mathbf{k}\mathbf{q}} d_{\mathbf{k}\mathbf{q}}^\dagger d_{\mathbf{k}\mathbf{q}} + \mathcal{H}_{P2}^{\text{intra}}. \quad (55)$$

This Hamiltonian is formally identical to the PZW Hamiltonian of the three-dimensional gas, considered in Ref. [3]. Following [3], and the method outlined in Appendix A we associate to Eq. (55) the following two-dimensional

characteristic tensor:

$$\boldsymbol{\zeta}_{\parallel}^{\text{intra}}(\omega, \mathbf{q}) = \mathbf{1}_2 - \frac{2e^2 J_{1,1}}{\hbar S \epsilon \epsilon_0} \sum_{\mathbf{k}} \Delta n_{\mathbf{k}\mathbf{q}1} \frac{(\boldsymbol{\beta}_{\mathbf{q}\mathbf{k}} \otimes \boldsymbol{\beta}_{\mathbf{q}\mathbf{k}}) \Delta\omega_{\mathbf{k}\mathbf{q}}}{\omega^2 - \Delta\omega_{\mathbf{k}\mathbf{q}}^2}. \quad (56)$$

Here, $\mathbf{1}_2$ is the in-plane unit tensor. The eigenvalues of the Hamiltonian (55) are then provided as the solutions of the characteristic equation

$$\|\boldsymbol{\zeta}_{\parallel}^{\text{intra}}(\omega, \mathbf{q})\| = 0. \quad (57)$$

According to the general properties of the characteristic function $\boldsymbol{\zeta}_{\parallel}^{\text{intra}}(\omega, \mathbf{q})$, discussed in Ref. [3], this equation has two types of solutions: (i) single-particle-like solutions, with frequencies that remain very close to the original excitations frequencies $\Delta\omega_{\mathbf{k}\mathbf{q}}$, or (ii) collective modes with frequencies that can be much larger than $\Delta\omega_{\mathbf{k}\mathbf{q}}$. The frequencies of the collective modes can be obtained explicitly in the long-wavelength limit of Eq. (56) where, just like for the homogeneous electron gas, the characteristic function $\boldsymbol{\zeta}_{\parallel}^{\text{intra}}(\omega, \mathbf{q})$ acquires the Drude-type diagonal form

$$\boldsymbol{\zeta}_{\parallel}^{\text{intra}}(\omega, \mathbf{q} \rightarrow \mathbf{0}) = \mathbf{1}_2 \left(1 - \frac{\omega_{P\parallel}^2}{\omega^2} \right). \quad (58)$$

Here, we defined the plasma frequency of the corresponding collective state, the intrasubband plasmon:

$$\omega_{P\parallel}^2 = \frac{e^2 N_1}{m^* \epsilon \epsilon_0 S L_1}, \quad L_1 = 1/J_{1,1}. \quad (59)$$

The effective length L_1 introduced above depends on the electronic wave functions through the coefficient $J_{1,1}$ [Eq. (48)], and takes into account the effect of the quantum confinement of the heterostructure potential $V(z)$. The resulting intrasubband modes feature no dispersion, and correspond to density waves in the (x, y) plane where the electrons oscillate at a frequency $\omega_{P\parallel}$. The associated bosonic operators are expressed as sums over all possible excitation wave vectors:

$$\begin{aligned} \pi_{\mathbf{q}\mathbf{n}}^\dagger &= \sqrt{\frac{J_{1,1} e^2}{2\hbar\omega_{P\parallel}\epsilon\epsilon_0 S}} \sum_{\mathbf{k}} \Delta n_{\mathbf{k}\mathbf{q}1} (\boldsymbol{\beta}_{\mathbf{q}\mathbf{k}} \cdot \mathbf{n}) \\ &\times \left\{ (d_{\mathbf{k}\mathbf{q}}^\dagger + d_{-\mathbf{k}-\mathbf{q}}) + \frac{\Delta\omega_{\mathbf{k}\mathbf{q}}}{\omega_{P\parallel}} (d_{\mathbf{k}\mathbf{q}}^\dagger - d_{-\mathbf{k}-\mathbf{q}}) \right\}. \end{aligned} \quad (60)$$

Here, \mathbf{n} is an in-plane unit vector that corresponds to the direction of the density wave. These collective excitations provide the dominant contribution in the polarization field of the gas. Let $\mathbf{n}_j, j = 1, 2$, be an orthogonal basis in the plane (x, y) , then neglecting the vanishing contributions from the single-particle-like excitations the expression of the polarization operator from Eq. (40) becomes

$$\begin{aligned} \hat{\mathbf{P}}_{\parallel} |_{\text{intra}} &= -i\eta_{11}(z) \sqrt{\frac{\omega_{P\parallel}\epsilon\epsilon_0\hbar}{2SJ_{1,1}}} \\ &\times \sum_{\mathbf{q}\mathbf{n}_j} e^{-i\mathbf{q}\mathbf{r}_{\parallel}} \mathbf{n}_j [\pi_{\mathbf{q}\mathbf{n}_j}^\dagger + \pi_{-\mathbf{q}\mathbf{n}_j}] \end{aligned} \quad (61)$$

and the intrasubband part of the Hamiltonian in Eq. (55) is unitary transformed into a diagonal form

$$\sum_{\mathbf{q}\mathbf{n}_j} \hbar\omega_{P\parallel} \pi_{\mathbf{q}\mathbf{n}_j}^\dagger \pi_{\mathbf{q}\mathbf{n}_j}. \quad (62)$$

According to Eq. (61), the polarization density of the intrasubband plasmon is decomposed into plane waves of the form $\eta_{11}(z) \exp(-i\mathbf{q}\mathbf{r}_{\parallel})$. This spatial variation has a clear physical meaning since according to the definition of the charge density operator from Eq. (31), the quantity $\eta_{11}(z) = \phi_1^2(z)$ describes the electronic density in the first subband along the direction of quantum confinement. Then, the intrasubband plasmon corresponds to a density wave, very similar to the bulk plasmon of a homogeneous electron gas, with the exception that the wave vector \mathbf{q} is constrained to the xy plane, while the electronic density in the z direction is set by the quantum confinement. Furthermore, just like the bulk plasma mode of the 3D electron gas, the intrasubband excitation obtained with our approach has a plasma frequency $\omega_{P\parallel}$ that is independent from the wave vector, in the long-wavelength limit. This result might appear in conflict with the well-known $\sqrt{|\mathbf{q}|}$ dispersion of the intrasubband plasmon of 2DEG [26]. Actually, this conventional excitation can be obtained as the longitudinal part of a the intrasubband plasmon mode derived above, as discussed in details in Sec. II D. As we pointed out in the end of Sec. II A, the polarization field that we consider has both longitudinal and transverse components, the latter allowing us to describe the coupling of the collective excitations with light. In particular, the Drude-type dielectric function in Eq. (58) leads to free-carrier absorption in the plane of the quantum wells owing to the intrasubband plasmon described above.

Note that the tensor $\zeta_{\parallel}^{\text{intra}}(\omega, \mathbf{q})$ can be used in its more general form in Eq. (56) to study the intrasubband excitations beyond the long-wavelength approximation, and the related Landau damping of collective excitations.

2. Intersubband plasmons

The intersubband part of the Hamiltonian [Eqs. (50)–(52)], that is, the part that corresponds to electrons evolving between two different subbands, is

$$\sum_{\mathbf{k}\mathbf{q}} \hbar\Delta\omega_{\mathbf{k}\mathbf{q}21} b_{\mathbf{k}\mathbf{q}}^\dagger b_{\mathbf{k}\mathbf{q}} + \mathcal{H}_{P2}^{\text{inter}}. \quad (63)$$

The corresponding characteristic tensor is now three dimensional:

$$\zeta(\omega, \mathbf{q}) = \mathbf{1}_3 - \frac{\hbar e^2}{2m^* \varepsilon \varepsilon_0 S} \sum_{\mathbf{k}} \frac{(\mathbf{V}_{\mathbf{q}\mathbf{k}} \otimes \mathbf{V}_{\mathbf{q}\mathbf{k}}) \Delta\omega_{\mathbf{k}\mathbf{q}21}}{\omega^2 - \Delta\omega_{\mathbf{k}\mathbf{q}21}^2}. \quad (64)$$

Using Eq. (52) for the vector $\mathbf{V}_{\mathbf{q}\mathbf{k}}$, we can split the tensor $\zeta(\omega, \mathbf{q})$ into a z component and a planar component that are not coupled to each other:

$$\zeta(\omega, \mathbf{q}) = (\mathbf{e}_z \otimes \mathbf{e}_z) \zeta_{zz}(\omega, \mathbf{q}) + \zeta_{\parallel}^{\text{inter}}(\omega, \mathbf{q}). \quad (65)$$

Since the two components in Eq. (65) are independent from each other, they will be treated separately. Equation (65) thus expresses an important property of the system, which states that, as long as we are restrained to bound states, or in other words, a closed system, the excitation of the gas along the

direction of the quantum confinement is completely decoupled from the in-plane excitations.

The tensor $\zeta(\omega, \mathbf{q})$ can be used to study the intersubband excitations for any value of the wave vector \mathbf{q} . Similarly to the case of the intrasubband plasmon, when the excitation wave vector \mathbf{q} is sufficiently small, most of the solutions remain close to the single-particle frequencies $\Delta\omega_{\mathbf{k}\mathbf{q}21}$ and are well separated from the collective excitations of the gas. The two characteristic tensors from Eq. (65) give rise, respectively, to charge oscillations along the z axis and in the (x, y) plane. However, unlike the intrasubband excitations of the previous paragraph, now the in-plane oscillations can have a zero-excitation wave vector. In this case, they correspond to a global change in the electronic density (related to the changing shape of the wave functions as the electrons hop from one subband to another), rather than an acousticlike density wave, as in the case of the intrasubband plasmon. In the long-wavelength approximation $\mathbf{q} \rightarrow \mathbf{0}$, we can neglect the change of the kinetic energy of the electrons with respect to the transition energy, and we have $\Delta\omega_{\mathbf{k}\mathbf{q}21} \approx \Delta\omega_{21}$ as well as $\Delta n_{\mathbf{k}\mathbf{q}21} \approx \Delta n_{\mathbf{k}\mathbf{0}21}$. The tensor components then take simple diagonal forms

$$\zeta_{zz}(\omega, \mathbf{q} \rightarrow \mathbf{0}) = 1 - \frac{\omega_{P21}^2}{\omega^2 - \Delta\omega_{21}^2}, \quad (66)$$

$$\zeta_{\parallel}^{\text{inter}}(\omega, \mathbf{q} \rightarrow \mathbf{0}) = \mathbf{1}_2 \left(1 - \frac{W_{P21}^2}{\omega^2 - \Delta\omega_{21}^2} \right). \quad (67)$$

Here, we introduced the two plasma frequencies

$$\omega_{P21}^2 = \frac{2\hbar e^2 I_{21,21}}{m^* \varepsilon \varepsilon_0 S \Delta\omega_{21}} \sum_{\mathbf{k}} \Delta n_{\mathbf{k}\mathbf{0}21}, \quad (68)$$

$$W_{P21}^2 = \frac{2\hbar e^2 J_{21,21}}{m^* \varepsilon \varepsilon_0 S \Delta\omega_{21}} \sum_{\mathbf{k}} \Delta n_{\mathbf{k}\mathbf{0}21} (\mathbf{k}\mathbf{n})^2, \quad (69)$$

and \mathbf{n} is a fixed direction in the plane. The summation over the wave vectors is readily performed to yield

$$\omega_{P21}^2 = \frac{e^2 N_e}{m^* \varepsilon \varepsilon_0 S L_{21}}, \quad L_{21} = \frac{2m^* \Delta\omega_{21}}{\hbar I_{21,21}}, \quad (70)$$

$$W_{P21}^2 = \frac{e^2 (N_e/2)}{m^* \varepsilon \varepsilon_0 S L_{21}^{\parallel}}, \quad L_{21}^{\parallel} = \frac{1}{J_{21,21}}. \quad (71)$$

Here, $N_e = \sum_{\mathbf{k}} \Delta n_{\mathbf{k}\mathbf{0}21}$ is the population difference between the two subbands, which is equal in this case to the total number of electrons in the system. Similarly to Eq. (59), the effective lengths L_{21} and L_{21}^{\parallel} take into account the quantum confinement of the gas, as they are expressed directly from the wave functions of the bound states. The solutions of the characteristic equation $\|\zeta(\omega, \mathbf{q})\| = 0$ are

$$\tilde{\omega}_{21} = \sqrt{\Delta\omega_{21}^2 + \omega_{P12}^2}, \quad (72)$$

$$\tilde{W}_{21} = \sqrt{\Delta\omega_{21}^2 + W_{P12}^2}. \quad (73)$$

The first solution [Eq. (72)] is the well-known intersubband plasmon mode oscillating in the z direction [33], which was already described in the PZW approach [4]. The second solution describes a less conventional plasmon mode where electrons oscillate in the plane. We will dub

it “in-plane intersubband plasmon,” while the first solution [Eq. (72)] will be called simply “intersubband plasmon” to comply with existing literature [27,33]. In order to understand the physical meaning of these excitations, we will explicit the corresponding polarization operators. Let $p_{\mathbf{q}21}^\dagger$ and $t_{\mathbf{q}\mathbf{n}21}^\dagger$ be the corresponding bosonic operators, respectively, for the conventional intersubband plasmon and in-plane intersubband plasmon, that diagonalize the quadratic Hamiltonian (55):

$$\sum_{\mathbf{q}} \hbar \tilde{\omega}_{21} p_{\mathbf{q}21}^\dagger p_{\mathbf{q}21} + \sum_{\mathbf{q}\mathbf{n}_j} \hbar \tilde{W}_{21} t_{\mathbf{q}\mathbf{n}_j21}^\dagger t_{\mathbf{q}\mathbf{n}_j21}. \quad (74)$$

As the dominant contribution into the polarization field arises from the collective excitations, the respective components can be expressed as

$$\begin{aligned} \hat{P}_z|_{\text{inter}} &= -\xi_{21}(z) \sqrt{\frac{\omega_{P21}^2}{2\tilde{\omega}_{21}} \frac{\hbar \varepsilon \varepsilon_0}{S I_{21,21}}} \\ &\times \sum_{\mathbf{q}} e^{-i\mathbf{q}\mathbf{r}_\parallel} (p_{\mathbf{q}21}^\dagger + p_{-\mathbf{q}21}), \end{aligned} \quad (75)$$

$$\begin{aligned} \hat{P}_\parallel|_{\text{inter}} &= -i\eta_{21}(z) \sqrt{\frac{W_{P21}^2}{2\tilde{W}_{21}} \frac{\hbar \varepsilon \varepsilon_0}{S J_{21,21}}} \\ &\times \sum_{\mathbf{q}\mathbf{n}_j} e^{-i\mathbf{q}\mathbf{r}_\parallel} \mathbf{n}_j [t_{\mathbf{q}\mathbf{n}_j21}^\dagger + t_{-\mathbf{q}\mathbf{n}_j21}]. \end{aligned} \quad (76)$$

According to the above equations, the z dependence for the polarization field of the conventional intersubband plasmon [Eq. (75)] is provided by the current function $\xi_{21}(z)$. Furthermore, the polarization field has a single component along the z axis. This excitation therefore corresponds to dynamical oscillations of the electronic density along the z direction, induced by the electronic transitions between the two subbands [8].

On the contrary, the polarization field of the in-plane plasmon (76) lies in the (x, y) plane and has a very similar form as the one of the intrasubband plasmon from the previous section [Eq. (61)], with the static electronic density $\eta_{11}(z) = \phi_1^2(z)$ now replaced by the intersubband term $\eta_{21}(z) = \phi_1(z)\phi_2(z)$. Once again, we have referred to the definition of the charge density operator from Eq. (31). Such static contribution can be interpreted as resulting from a quantum superposition of states $[\phi_1(z) + \phi_2(z)]/\sqrt{2}$, where the excited electrons occupy virtually both subbands with equal probability. Furthermore, since both the in-plane intersubband plasmon and the intrasubband plasmon have polarization fields that are contained in the (x, y) plane, they are generally coupled through the square-polarization term of the matter Hamiltonian (19). This coupling is analyzed in the next section.

The explicit expressions for the operators $p_{21\mathbf{q}}^\dagger$ and $t_{21\mathbf{q}\mathbf{n}}^\dagger$ can be obtained following the approach described in Ref. [3]. Here, we specify the collective operator $p_{21\mathbf{q}}^\dagger$ which corresponds to the intersubband plasmon:

$$\begin{aligned} p_{\mathbf{q}21}^\dagger &= \frac{\omega_{P21}^2}{2\sqrt{\tilde{\omega}_{21}} \Delta\omega_{21} N_e} \sum_{\mathbf{k}} \Delta n_{\mathbf{k}021} \\ &\times \left\{ \frac{b_{\mathbf{k}\mathbf{q}}^\dagger}{\tilde{\omega}_{21} - \Delta\omega_{21}} + \frac{b_{-\mathbf{k}-\mathbf{q}}}{\tilde{\omega}_{21} + \Delta\omega_{21}} \right\}. \end{aligned} \quad (77)$$

This operator then sums coherently over all allowed single-particle intersubband transitions. In Eq. (77), let us consider the case of a lightly doped quantum well such as $\omega_{P21} \ll \Delta\omega_{21}$. Then, neglecting the antiresonant contribution we obtain an approximate expression for the plasmon operator:

$$p_{\mathbf{q}21}^\dagger \approx \frac{1}{\sqrt{N_e}} \sum_{\mathbf{k}} \Delta n_{\mathbf{k}021} b_{\mathbf{k}\mathbf{q}}^\dagger. \quad (78)$$

This expression is formally identical to the one introduced for the first theoretical description of the ultrastrong coupling regime with intersubband polaritons in Ref. [5].

3. Intersubband-intrasubband coupling and numerical examples

Having separated the single-particle from the collective excitations in the long-wavelength limit, we now replace the electronic Hamiltonian from Eqs. (50)–(45) with an effective bosonic Hamiltonian that acts only on the collective operators:

$$\begin{aligned} \mathcal{H}_{\text{coll}} &= \sum_{\mathbf{q}} \hbar \tilde{\omega}_{21} p_{\mathbf{q}21}^\dagger p_{\mathbf{q}21} + \sum_{\mathbf{q}\mathbf{n}_j} \hbar \tilde{W}_{21} t_{\mathbf{q}\mathbf{n}_j21}^\dagger t_{\mathbf{q}\mathbf{n}_j21} \\ &+ \sum_{\mathbf{q}\mathbf{n}_j} \hbar \omega_{P\parallel} \pi_{\mathbf{q}\mathbf{n}_j}^\dagger \pi_{\mathbf{q}\mathbf{n}_j} + C_{1,21}^J \frac{\hbar W_{P21}}{2} \sqrt{\frac{\omega_{P\parallel}}{\tilde{W}_{21}}} \\ &\times \sum_{\mathbf{q}\mathbf{n}_j} (\pi_{\mathbf{q}\mathbf{n}_j}^\dagger + \pi_{-\mathbf{q}\mathbf{n}_j}) (t_{-\mathbf{q}\mathbf{n}_j21}^\dagger + t_{\mathbf{q}\mathbf{n}_j21}). \end{aligned} \quad (79)$$

As indicated in the previous section, only the conventional intersubband plasmon oscillates in the direction of quantum confinement, and therefore it forms an independent contribution [first term in the right-hand side of Eq. (79)]. The two other collective excitations that we considered oscillate both in the plane and are coupled by the quadratic interaction term in Eq. (19). This interaction is contained in the last term of Eq. (79) through the expression of the inter-intra subband coupling term $\mathcal{H}_{P2}^{\text{inter-intra}}$ [Eq. (54)] through Eqs. (61) and (76). The overlap coefficient $C_{1,21}^J$ has been defined as

$$C_{1,21}^J = \frac{J_{1,21}}{\sqrt{J_{1,1} J_{21,21}}}. \quad (80)$$

The inter-intra subband coupling concerns only the in-plane collective mode. For each wave vector \mathbf{q} and each direction in the plane \mathbf{n} we recover a set of two coupled quantum harmonic oscillators, described by the ladder operators $t_{\mathbf{q}\mathbf{n}21}^\dagger$ and $\pi_{\mathbf{q}\mathbf{n}}^\dagger$. The corresponding eigenvalue equation is

$$(\omega^2 - \omega_{P\parallel}^2)(\omega^2 - \tilde{W}_{21}^2) = (C_{1,21}^J)^2 W_{P21}^2 \omega_{P\parallel}^2. \quad (81)$$

Clearly, the overlap coefficient $C_{1,21}^J$ provides directly the strength of the coupling between the two kinds of in-plane plasmonic modes. In particular, for the case of centrosymmetric potential, the wave functions ϕ_1 and ϕ_2 have different parities, we therefore have $J_{1,21} = 0$ and the inter-intra subband coupling vanishes.

Let us at present illustrate the collective modes derived in this section with two numerical examples. The first example is an infinite square quantum well, as depicted in the inset of Fig. 4(a), and the second example is a finite asymmetric potential [Fig. 4(b), inset]. We restrict our discussion only to the first two subbands separated by a frequency $\Delta\omega_{21} =$

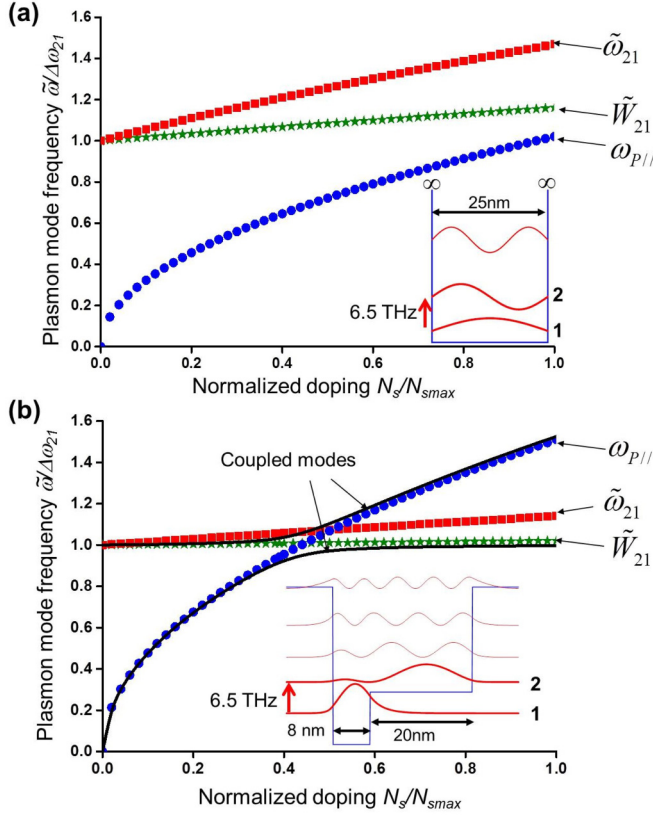


FIG. 4. (Color online) (a) The frequencies of the three collective modes arising between the fundamental and first excited subbands for the case of an infinite square quantum well. Circles: intrasubband plasmon; squares: conventional intrasubband plasmon; stars: in-plane intersubband plasmon. (b) Similar plot for a finite asymmetric potential. The asymmetry of the potential induces a coupling between the intrasubband plasmon and the in-plane intersubband plasmon. The coupled modes are plotted in continuous lines.

6.5 THz by design. Respectively, the maximum areal density of charges N_{smax} in the wells is set by the condition $E_F = \hbar\omega_2$ and equal to $N_{smax} = m^* \Delta\omega_{21} / \pi \hbar$. For concreteness, we consider GaAs material for the quantum wells with $m^* = 0.067m_0$, with m_0 the electron mass. This provides a maximum areal density of charges $N_{smax} = 7.5 \times 10^{11} \text{ cm}^{-2}$. Furthermore, we shall ignore the phonon dispersion of the material for simplicity.

In the case of the infinite quantum well with a thickness L_{QW} the confined wave functions are provided by $\phi_i(z) = \sqrt{2/L_{QW}} \sin(i\pi z/L_{QW})$ with $i \geq 1$. We can therefore compute directly the three characteristic lengths introduced by Eqs. (59), (70), and (71):

$$L_1 = \frac{2}{3}L_{QW}, \quad L_{21} = \frac{3}{5}L_{QW}, \quad L_{21}^{\parallel} = L_{QW}. \quad (82)$$

We can therefore use the definitions (59), (72), and (73) to compute the collective mode frequencies as a function of the areal charge density in the well N_s with $N_s \leq N_{smax}$. These frequencies have been normalized to the transition frequency $\Delta\omega_{21}$:

$$\frac{\omega_{P\parallel}}{\Delta\omega_{21}} = \sqrt{\frac{2}{3} \frac{N_s}{N_{smax}} \frac{L_{QW}}{L^*}}, \quad (83)$$

$$\frac{\tilde{\omega}_{21}}{\Delta\omega_{21}} = \sqrt{1 + \frac{3}{5} \frac{N_s}{N_{smax}} \frac{L_{QW}}{L^*}}, \quad (84)$$

$$\frac{\tilde{W}_{21}}{\Delta\omega_{21}} = \sqrt{1 + \frac{1}{2} \frac{N_s}{N_{smax}} \frac{L_{QW}}{L^*}}. \quad (85)$$

Here, we introduced a unique parameter that scales like a characteristic thickness:

$$L^* = \frac{3\pi\epsilon\epsilon_0\hbar^2}{8m^*e^2} \quad (86)$$

and $\hbar = 2\pi\hbar$. The characteristic thickness L^* has an expression that is very similar to the Bohr radius [37]. This parameter appears naturally while computing the ratio between the plasma frequencies and the transition frequency $\Delta\omega_{21}$. It therefore corresponds to the ratio between the potential energy associated to the particle-particle interactions over the characteristic kinetic energy of the particles (in this case, the transition energy $\hbar\Delta\omega_{21}$). Clearly, this parameter allows us to evaluate rapidly the pertinence of the collective effects in the system. Indeed, as seen from the set of equations (83)–(85), when $L_{QW} \ll L^*$, the collective effects have little impact on the system, no matter the doping level, as the collective mode frequencies remain close to the “bare” transition frequency $\Delta\omega_{21}$. On the contrary, in the case of large quantum wells $L_{QW} \gg L^*$, the collective effects can become important even for moderate doping levels. For the case of a GaAs well we estimate $L^* = 37 \text{ nm}$. We shall, however, bear in mind that this value is not universal, but restricted to the first transition of an infinite quantum well. Yet, it provides a quick guide for the impact on the collective effects in simple potentials.

The corresponding collective mode frequencies provided by Eqs. (83)–(85) have been plotted in Fig. 4(a), for the case $L_{QW} = 25 \text{ nm}$. In this case, as the potential is centrosymmetric the coupling between the in-plane plasmons is null.

The effective lengths introduced by Eqs. (59), (70), and (71) can be very sensitive to the shape of the confining potential. In Fig. 4(b), we have plotted an asymmetric quantum well, where the wave functions have been obtained through a numerical solution of the Schrödinger equation. For simplicity, we do not consider the static Hartree effects due to the charge impurities. In this case, we obtain the effective lengths $L_1 = 7.8 \text{ nm}$, $L_{21} = 59 \text{ nm}$, and $L_{21}^{\parallel} = 432 \text{ nm}$. While the effective length of the intrasubband plasmon remains close to the size of confining region for the first wave function $\phi_1(z)$ [$\approx 8 \text{ nm}$, Fig. 4(b)], the intersubband effective lengths are very large as compared to the total size of the potential, 28 nm. Indeed, both L_{21} and L_{21}^{\parallel} are roughly inversely proportional to the overlap between the wave functions $\phi_1(z)$ and $\phi_2(z)$, which in that case is designed to be very small. Furthermore, now that the potential is highly asymmetric, the overlap coefficient in Eq. (80) becomes important: $C_{1,21}^J = 0.88$. This results in a sizable splitting between the intrasubband and in-plane intersubband plasmons, as illustrated in the plot from Fig. 4(b).

D. Longitudinal (Coulomb) projections

The polarization field operator $\hat{\mathbf{P}}$ that was defined in Sec. II B is neither purely transverse nor longitudinal, and as

such it mediates both the retarded and instantaneous interaction between particles in the nonrelativistic PZW Hamiltonian from Eq. (1). Therefore, the collective modes that were described in the previous sections encapsulate both transverse and longitudinal degrees of freedom. The transverse part of $\hat{\mathbf{P}}$ couples to the purely transverse displacement field $\hat{\mathbf{D}}$ to yield new light-coupled plasmon-polariton modes. These will be discussed in Sec. III. The remaining longitudinal part of $\hat{\mathbf{P}}$ describes the instantaneous Coulomb interaction between particles and can couple to quasistatic electric fields, such as those arising in the evanescent near field of metal gratings [25,26] or nanoresonators [9,23,38]. Actually, these quasistatic electric fields can also be described in terms of polarization fields that are associated to the oscillating charges on the metal surfaces [39]. In this section, we illustrate how the longitudinal part of the polarization field and the corresponding dispersion can be derived from our results. To this end, we shall consider only the case of the intrasubband and intersubband excitations of two-level system hosted by infinite homogeneous media. In particular, we shall illustrate how the well known $\sqrt{|\mathbf{q}|}$ dispersion for the intrasubband plasmon is recovered from the almost dispersionless intrasubband mode discussed in Sec. II C 1. A very general treatment including all possible excitations combined with boundary-condition problem for the electromagnetic field will be discussed in Sec. III C 1.

Let us consider an electromagnetic wave perturbation propagating in the system, with a general three-dimensional wave vector \mathbf{Q} . The spatial variations of the wave are provided by the exponential factor

$$e^{i\mathbf{Q}\mathbf{r}} = e^{i\mathbf{q}\mathbf{r}_\parallel} e^{iq_z z}. \quad (87)$$

We have split the wave vector \mathbf{Q} into components \mathbf{q} and q_z that are, respectively, parallel and perpendicular to the 2DEG layer. The longitudinal components of the polarization field are those that are collinear with the propagation vector \mathbf{Q} . In order to isolate the longitudinal excitations, we will work directly with the characteristic tensors from Eqs. (56) and (65). Let us consider the intrasubband characteristic tensor $\xi_{\parallel}^{\text{intra}}(\omega, \mathbf{q})$ [Eq. (56)]. The overlap integral $J_{1,1}$ can be expanded in a Fourier series:

$$J_{1,1} = \int \eta_{11}^2(z) dz = \sum_{q_z} |\tilde{\eta}_{11}(q_z)|^2. \quad (88)$$

Here, $\tilde{\eta}_{11}(q_z)$ is the Fourier component of $\eta_{11}(z)$ with respect to the perpendicular wave vectors q_z . With the above expression, the characteristic tensor $\xi_{\parallel}^{\text{intra}}(\omega, \mathbf{q})$ appears as a sum over both components q_z, \mathbf{q} of the three-dimensional vector \mathbf{Q} . To isolate the longitudinal part, we notice that

$$\frac{\mathbf{Q}(\boldsymbol{\beta}_{\mathbf{q}\mathbf{k}} \otimes \boldsymbol{\beta}_{\mathbf{q}\mathbf{k}})\mathbf{Q}}{Q^2} = \frac{1}{\mathbf{q}^2 + q_z^2}. \quad (89)$$

Indeed, $\mathbf{Q}\boldsymbol{\beta}_{\mathbf{q}\mathbf{k}} = \mathbf{q}\boldsymbol{\beta}_{\mathbf{q}\mathbf{k}} = 1$. By summing only over the longitudinal projection of $(\boldsymbol{\beta}_{\mathbf{q}\mathbf{k}} \otimes \boldsymbol{\beta}_{\mathbf{q}\mathbf{k}})$ and using the well-known result from the distribution theory [40]

$$\sum_{q_z} \frac{|\tilde{\eta}_{11}(q_z)|^2}{q^2 + q_z^2} = \frac{1}{q} \iint dz dz' \eta_{11}(z) \eta_{11}(z') e^{-q|z-z'|}, \quad (90)$$

we arrive at the following expression for the scalar longitudinal component of $\xi_{\parallel}^{\text{intra}}(\omega, \mathbf{q})$:

$$\xi_{\parallel}^{\text{intra}}(\omega, \mathbf{q})|_{ll} = 1 - \sum_{\mathbf{k}} \frac{2\Delta n_{\mathbf{k}\mathbf{q}} \Delta \omega_{\mathbf{k}\mathbf{q}}}{\omega^2 - \Delta \omega_{\mathbf{k}\mathbf{q}}^2} \frac{V_{11,11}(q)}{\hbar}, \quad (91)$$

$$V_{11,11}(q) = \frac{e^2}{\varepsilon \varepsilon_0 S q} \iint dz dz' \eta_{11}(z) \eta_{11}(z') e^{-q|z-z'|}. \quad (92)$$

Here, $V_{11,11}(q)$ is nothing else but the intrasubband matrix element of the Coulomb potential [18]. Clearly, Eqs. (91) and (92) can be used to study the excitations of the system for any excitation wave vector \mathbf{q} at the dipole-dipole order of the Coulomb interaction [3] (see also Sec. III C 1). In particular, taking the long-wavelength limit of Eq. (91) we obtain

$$\xi_{\parallel}^{\text{intra}}(\omega, \mathbf{q})|_{ll} = 1 - \frac{\Omega_{\parallel}^2(\mathbf{q})}{\omega^2}. \quad (93)$$

Here, $\Omega_{\parallel}^2(\mathbf{q})$ is the \mathbf{q} -dependent plasma frequency

$$\begin{aligned} \Omega_{\parallel}^2(\mathbf{q}) &= q\omega_{P\parallel}^2 \frac{\iint dz dz' \eta_{11}(z) \eta_{11}(z') e^{-q|z-z'|}}{J_{1,1}} \Big|_{q \rightarrow 0} \\ &\approx q\omega_{P\parallel}^2 \frac{\int dz dz' \eta_{11}(z) \eta_{11}(z')}{J_{1,1}} \\ &= \frac{e^2}{m^* \varepsilon \varepsilon_0} |\mathbf{q}|. \end{aligned} \quad (94)$$

We therefore recover the longitudinal intrasubband mode of the 2DEG with a square-root wavelength dispersion $\Omega_{\parallel}(\mathbf{q}) \propto \sqrt{|\mathbf{q}|}$.

Furthermore, let us also examine the formal limit of the expression $\Omega_{\parallel}^2(\mathbf{q})$ at very large wave vectors $q \rightarrow \infty$. In this case, $q e^{-q|z-z'|} \rightarrow \delta(z-z')$ and therefore we have the asymptotic expression

$$\Omega_{\parallel}^2(\mathbf{q})|_{q \rightarrow \infty} \rightarrow \omega_{P\parallel}^2. \quad (95)$$

This expression remains valid as long as the plasma frequency $\omega_{P\parallel}$ is far from the particle-hole continuum of uncoupled excitations $\Delta \omega_{\mathbf{k}\mathbf{q}}$. Indeed, for wave vectors beyond the light cone, the intrasubband excitation considered in Sec. II C 1 is a purely longitudinal excitation.

Similar considerations apply also for the intrasubband plasmon mode described by Eq. (65). For the sake of illustration, we shall consider only the z component with characteristic function $\xi_{zz}(\omega, \mathbf{q})$. In this case, we compute the Fourier components of the overlap integral

$$I_{21,21} = \sum_{q_z} |\tilde{\xi}_{21}(q_z)|^2. \quad (96)$$

Now, $\tilde{\xi}_{21}(q_z)$ is the Fourier component of the intersubband current density $\xi_{21}(z)$. Furthermore, we use the projection identity

$$\frac{\mathbf{Q}(\mathbf{e}_z \otimes \mathbf{e}_z)\mathbf{Q}}{Q^2} = \frac{q_z^2}{\mathbf{q}^2 + q_z^2}. \quad (97)$$

We must then sum up the Fourier integral that appears in the longitudinal projection of $\zeta_{zz}(\omega, \mathbf{q})$:

$$\begin{aligned} & \sum_{q_z} \frac{q_z^2 |\tilde{\xi}_{21}(q_z)|^2}{\mathbf{q}^2 + q_z^2} \\ &= \frac{1}{q} \iint dz dz' \partial_z \xi_{21}(z) \partial_z \xi_{21}(z') e^{-q|z-z'|} \\ &= \frac{4m^{*2} \Delta\omega_{21}}{\hbar^2 q} \iint dz dz' \eta_{21}(z) \eta_{21}(z') e^{-q|z-z'|}. \end{aligned} \quad (98)$$

The second line of Eq. (98) is obtained by noticing that $q_z \tilde{\xi}_{21}(q_z)$ is the Fourier image of $\partial_z \xi_{21}(z)$, and the third line by using Eq. (204). We can then cast the longitudinal projection of the z component in the form

$$\zeta_{zz}(\omega, \mathbf{q})_{||} = 1 - \frac{V_{21,21}(q)}{2\hbar} \sum_{\mathbf{k}} \frac{\Delta\omega_{21}^2 \Delta n_{\mathbf{kq}21}}{\Delta\omega_{\mathbf{kq}21}(\omega^2 - \Delta\omega_{\mathbf{kq}21}^2)}. \quad (99)$$

Here, $V_{21,21}(q)$ has the same expression as Eq. (92) with $\eta_{21}(z)$ instead of $\eta_{11}(z)$. The long-wavelength limit of Eq. (99) then coincides with Eq. (66), as we have the following identity (see Ref. [4], Appendix C):

$$\omega_{P21}^2 = \frac{V_{21,21}(q \rightarrow 0) \Delta\omega_{21} N_e}{2\hbar}. \quad (100)$$

We see that the intersubband plasmon becomes a purely longitudinal mode at very small wave vectors. Indeed, this is the reason why the intersubband transitions can not couple to a normally incident light [34]. Using the same method, we can show that longitudinal projection of the in-plane intrasubband plasmon is provided a very similar expression as (99), and the only difference is that the square $\Delta\omega_{21}^2$ is replaced with the square of the change in the kinetic energy $\hbar\mathbf{q}(2\mathbf{k} + \mathbf{q})/m^*$. It is therefore clear that the in-plane intrasubband plasmon has a vanishing contribution to the longitudinal part of the characteristic tensor (65).

Note also that, as the wave vector \mathbf{q} increases, the Coulomb matrix element $V_{21,21}(q)$ tends to zero, as it becomes proportional to the square of the overlap integral between two orthogonal wave functions $\int \eta_{21}(z) dz$ and therefore we would expect a red-shift of the plasmon mode at higher wave vectors. This analysis must be completed also considering the intra-inter subband coupling; however, we refer to the very general multitransition case discussed in Sec. III C 1.

These results are graphically summarized in the diagram of Fig. 5, where we have sketched the dispersion-less plasmon modes obtained in the previous paragraph together with their longitudinal projections, as well as the one-particle solutions of the characteristic tensors. Clearly, beyond the light cone described with the equation $\omega = cq/\sqrt{\epsilon}$, only the longitudinal projections should be considered. The interaction of the collective modes with the transverse photon field inside the light cone gives rise to mixed polariton modes, as described in Sec. III. For instance, this coupling at the frequency of the intrasubband plasmon is responsible for a free-carrier absorption at the frequency $\omega_{P||}$. In a similar way, the coupling of the intrasubband plasmon with light for finite wave vectors $q \neq 0$ gives rise to an absorption resonance at a frequency $\tilde{\omega}_{21}$.

Note that the diagram in Fig. 5 holds only for the case of electromagnetic waves in free space, and will generally be different depending on the boundary conditions for the electromagnetic field. However, the dispersionless collective modes derived in the previous paragraph, together with the one-particle solutions of the characteristic tensors, are universal. As shown in the previous section, these modes have a simpler structure than, for instance, the longitudinal modes obtained by working directly with the Coulomb potential in the minimal coupling representation [41].

Once the full set of the electromagnetic modes are known for a particular geometry, we can define longitudinal and transverse projections of the ‘‘universal’’ collective modes, in order to work out the corresponding polariton and quasistatic excitations. In practice, we can work with a finite set of electromagnetic modes to obtain reasonable approximations. This approach is very convenient in the case of confined geometries, where there are usually only a few electromagnetic modes that resonate closely to the frequencies of the collective electronic modes. In Sec. III C, we provide a systematic method to obtain such modal development based on the inverse PZW transformation. In the case where surface waves are present they can be treated in a similar approach as the one employed for the surface plasmon polariton in Ref. [3].

E. General case of multiple subbands

We now turn to a more general case where several subbands can be occupied. In this case, the Fermi level of the gas lies higher than at least two discrete energy levels of the bounding potential $V(z)$. In particular, we will be interested in the interaction of such systems with light, which will be considered in the next part. As the single-particle excitations carry very low oscillator strength, we will exclude them from our discussion, and we will consider only the collective plasmon modes described in the previous paragraph.

In such system with several occupied subbands, each occupied subband yields an intrasubband plasmon, and each pair of subbands $j > i$ gives rise to two intersubband plasmons. The self-polarization term $\hat{\mathbf{P}}^2$ then induces coupling between

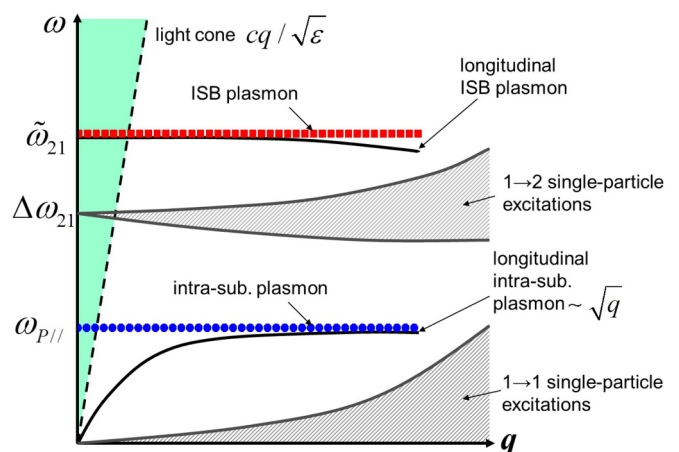


FIG. 5. (Color online) Sketch of the excitation diagram of a two-subband system (not at scale). The dispersionless intersubband and intrasubband plasmons are traced, respectively, in squares and circles, and their Coulomb projections in continuous curves.

the plasmons issued from different subbands or subband pairs, as well as couplings between the intrasubband and in-plane intersubband plasmons. Our formalism then allows us to reduce the problem into a finite number of coupled quantum harmonic oscillators [4,8,42], which can therefore be diagonalized numerically.

For simplicity, and as we are interested in the interaction of the collective plasmonic modes with light, in the following discussion we shall neglect the contribution of the in-plane intersubband plasmon, as well as its interaction with the intrasubband plasmons. Indeed, the in-plane intrasubband plasmon is intrinsically a dark mode with a very low oscillator strength. This can be understood by considering its contribution to the polarization field $\hat{P}_{\parallel|\text{inter}}$, as described by Eq. (39) or (76). Since the coupling with light is provided by the linear term $\hat{\mathbf{D}} \cdot \hat{\mathbf{P}}$ of the PZW Hamiltonian (1), the coupling constant between the in-plane intersubband plasmon and the electromagnetic field is proportional to the overlap integral

$$\int f(z)\eta_{\alpha}(z)dz = \int f(z)\phi_i(z)\phi_j(z)dz, \quad i > j. \quad (101)$$

Here, $f(z)$ is a function that describes the spatial variations of the displacement field $\hat{\mathbf{D}}$ along the z direction. The typical scale of variation of $f(z)$ is the wavelength of light, which is much larger than the scale of the typical confined electronic wave functions. As the function $f(z)$ varies slowly compared to the product $\phi_i(z)\phi_j(z)$ we can take it out from the integral sign, and the remaining integral vanishes owing to the orthogonality of the wave functions $\phi_i(z)$ and $\phi_j(z)$.

Even if the coupling of the in-plane intersubband plasmon with light is negligible, it could still influence the optical properties of the system through its coupling with the bright intrasubband plasmon. We already saw that this coupling is zero in the two-subband case, for a confining potential that has an inversion symmetry. This argument can be extended in the multiple subband case. Indeed, the first term in Eq. (45) can be expressed from the overlap integrals (49):

$$J_{\alpha j'} = \int \eta_{\alpha}(z)\eta_{j'}(z)dz = \int \phi_i(z)\phi_j(z)\phi_{j'}^2(z)dz, \quad i > j. \quad (102)$$

As the wave functions $\phi_i(z)$ form an orthogonal set, it is clear that the overlap integrals $J_{\alpha j'}$ will take generally very small, although finite values. Furthermore, if the confining potential has an inversion symmetry, then the wave functions have a well-defined parity and Eq. (102) is zero for wave functions $i > j$ with different parities. The term Eq. (102) can then become influential only in the case where $\phi_i(z)$ and $\phi_j(z)$ have the same parity, that is, for instance, for nonconsecutive transitions. This case can be achieved for high doping levels. We can, however, observe that, even for an asymmetric potential, such as the one described in Fig. 4(b), the range of doping levels where the coupling is significant is limited. We see that there are a number of situations where the coupling between the in-plane intersubband plasmon and the intrasubband plasmon can be ignored, and therefore we discard that coupling in the following discussion. Nevertheless, our formalism allows recovering the optical response of the system when this coupling is not zero, if needed.

Under the above assumptions, the collective behavior of the gas is described by plasma oscillations that are well separated as intersubband plasmons in the direction of confinement (z axis) and intrasubband plasmons in the (x, y) plane. The effective matter Hamiltonian is expressed from the collective excitations only:

$$\mathcal{H}_e + \frac{1}{2\epsilon\epsilon_0} \int \hat{\mathbf{P}}^2 d^3\mathbf{r} \rightarrow \mathcal{H}_{\text{coll}}^{\text{inter}} + \mathcal{H}_{\text{coll}}^{\text{intra}}. \quad (103)$$

The intersubband Hamiltonian $\mathcal{H}_{\text{coll}}^{\text{inter}}$ contains only the $\hat{P}_z|_{\text{inter}}$ component of the polarization field, while the intrasubband Hamiltonian $\mathcal{H}_{\text{coll}}^{\text{intra}}$ only the $\hat{\mathbf{P}}_{\parallel|\text{intra}}$ component. The Hamiltonian describing the intersubband plasmons $\mathcal{H}_{\text{coll}}^{\text{inter}}$ was already considered in Refs. [4,8]. We shall reproduce briefly the discussion in those references for completeness. The square-polarization term $\hat{P}_z|_{\text{inter}}^2$ now involves both contributions from the same subband pair α , together with cross terms from different subbands pairs $\alpha \neq \beta$. The polarization self-energies arising from the same transition α are combined with the electronic part to define collective intersubband plasmon operators $p_{q\alpha}^{\dagger}$ as in Sec. II C. The polarization field $\hat{P}_z|_{\text{inter}}$ is now expressed only from these collective contributions:

$$\hat{P}_z|_{\text{inter}} = - \sum_{q\alpha} \xi_{\alpha}(z) \sqrt{\frac{\omega_{P\alpha}^2}{2\tilde{\omega}_{\alpha}} \frac{\hbar\epsilon\epsilon_0}{SI_{\alpha,\alpha}}} e^{-i\mathbf{q}\mathbf{r}_{\parallel}} (p_{q\alpha}^{\dagger} + p_{-q\alpha}). \quad (104)$$

Here, all definitions are identical to the ones in Sec. II C, by replacing the indexes “21” with “ α .” The plasma frequencies $\omega_{P\alpha}$ are also defined as in Sec. II C [Eq. (70)]:

$$\omega_{P\alpha}^2 = \frac{e^2 \Delta N_{\alpha}}{m^* \epsilon \epsilon_0 S L_{\alpha}}, \quad L_{\alpha} = \frac{2m^* \Delta \omega_{21}}{\hbar I_{\alpha,\alpha}} \quad (105)$$

except that now we have the population difference between the subbands ΔN_{α} instead of the total number of electrons N_e . With all the self-energy polarization terms diagonalized, the remaining contributions from the square-polarization term in $\mathcal{H}_{\text{coll}}^{\text{inter}}$ arise from the interactions between distinct pairs of subbands $\alpha \neq \beta$:

$$\mathcal{H}_{\text{coll}}^{\text{inter}} = \sum_{q\alpha} \hbar \tilde{\omega}_{\alpha} p_{q\alpha}^{\dagger} p_{q\alpha} + \sum_{q\alpha \neq \beta} C_{\alpha\beta}^I \frac{\hbar \omega_{P\alpha} \omega_{P\beta}}{4\sqrt{\tilde{\omega}_{\alpha} \tilde{\omega}_{\beta}}} \times (p_{q\alpha}^{\dagger} + p_{-q\alpha})(p_{-q\beta}^{\dagger} + p_{q\beta}), \quad (106)$$

$$C_{\alpha\beta}^I = \frac{I_{\alpha,\beta}}{\sqrt{I_{\alpha,\alpha} I_{\beta,\beta}}}. \quad (107)$$

This equation describes an ensemble of coupled intersubband plasmon modes. The advantage of this representation is that now we can choose a finite number of subbands that describe the problem, which renders the diagonalization of the Hamiltonian (106) a well-defined numerical problem. A complete analytical solution would be possible only in the case where all coupling coefficients $C_{\alpha\beta}^I$ are identical [4]. This is approximately the case for the consecutive transitions of a square quantum well [8,15]. When the remaining plasmon-plasmon interaction is diagonalized away, the Hamiltonian (106) is decomposed into a sum of independent intersubband

plasmon modes, which mix plasmons from different subbands:

$$\mathcal{H}_{\text{coll}}^{\text{inter}} = \sum_{\mathbf{q}K} \hbar \Omega_K P_{\mathbf{q}K}^\dagger P_{\mathbf{q}K}. \quad (108)$$

The new operators $P_{\mathbf{q}K}^\dagger$ are linear combinations of the old ones:

$$P_{\mathbf{q}K}^\dagger = \sum_{\alpha} (m_{\alpha K} P_{\mathbf{q}\alpha}^\dagger + h_{\alpha K} P_{-\mathbf{q}\alpha}). \quad (109)$$

The Hopfield coefficients $m_{\alpha K}$, $h_{\alpha K}$ and the new collective frequencies Ω_K are obtained from a numerical Hopfield-Bogoliubov procedure, and it can be shown that they are real [42]. For a particular physical problem, one always retains a finite number of intersubband pairs α , then the Hopfield-Bogoliubov procedure will deliver the same number of uncoupled plasmons $P_{\mathbf{q}K}^\dagger$. Equation (109) can then be inverted to express the old operators $p_{\alpha\mathbf{q}}^\dagger$ as a function of new ones $P_{\mathbf{q}K}^\dagger$:

$$\begin{aligned} p_{\mathbf{q}\alpha}^\dagger + P_{-\mathbf{q}\alpha} &= \sum_K (m_{\alpha K} + h_{\alpha K})^{-1} (P_{\mathbf{q}K}^\dagger + P_{-\mathbf{q}K}) \\ &= \sum_K M_{\alpha K}^{-1} (P_{\mathbf{q}K}^\dagger + P_{-\mathbf{q}K}). \end{aligned} \quad (110)$$

We introduced here the square matrix $M_{\alpha K} = m_{\alpha K} + h_{\alpha K}$ constructed from the Hopfield coefficients. This relation allows us to express the collective electronic polarization in Eq. (104) as a function of the new collective operators:

$$\hat{P}_z|_{\text{inter}} = -\sqrt{\frac{\hbar \varepsilon \varepsilon_0}{2S}} \sum_{\mathbf{q}K} \frac{\Xi_K(z) e^{-i\mathbf{q}\mathbf{r}_\parallel}}{\sqrt{\Omega_K}} (P_{\mathbf{q}K}^\dagger + P_{-\mathbf{q}K}), \quad (111)$$

$$\Xi_K(z) = \sum_{\alpha} M_{\alpha K}^{-1} \xi_{\alpha}(z) \omega_{P\alpha} \sqrt{\frac{\Omega_K}{\tilde{\omega}_{\alpha} I_{\alpha,\alpha}}}. \quad (112)$$

The function $\Xi_K(z)$ is expressed as a linear combination of the intersubband microcurrents $\xi_{\alpha}(z)$, and therefore can be interpreted as the ‘‘microcurrent’’ of the new collective mode K [8]. It allows us to express the light-matter coupling constant for intersubband plasmons, as described in the next part. An experimental example of a collective mode that arises from the interaction of several intersubband plasmons is provided in Ref. [15]. In particular, the bright plasmon mode that appears in a parabolic quantum well according to the Kohn theorem [43–45] is another example of that kind [15].

The intrasubband part of the Hamiltonian (103) is treated in the same way. Generalizing the notations from Sec. II C for the multisubband case, we can express $\mathcal{H}_{\text{coll}}^{\text{intra}}$ as a sum of interacting intrasubband plasmons arising from different subbands i :

$$\begin{aligned} \mathcal{H}_{\text{coll}}^{\text{intra}} &= \sum_{\mathbf{q}ni} \hbar \omega_{iP}^{\parallel} \pi_{\mathbf{q}ni}^\dagger \pi_{\mathbf{q}ni} + \sum_{\mathbf{q}ni \neq j} C_{ij}^J \frac{\hbar \sqrt{\omega_{iP}^{\parallel} \omega_{jP}^{\parallel}}}{4} \\ &\times (\pi_{\mathbf{q}ni}^\dagger + \pi_{-\mathbf{q}ni}) (\pi_{-\mathbf{q}nj}^\dagger + \pi_{\mathbf{q}nj}), \end{aligned} \quad (113)$$

$$C_{ij}^J = \frac{J_{i,j}}{\sqrt{J_{i,i} J_{j,j}}}. \quad (114)$$

Here, $\mathbf{n} = (\mathbf{n}_1, \mathbf{n}_2)$ is a basis in the (x, y) plane and the plasma frequencies are defined as in Sec. II C:

$$(\omega_{iP}^{\parallel})^2 = \frac{e^2 N_i}{m^* \varepsilon \varepsilon_0 S L_i}, \quad L_i = 1/J_{i,i}. \quad (115)$$

Now, N_i is the electronic population in the subband i . The Hamiltonian $\mathcal{H}^{\text{intra}}$ can be further diagonalized into a sum of independent plasmon modes with frequencies W_L :

$$\mathcal{H}_{\text{coll}}^{\text{intra}} = \sum_{\mathbf{q}nL} \hbar W_L \Pi_{\mathbf{q}nL}^\dagger \Pi_{\mathbf{q}nL}, \quad (116)$$

$$\Pi_{\mathbf{q}nL}^\dagger = \sum_i (l_{iL} \pi_{\mathbf{q}ni}^\dagger + g_{iL} \pi_{-\mathbf{q}ni}). \quad (117)$$

Let us introduce the matrix constructed from the Hopfield coefficients

$$N_{Li} = l_{iL} + g_{iL}. \quad (118)$$

Then, the polarization field is expressed, respectively,

$$\hat{\mathbf{P}}_{\parallel}|_{\text{intra}} = -i \sqrt{\frac{\hbar \varepsilon \varepsilon_0}{2S}} \sum_{\mathbf{q}nK} \sqrt{W_L} \Upsilon_L(z) e^{-i\mathbf{q}\mathbf{r}_\parallel} \mathbf{n} (\Pi_{\mathbf{q}nK}^\dagger + \Pi_{-\mathbf{q}nL}), \quad (119)$$

$$\Upsilon_L(z) = \sum_i N_{Li}^{-1} \eta_{ii}(z) \sqrt{\frac{\omega_{Pi}^{\parallel}}{W_L J_{i,i}}}. \quad (120)$$

This expression will be used in the next part to study the coupling of the collective excitations of the gas with light.

Before concluding this section, let us provide an example of a collective intrasubband excitation that combines intrasubband plasmons from different subbands. Consider an infinite square quantum well, like the one in Sec. II C 3. Using the expressions of the wave functions $\phi_i(z)$ provided in that section, it is straightforward to show that all the coefficients $J_{i,i}$ are identical: $J_{i,i} = 3/2L_{\text{QW}}$. Furthermore, the cross-correlation coefficients $J_{i,j}, i \neq j$ are also identical: $J_{i,j} = 1/L_{\text{QW}}$. In that case, $C_{ij}^J = \frac{2}{3}$, and the Hamiltonian (113) falls into the one of the cases described in Appendix A where analytical diagonalization becomes possible. Relying on the results from Appendix A, we can write the characteristic equation that provides the new collective frequencies:

$$1 = \sum_i \frac{2}{3} (\omega_{iP}^{\parallel})^2 \frac{1}{W_L^2 - (\omega_{iP}^{\parallel})^2/3}. \quad (121)$$

Equations of such type were already encountered in Ref. [3]. As discussed in that reference, a general property of such equation is that if the number of individual contributions i is sufficiently high, then we can isolate a single collective solution, which is far from the individual plasma frequencies ω_{iP}^{\parallel} and sums coherently all the plasma contributions:

$$\begin{aligned} W_{L\text{max}}^2 &\approx \sum_i \frac{2}{3} (\omega_{iP}^{\parallel})^2 \\ &= \frac{e^2}{m^* \varepsilon \varepsilon_0 L_{\text{QW}} S} \sum_i N_i = \frac{e^2 N_e}{m^* \varepsilon \varepsilon_0 L_{\text{QW}} S}. \end{aligned} \quad (122)$$

Here, N_e is the total number of electrons in the system. Therefore, in the limit of a large number of occupied subbands, we obtain the classical plasma frequency, as should be expected. Our microscopic model then correctly recovers the case of a classical three-dimensional plasma.

III. COUPLING BETWEEN A 2DEG AND A PLANAR METALLIC WAVEGUIDE

A. Light-matter coupling Hamiltonian

We now investigate the coupling of the collective excitations of the gas, described in the previous section, with the transverse photons in a confined geometry. For this purpose, we choose a photonic structure that has a translational symmetry identical to that of the heterostructure potential that confines the electron gas. This structure is the planar metallic waveguide, which consists of two perfectly conducting mirrors, perpendicular to the z axis and separated by a distance L . This arrangement, that shall be called in the following “double-metal” (DM) waveguide, is well known from quantum optics [46,47] and far-infrared optoelectronics [48]. In this geometry, light propagates in the in-plane direction with a planar wave vector \mathbf{q} , whereas it vibrates in a sinusoidal standing wavelike patterns along the z direction. We shall suppose that the waveguide is filled with a homogeneous medium with a real dielectric constant ε , that plays the role of a host for the 2D electron gas. The interaction of the gas with the guided modes is described by the nonmagnetic PZW Hamiltonian from Eq. (1), and according to the general properties of the PZW representation, we need to express the transverse electromagnetic field vectors $\hat{\mathbf{D}}$ and $\hat{\mathbf{H}}$ independently from polarization field of the gas $\hat{\mathbf{P}}$. The diagonalization of the full Hamiltonian in Eq. (1) then will provide the coupled plasmon-polariton modes of the system, both in the intersubband and intrasubband cases, as well as the corresponding effective dielectric constants. The PZW approach, illustrated here for this particular geometry, can then be generalized to more complex situations.

Taking of the conceptual simplicity of the DM waveguide, our motivation is to provide the most general light-matter coupling Hamiltonian of the problem, which takes into account all possible waveguide modes. As these modes constitute a complete orthonormal set, we obtain a complete treatment of an electromagnetic problem with boundary conditions. The importance of such multimode treatment has been already outlined by previous authors [30], in the context of a semiclassical description of the electromagnetic field. In the present case, we adopt a fully quantum-mechanical description, by discarding dissipation effects [49]. This general formulation will allow us to relate to previous results that were established by a single-mode approximation [4]. More generally, the full multimode treatment will enable us to study the correspondence between our PZW model and the minimal-coupling representation of the full electromagnetic Hamiltonian, as shall be outlined in Sec. III C. In particular, we will show that this approach leads to a longitudinal Coulomb potential, that takes into account automatically the boundary conditions imposed by the cavity walls. Such investigation is important in the context of light-matter coupled systems operating in the ultrastrong

light-matter coupling regime, where the image effects of the dipole-dipole forces can no longer be ignored owing to the increased density of interacting particles. More generally, such a study is pertinent in the context of quantum optics problems with condensed matter systems, where the full electromagnetic Hamiltonian, including both the square-vector potential term and the Coulomb potential, must be taken into account [12,14].

The modes of a perfect mirror DM waveguide break into “transverse magnetic” (TM) and “transverse electric” (TE) polarized modes [50]. The TM modes have nonzero z component of the electric field, whereas the TE have nonzero z component of the magnetic field. The modal dispersion of both kinds of modes depends on two quantum numbers m and \mathbf{q} and is described by the unique formula

$$\varepsilon \frac{\omega_{cm\mathbf{q}}^2}{c^2} = \mathbf{q}^2 + \frac{\pi^2 m^2}{L^2}. \quad (123)$$

Here, $\omega_{cm\mathbf{q}}$ is the frequency of the guided mode and m is an integer describing the confinement in the z direction; $m > 0$ for TE modes and $m \geq 0$ for TM modes. We will make use of the lateral wave vector

$$k_{zm} = \frac{\pi m}{L}, \quad (124)$$

which describes the standing-wave patterns of the modes in the z direction. These patterns are expressed through the normalized functions

$$u_m(z) = \sqrt{\frac{2}{1 + \delta_{0m}}} \cos(k_{zm} z) \quad (125)$$

and their derivatives, that are nonzero for $m > 0$:

$$w_m(z) = \frac{1}{k_{zm}} \frac{du_m}{dz} = \sqrt{2} \sin(k_{zm} z). \quad (126)$$

The electromagnetic field components are expressed in an orthonormal basis ($\mathbf{e}_q, \mathbf{e}_\perp, \mathbf{e}_z$), where \mathbf{e}_z is the unit vector of the z axis, $\mathbf{e}_q = \mathbf{q}/q$, and $\mathbf{e}_\perp = \mathbf{e}_q \wedge \mathbf{e}_z$. The field operators are expressed in terms of creation and annihilation operators a_{qmh}^\dagger, a_{qmh} , and a_{qme}^\dagger, a_{qme} for each waveguide mode m, \mathbf{q} . The index h stands for the TM modes, and e stands for the TE modes. The full expressions of the quantized electromagnetic fields operators, that describe the displacement field $\hat{\mathbf{D}}$, the magnetic field $\hat{\mathbf{H}}$, and the vector potential $\hat{\mathbf{A}}$, are then

$$\hat{D}_{hz} = i \sum_{qm} A_{qm} \frac{q u_m(z)}{\omega_{cm\mathbf{q}}} e^{i\mathbf{q}\mathbf{r}_\parallel} (a_{qmh} - a_{-qmh}^\dagger), \quad (127)$$

$$\hat{D}_{h\parallel} = - \sum_{qm} A_{qm} \frac{\mathbf{e}_q k_{zm} w_m(z)}{\omega_{cm\mathbf{q}}} e^{i\mathbf{q}\mathbf{r}_\parallel} (a_{qmh} - a_{-qmh}^\dagger), \quad (128)$$

$$\hat{H}_{h\perp} = i \sum_{qm} A_{qm} \mathbf{e}_\perp u_m(z) e^{i\mathbf{q}\mathbf{r}_\parallel} (a_{qmh} + a_{-qmh}^\dagger), \quad (129)$$

$$\hat{A}_{hz} = \sum_{qm} \frac{A_{qm}}{\varepsilon \varepsilon_0} \frac{q u_m(z)}{\omega_{cm\mathbf{q}}^2} e^{i\mathbf{q}\mathbf{r}_\parallel} (a_{qmh} + a_{-qmh}^\dagger), \quad (130)$$

$$\hat{A}_{h\parallel} = i \sum_{qm} \frac{A_{qm}}{\varepsilon \varepsilon_0} \frac{\mathbf{e}_q k_{zm} w_m(z)}{\omega_{cm\mathbf{q}}^2} e^{i\mathbf{q}\mathbf{r}_\parallel} (a_{qmh} + a_{-qmh}^\dagger) \quad (131)$$

for the TM modes. These expressions are valid only in the dielectric slab, as the fields will be considered as identically zero in the metal (see the discussion in the end of this section). For TE modes, we have

$$\hat{\mathbf{D}}_{e\perp} = \sum_{\mathbf{qm}} A_{\mathbf{qm}} \frac{\sqrt{\varepsilon}}{c} \mathbf{e}_{\perp} w_m(z) e^{i\mathbf{q}\mathbf{r}_{\parallel}} (a_{\mathbf{q}me} - a_{-\mathbf{q}me}^{\dagger}), \quad (132)$$

$$\hat{H}_{ez} = \sum_{\mathbf{qm}} A_{\mathbf{qm}} \frac{cq}{\sqrt{\varepsilon}\omega_{c\mathbf{m}\mathbf{q}}} w_m(z) e^{i\mathbf{q}\mathbf{r}_{\parallel}} (a_{\mathbf{q}me} + a_{-\mathbf{q}me}^{\dagger}), \quad (133)$$

$$\hat{\mathbf{H}}_{e\parallel} = -i \sum_{\mathbf{qm}} A_{\mathbf{qm}} \frac{ck_{zm}}{\sqrt{\varepsilon}\omega_{c\mathbf{m}\mathbf{q}}} \mathbf{e}_{\mathbf{q}} u_m(z) e^{i\mathbf{q}\mathbf{r}_{\parallel}} (a_{\mathbf{q}me} + a_{-\mathbf{q}me}^{\dagger}), \quad (134)$$

$$\hat{\mathbf{A}}_{e\perp} = -i \sum_{\mathbf{qm}} \frac{A_{\mathbf{qm}}}{\varepsilon\varepsilon_0} \frac{\sqrt{\varepsilon}}{c\omega_{c\mathbf{m}\mathbf{q}}} \mathbf{e}_{\perp} w_m(z) e^{i\mathbf{q}\mathbf{r}_{\parallel}} (a_{\mathbf{q}me} + a_{-\mathbf{q}me}^{\dagger}). \quad (135)$$

We have used unique normalization constant for both types of modes:

$$A_{\mathbf{qm}} = \sqrt{\frac{\hbar\omega_{c\mathbf{m}\mathbf{q}}}{2\mu_0 SL}}. \quad (136)$$

The free-field Hamiltonians are, respectively,

$$\begin{aligned} \mathcal{H}_{\text{ph}}^h &= \int \left[\frac{\hat{D}_{hz}^2 + \hat{\mathbf{D}}_{h\parallel}^2}{2\varepsilon_0\varepsilon} + \frac{\mu_0 \hat{\mathbf{H}}_{h\perp}^2}{2} \right] d^3\mathbf{r} \\ &= \sum_{\mathbf{qm}} \hbar\omega_{c\mathbf{m}\mathbf{q}} \left(a_{\mathbf{q}mh}^{\dagger} a_{\mathbf{q}mh} + \frac{1}{2} \right), \end{aligned} \quad (137)$$

$$\begin{aligned} \mathcal{H}_{\text{ph}}^e &= \int \left[\frac{\hat{\mathbf{D}}_{e\perp}^2}{2\varepsilon_0\varepsilon} + \frac{\mu_0 (\hat{H}_{ez}^2 + \hat{\mathbf{H}}_{e\parallel}^2)}{2} \right] d^3\mathbf{r} \\ &= \sum_{\mathbf{qm}} \hbar\omega_{c\mathbf{m}\mathbf{q}} \left(a_{\mathbf{q}me}^{\dagger} a_{\mathbf{q}me} + \frac{1}{2} \right). \end{aligned} \quad (138)$$

Before providing the coupling of the waveguide modes of the DM resonator with light, let us discuss the physical meaning of the displacement field $\hat{\mathbf{D}}$ from the point of view of the PZW representation. In that representation, and for globally charge neutral system the field $-\hat{\mathbf{D}}$ plays the role of conjugate momentum to the vector potential $\hat{\mathbf{A}}$, and therefore it is required that $\hat{\mathbf{D}}$ is a purely transverse field [2]. It is clear from Eq. (132) that this is the case for the TE-polarized modes, as the only nonzero component $\hat{\mathbf{D}}_{e\perp}$ has a zero divergence. Indeed, each contribution in Eq. (132) points along the \mathbf{e}_{\perp} direction, whereas the spatial variations of the field arise from the directions $\mathbf{e}_{\mathbf{q}}$ and \mathbf{e}_z . Furthermore, the field $\hat{\mathbf{D}}_{e\perp}$ vanishes identically on the metal walls.

The fact that $\hat{\mathbf{D}}$ also has a zero divergence for the TM modes seems less evident. Let us consider the lowest-order ($m=0$) TM_0 mode, for which according to Eqs. (127) and (128) the only nonvanishing component of displacement vector is the z component:

$$\hat{D}_{hz}|_{m=0} = i \sum_{\mathbf{q}} \frac{A_{\mathbf{q}0} \sqrt{2\varepsilon}}{c} \chi_{[0,L]}(z) e^{i\mathbf{q}\mathbf{r}_{\parallel}} (a_{\mathbf{q}0h} - a_{-\mathbf{q}0h}^{\dagger}). \quad (139)$$

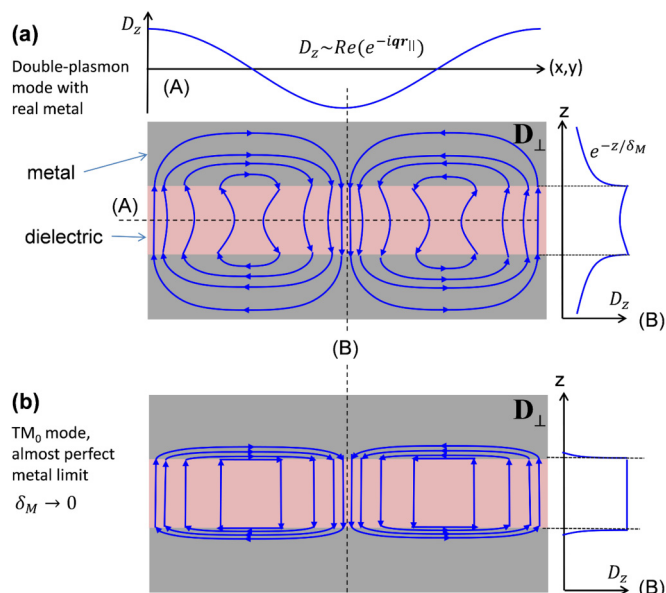


FIG. 6. (Color online) Transverse field \mathbf{D} of the lowest-frequency symmetric guided mode from nonperfect (a) and almost perfect (b) metal-dielectric-metal waveguide. Here, δ_M indicates the penetration depth of the mode into the metal walls, that is identically zero for a perfect metal.

Here, the function $\chi_{[0,L]}(z) = 1$ when z runs inside the dielectric slab and $\chi_{[0,L]}(z) = 0$ everywhere else. Since the function $\chi_{[0,L]}(z)$ is discontinuous at the metal walls it might seem that $\text{div} \hat{D}_{hz}|_{m=0} = \partial \hat{D}_{hz}|_{m=0} / \partial z$ is not zero everywhere in space, but has instead a very strong value at the metal walls. This, however, is not true; indeed, consider the situation where the metal is not perfect but behaves instead as a three-dimensional electronic plasma with some finite plasma frequency. In that case, the field penetrates into the metal [Fig. 6(a)], furthermore, the lowest-order symmetric guided mode can be seen as a combination of two surface plasmon waves [51,52]. Solving the classical electromagnetic problem with the usual boundary conditions one finds that the classical displacement field \mathbf{D} has zero divergence everywhere in space, and its force lines are closed loops, like the one sketched in Fig. 6(a). (This mode can also be described quantum mechanically by using the microscopic model of the 3D gas from Ref. [3].) As the field decays exponentially into the metal with a characteristic skin depth δ_M the force lines extend inside the metal over a distance δ_M . The classical analysis indicates that, in the case of an almost perfect metal, $\delta_M \rightarrow 0$ and the force lines are strongly compressed around the metal-dielectric interface, as illustrated in Fig. 6(b). Nevertheless, the force lines of \mathbf{D} are still closed loops, and we have $\text{div} \mathbf{D} = 0$ everywhere in space. Finally, in the perfect metal case all force lines run only on the surface of the metal walls. This is the sense in which Eqs. (127), (128), and (139) should be understood as describing a purely transverse field.

Furthermore, the requirement that the force lines of \mathbf{D} are closed loops leads to the fact that the propagation vector \mathbf{q} can never be zero. To show this, let us take the case of the TM_0 mode, where the force lines running in the dielectric slab are all parallel to the z axis. Consider then a particular line pointing upwards while in the dielectric, at a position x_0 , then

necessarily it is closed by a line running downwards in some further position, say $x_0 + \delta x$. The maximum such distance δx corresponds to the spatial wave vector $q = \pi/\delta x$ which is then necessarily nonzero, although it can be rendered arbitrarily small in an infinite waveguide. We recover once again the fact that the displacement vector \mathbf{D} describes a purely transverse, propagating field as required by the PZW representation.

We are now in a position to express the nonmagnetic PZW Hamiltonian (1) for the coupling between the 2D electron gas with the guided modes of the DM structure. We consider only the collective excitations of the gas which, according to the results from the previous sections, are the only ones to have a nonvanishing contribution to the polarization field of the gas. The PZW Hamiltonian of our system then becomes

$$\mathcal{H} = \mathcal{H}_{\text{ph}}^h + \mathcal{H}_{\text{ph}}^e + \mathcal{H}_{\text{coll}}^{\text{inter}} + \mathcal{H}_{\text{coll}}^{\text{intra}} + \mathcal{H}_{\text{int}}^h|_{\text{inter}} + \mathcal{H}_{\text{int}}^h|_{\text{intra}} + \mathcal{H}_{\text{int}}^e. \quad (140)$$

Here, we have split the interaction terms according to the polarization of the guided modes:

$$\mathcal{H}_{\text{int}}^h|_{\text{inter}} = -\frac{1}{\varepsilon\varepsilon_0} \int \hat{\mathbf{D}}_{hz} \hat{\mathbf{P}}_z|_{\text{inter}} d^3\mathbf{r}, \quad (141)$$

$$\mathcal{H}_{\text{int}}^h|_{\text{intra}} = -\frac{1}{\varepsilon\varepsilon_0} \int \hat{\mathbf{D}}_{h\parallel} \hat{\mathbf{P}}_{\parallel}|_{\text{intra}} d^3\mathbf{r}, \quad (142)$$

$$\mathcal{H}_{\text{int}}^e = -\frac{1}{\varepsilon\varepsilon_0} \int \hat{\mathbf{D}}_{e\perp} \hat{\mathbf{P}}_{\parallel}|_{\text{intra}} d^3\mathbf{r}. \quad (143)$$

As the displacement field is purely transverse, the above coupling terms select automatically the transverse part of the polarization field, whereas the longitudinal field must be treated apart, as described for instance in Sec. IID (in the case of the confined photonic DM geometry, we should use the discrete wave vectors k_z^m instead of the continuous set q_z). The TM modes are coupled to both intersubband and intrasubband plasmons, as they have both z and in-plane components. The $m=0$ (TM₀) mode is an important exception, as it has only z component in the dielectric and couples only to intersubband plasmons [4]. The TE modes couple only to intrasubband plasmons. Using the decomposition of the matter polarization field into independent plasmon modes [Eqs. (111) and (119)], we can explicit the coupling terms as

$$\mathcal{H}_{\text{int}}^h|_{\text{inter}} = i \sum_{\mathbf{q}K m} \frac{\hbar R_{Km}}{2} \frac{qc/\sqrt{\varepsilon}}{\sqrt{\Omega_K \omega_{cm\mathbf{q}}}} \times (P_{\mathbf{q}K}^\dagger + P_{-\mathbf{q}K}) (a_{\mathbf{q}m h} - a_{-\mathbf{q}m h}^\dagger), \quad (144)$$

$$\mathcal{H}_{\text{int}}^h|_{\text{intra}} = -i \sum_{\mathbf{q}L m} \frac{\hbar k_{mz} c/\sqrt{\varepsilon}}{2} \sqrt{\frac{W_L}{\omega_{cm\mathbf{q}}}} Q_{Lm} \times (\Pi_{\mathbf{q}\parallel L}^\dagger + \Pi_{-\mathbf{q}\parallel L}) (a_{\mathbf{q}m h} - a_{-\mathbf{q}m h}^\dagger), \quad (145)$$

$$\mathcal{H}_{\text{int}}^e = i \sum_{\mathbf{q}L m} \frac{\hbar \sqrt{W_L \omega_{cm\mathbf{q}}}}{2} Q_{Lm} \times (\Pi_{\mathbf{q}\perp L}^\dagger + \Pi_{-\mathbf{q}\perp L}) (a_{\mathbf{q}m e} - a_{-\mathbf{q}m e}^\dagger). \quad (146)$$

In the above expressions, the intrasubband plasmons have been split into components parallel \parallel and perpendicular \perp to the propagation wave vector \mathbf{q} . We introduced two light-matter overlap integrals:

$$R_{Km} = \frac{1}{\sqrt{L}} \int \Xi_K(z) u_m(z) dz, \quad (147)$$

$$Q_{Lm} = \frac{1}{\sqrt{L}} \int \Upsilon_L(z) w_m(z) dz. \quad (148)$$

The first one, R_{Km} , describes the coupling strength of the K th intersubband plasmon mode with the m th waveguide mode, while the second Q_{Lm} provides analogous coupling for the L th intrasubband plasmon mode. Let us seek to express Eqs. (147) and (148) in a more familiar way. Using Eqs. (105) and (112), we can express the overlap integral R_{Km} as

$$R_{Km} = \sum_{\alpha} M_{\alpha K}^{-1} \sqrt{f_{\alpha}^w f_{\alpha m}^o} \omega_{P\alpha} \sqrt{\frac{\Omega_K}{\omega_{\alpha}}} \text{sgn}_{\alpha}. \quad (149)$$

Here, we introduced the spatial overlap coefficient f_{α}^w and the oscillator strength of the transition $f_{\alpha m}^o$:

$$f_{\alpha}^w = \frac{L_{\alpha}}{L}, \quad (150)$$

$$f_{\alpha m}^o = \frac{\hbar}{2m^* \Delta\omega_{\alpha}} \left(\int \xi_{\alpha}(z) u_m(z) dz \right)^2. \quad (151)$$

The coefficient sgn_{α} in Eq. (149) is the sign of the overlap integral in the definition of $f_{\alpha m}^o$. These definitions can be considered as a generalization of the previous results established for intersubband plasmons [4,8,42]. Now, the oscillator strength $f_{\alpha m}^o$ becomes mode dependent, however, in the case where the variations of the function $u_m(z)$ are slow as compared to the function $\xi_{\alpha}(z)$ we can recover the well-known definition of the oscillator strength [34].

Equation (149) shows that the coefficient R_{Km} has a dimension of a frequency. This quantity can be regarded as an effective plasma frequency of the collective mode K , that is expressed as a linear combination of the initial plasma frequencies $\omega_{P\alpha}$, each being weighted by the respective oscillator strength and spatial overlap. The coefficients $M_{\alpha K}^{-1}$ provide the weight of each transition α in the collective mode K through the dipole-dipole coupling between intersubband plasmons.

Using Eqs. (115) and (120), we can also provide a similar version of the overlap integral Q_{Lm} :

$$Q_{Lm} = \sum_i N_{Li}^{-1} \sqrt{\frac{L_i}{L}} \int \eta_{ii}(z) w_m(z) dz \sqrt{\frac{\omega_{Pi}^{\parallel}}{W_L}}. \quad (152)$$

However, this overlap integral is dimensionless, and we can not assign a meaning of an oscillator strength to the integrals between $\eta_{ii}(z)$ and $w_m(z)$.

B. Confined plasmon-polariton modes

According to Eq. (146), the TE-polarized waveguide modes can couple only to the intrasubband plasmon modes $\Pi_{\mathbf{q}\perp L}^\dagger$ oscillating perpendicular to the propagation wave vector \mathbf{q} . Respectively, the TM modes couple both to the intersubband

plasmons $P_{\mathbf{q}K}^\dagger$ and the intrasubband plasmons $\Pi_{\mathbf{q}\parallel L}^\dagger$ that oscillate along the propagation wave vector. Therefore, we can split the full light-matter Hamiltonian (140) into two independent parts, according to the type of waveguide modes: $\mathcal{H} = \mathcal{H}_{\text{TE}} + \mathcal{H}_{\text{TM}}$. In the following, we examine the plasmon-polariton modes that arise from each part.

1. TE intrasubband plasmon polaritons

The TE part of the light-matter Hamiltonian is

$$\begin{aligned} \mathcal{H}_{\text{TE}} = & \sum_{\mathbf{q}m} \hbar\omega_{\mathbf{c}m\mathbf{q}} \left(a_{\mathbf{q}me}^\dagger a_{\mathbf{q}me} + \frac{1}{2} \right) + \sum_{\mathbf{q}L} \hbar W_L \Pi_{\mathbf{q}\perp L}^\dagger \Pi_{\mathbf{q}\perp L} \\ & + i \sum_{\mathbf{q}mL} \hbar \mathcal{W}_{mL}^\perp (\Pi_{\mathbf{q}\perp L}^\dagger + \Pi_{-\mathbf{q}\perp L}) (a_{\mathbf{q}me} - a_{-\mathbf{q}me}^\dagger), \end{aligned} \quad (153)$$

$$\mathcal{W}_{\mathbf{q}mL}^\perp = \frac{1}{2} \sqrt{W_L \omega_{\mathbf{c}m\mathbf{q}}} Q_{Lm}. \quad (154)$$

The mode TE_m thus interacts with intrasubband plasmons L with the coupling constant $\mathcal{W}_{\mathbf{q}mL}^\perp$. The above Hamiltonian is solved by introducing the coupled-mode operators

$$\begin{aligned} Y_{\mathbf{q}\perp} = & \sum_m (x_{\mathbf{q}m} a_{\mathbf{q}me} + y_{\mathbf{q}m} a_{-\mathbf{q}me}^\dagger) \\ & + \sum_L (m_{\mathbf{q}L} \Pi_{\mathbf{q}\perp L} + h_{\mathbf{q}L} \Pi_{-\mathbf{q}\perp L}^\dagger). \end{aligned} \quad (155)$$

Let $\omega_{\mathbf{q}}$ be the frequency of the coupled polariton modes. Then, using the relation $[Y_{\mathbf{q}\perp}, \mathcal{H}_{\text{TE}}] = \hbar\omega_{\mathbf{q}} Y_{\mathbf{q}\perp}$ (Hopfield-Bogoliubov procedure) it is straightforward to obtain the following relationships between the Hopfield coefficients introduced in the definition of $Y_{\mathbf{q}\perp}$ [Eq. (155)]:

$$m_{\mathbf{q}L} = \frac{-i}{\omega_{\mathbf{q}} - W_L} \sum_m \mathcal{W}_{\mathbf{q}mL}^\perp (x_{\mathbf{q}m} + y_{\mathbf{q}m}), \quad (156)$$

$$h_{\mathbf{q}L} = \frac{-i}{\omega_{\mathbf{q}} + W_L} \sum_m \mathcal{W}_{\mathbf{q}mL}^\perp (x_{\mathbf{q}m} + y_{\mathbf{q}m}), \quad (157)$$

$$x_{\mathbf{q}m} = \frac{i}{\omega_{\mathbf{q}} - \omega_{\mathbf{c}m\mathbf{q}}} \sum_L \mathcal{W}_{\mathbf{q}mL}^\perp (m_{\mathbf{q}L} + h_{\mathbf{q}L}), \quad (158)$$

$$y_{\mathbf{q}m} = \frac{-i}{\omega_{\mathbf{q}} + \omega_{\mathbf{c}m\mathbf{q}}} \sum_L \mathcal{W}_{\mathbf{q}mL}^\perp (m_{\mathbf{q}L} + h_{\mathbf{q}L}). \quad (159)$$

These equations must be supplemented by the normalization condition

$$\sum_m (|x_{\mathbf{q}m}|^2 - |y_{\mathbf{q}m}|^2) + \sum_L (|m_{\mathbf{q}L}|^2 - |h_{\mathbf{q}L}|^2) = 1 \quad (160)$$

which arises from the requirement that $Y_{\mathbf{q}\perp}$ is a boson destruction operator: $[Y_{\mathbf{q}\perp}, Y_{\mathbf{q}\perp}^\dagger] = \delta_{\mathbf{q}\mathbf{q}'}$. This set of equations is sufficient to determine the Hopfield coefficients, up to an arbitrary phase, as well as the polariton dispersion $\omega_{\mathbf{q}} = f(\mathbf{q})$. There are two possible approaches in order to handle the algebra in Eqs. (156)–(159). We can eliminate the matter Hopfield coefficients $m_{\mathbf{q}L}$ and $h_{\mathbf{q}L}$ in favor of the photonic coefficients $x_{\mathbf{q}m}$ and $y_{\mathbf{q}m}$. Then, the polariton eigenmodes $\omega_{\mathbf{q}}$

are determined by the following eigenvalue matrix equation:

$$\|\mathcal{M}_{mm'}^e(\omega_{\mathbf{q}})\| = 0, \quad (161)$$

$$\begin{aligned} \mathcal{M}_{mm'}^e(\omega) = & \delta_{mm'} (\omega^2 - \omega_{\mathbf{c}m\mathbf{q}}^2) \\ & - \sum_L \frac{4\omega_{\mathbf{c}m\mathbf{q}} W_L}{(\omega^2 - W_L^2)} \mathcal{W}_{\mathbf{q}mL}^\perp \mathcal{W}_{\mathbf{q}m'L}^\perp. \end{aligned} \quad (162)$$

In a similar way, by eliminating the photonic coefficients in favor of the matter ones, we can define an alternative matrix $\widetilde{\mathcal{M}}_{LL'}^e(\omega)$ that sums over all cavity modes (we shall not provide its expression explicitly here). In both approaches, the polariton dispersion is obtained numerically by truncating the matrix $\mathcal{M}_{mm'}^e(\omega)$ or $\widetilde{\mathcal{M}}_{LL'}^e(\omega)$; the choice of a particular matrix depends on whether the numerical truncation is more advantageous over the plasmon or photon indexes.

The lowest-order truncation corresponds to a single plasmon mode L coupled with a single waveguide mode TE_m . In this case, Eq. (161) provides the following secular equation:

$$(\omega^2 - \omega_{\mathbf{c}m\mathbf{q}}^2)(\omega^2 - W_L^2) = \omega_{\mathbf{c}m\mathbf{q}}^2 W_L^2 Q_{mL}^2. \quad (163)$$

We rearrange this equation in a form of a Helmholtz-type dispersion relation with an effective dielectric constant $\varepsilon_{\perp mL}(\omega)$:

$$\mathbf{q}^2 + k_{zm}^2 = \varepsilon \frac{\omega_{\mathbf{c}m\mathbf{q}}^2}{c^2} = \varepsilon_{\perp mL}(\omega_{\mathbf{q}}) \frac{\omega_{\mathbf{q}}^2}{c^2}, \quad (164)$$

$$\begin{aligned} \frac{1}{\varepsilon_{\perp mL}(\omega)} = & \frac{1}{\varepsilon} \left(1 + \frac{W_L^2 Q_{mL}^2}{\omega^2 - W_L^2} \right) \\ = & \frac{1 - Q_{mL}^2}{\varepsilon} + \frac{Q_{mL}^2}{\varepsilon(1 - W_L^2/\omega^2)}. \end{aligned} \quad (165)$$

We recognize in the second denominator of Eq. (165) a Drude-type dielectric constant $\varepsilon(1 - W_L^2/\omega^2)$ of the plasmon layer. Clearly, the coefficient Q_{mL}^2 plays the role of a spatial filling factor of the plasmon mode in the waveguide slab. In the following, we shall see that for TE modes resonant with the intrasubband plasmon mode, this filling factor is typically very small $Q_{mL}^2 \ll 1$. Furthermore, let us consider the high-frequency limit $\omega \gg W_L$; under these conditions, Eq. (165) can be rewritten as

$$\varepsilon_{\perp mL}(\omega) \approx (1 - Q_{mL}^2)\varepsilon + Q_{mL}^2 \varepsilon \left(1 - \frac{W_L^2}{\omega^2} \right). \quad (166)$$

This is the effective dielectric constant that would be obtained applying the classical boundary conditions for a sub-wavelength layer with an in-plane dielectric tensor component $\varepsilon(1 - W_L^2/\omega^2)$ and TE-polarized wave [28]. However, such interpretation is impossible in the general case as the quantity $\varepsilon_{\perp mL}(\omega)$ does not play a role of a macroscopic dielectric constant of the medium. This is already seen from the fact that it is strongly dependent on the waveguide index m through the overlap integral Q_{mL} . As a result, the dispersion relation in Eq. (164) also depends on the waveguide mode, and we can no longer define a global dielectric function in the sense of the macroscopic Maxwell's equations, contrary to the case of a homogeneous system from Ref. [3]. We will see further that we can still recover an effective dielectric function, independent

from the waveguide mode index, only as an average on scales much larger than the typical size of the quantum confinement.

Let us at present estimate the coupling strength for intrasubband plasmon polaritons. To this end, we consider the intrasubband plasmon from an infinite quantum well of a thickness L_{QW} and a single occupied subband, as discussed in Sec. II C 3. First, we look for the condition where the excitation frequency of the plasmon $\omega_{P\parallel} = \sqrt{(2/3)(e^2 N_s)/(m^* \epsilon \epsilon_0 L_{QW})}$ matches the cutoff frequency $\omega_{c10} = c\pi/\sqrt{\epsilon}L$ of the lowest-order $TE_{m=1}$ mode. We take the maximal doping level $N_{smax} = m^* \Delta\omega_{21}/\pi\hbar$ so that only the fundamental subband of the well remains occupied $E_F = \hbar\Delta\omega_{21}$. Since for an infinite quantum well we have $\hbar\Delta\omega_{21} = 3\pi^2\hbar^2/2m^*L_{QW}$ [35], we obtain $N_{smax} = 3\pi/2L_{QW}$. Then, the condition $\omega_{P\parallel} = \omega_{c10}$ can be rewritten as a relation that involves only the quantum well thickness L_{QW} and the waveguide thickness L :

$$L^2 = \frac{L_{QW}^3}{4a_c}. \quad (167)$$

Here, we introduced the ‘‘classical electron radius’’ a_c [37] of the electron with an effective mass m^* :

$$a_c = \frac{e^2}{4\pi\epsilon_0 m^* c^2} = 4.2 \times 10^{-5} \text{ nm}. \quad (168)$$

Clearly, this quantity sets the order of magnitude for the geometrical overlap $L_{QW}/L = \sqrt{4a_c/L_{QW}}$ between the quantum well and the waveguide mode which is resonant with the plasmon excitation. Since typically the quantum well thickness is on the order of tens of nanometers, we obtain that L_{QW}/L is on the order of 10^{-3} , which means extremely small coupling of the intrasubband plasmons of a single well with the transverse electromagnetic field [53].

Even if the coupling of a single quantum well with the waveguide mode is weak, we can recover strong collective coupling of an ensemble of quantum wells, that are homogeneously distributed inside the whole thickness of the waveguide slab, as depicted in Fig. 7(a). Let us consider a $L_{QW} = 23$ nm quantum well, which has an intrasubband plasmon excitation at $\omega_{P\parallel}/2\pi = 5$ THz. Then, according to Eq. (167) the corresponding waveguide thickness is $L = 8.8 \mu\text{m}$. As depicted in Fig. 7(a), we consider a quantum well/barrier superlattice of a period $L_{QW} + L_{bar} = 50$ nm; such system is feasible with the actual technology of THz quantum cascade lasers [48].

We look for a solution of the secular equation (161) by taking into account all possible waveguide modes. We first consider the off-diagonal terms of the matrix $\mathcal{M}_{mm'}^e(\omega)$. In the present case, the index L labels the position of the quantum well along the z axis. Since $W_L = \omega_{P\parallel}$ are identical for all wells, the off-diagonal elements ($m' \neq m$) are proportional to

$$\begin{aligned} \sum_L Q_{m'L} Q_{mL} &= \frac{2L_{QW}}{3L} \sum_{j=0}^{N_{QW}} w_{m'}(z_j) w_m(z_j) \\ &= \frac{4L_{QW}}{3L} \sum_{j=0}^{N_{QW}} \sin\left(\frac{m'\pi z_j}{L}\right) \sin\left(\frac{m\pi z_j}{L}\right) \end{aligned}$$

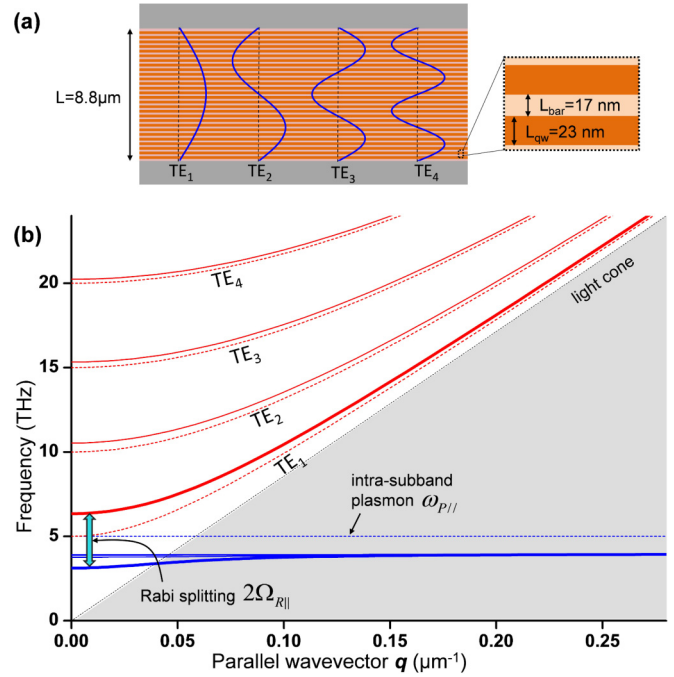


FIG. 7. (Color online) TE intrasubband plasmon polaritons. (a) Schematics of a DM waveguide filled with identical pairs of quantum wells and barriers. (b) The resulting coupled-mode dispersion, for the case where the plasma frequency $\omega_{P\parallel}$ is resonant with the cutoff frequency of the lowest-order $TE_{m=1}$ mode. Each waveguide mode TE_m interacts with the intrasubband plasmons, giving rise to two coupled modes indicated by continuous lines. The original uncoupled excitations are indicated in dashed lines. The polariton modes resulting from the resonant interaction between the intrasubband plasmon and the $TE_{m=1}$ mode are indicated by thick lines. Note the significant red-shift for all lower polariton modes, even if the TE_m waveguide modes are strongly detuned from the plasmon as the index m increases.

$$\begin{aligned} &= \frac{4}{3} \frac{L_{QW}}{L_{QW} + L_{bar}} \frac{1}{\pi} \int_0^\pi \sin(m'x) \sin(mx) dx \\ &= \frac{2}{3} \frac{L_{QW}}{L_{QW} + L_{bar}} \delta_{mm'}. \end{aligned} \quad (169)$$

Here, $z = j(L_{QW} + L_{bar})$, $j = 0 \dots N_{QW} - 1$, is the position of the j th quantum well inside the waveguide slab, and $N_{QW} = L/(L_{QW} + L_{bar})$ is the total number of quantum wells. Since $L_{QW} + L_{bar} \ll L$ we can convert the above sum into integral which vanishes for $m \neq m'$ thanks to the orthogonality of the waveguide modes $w_m(z)$. The matrix equation (161) then breaks into independent equations for each waveguide mode:

$$(\omega^2 - \omega_{cmq}^2)(\omega^2 - \omega_{P\parallel}^2) = \omega_{cmq}^2 \omega_{P\parallel}^2 \sum_L Q_{mL}^2. \quad (170)$$

The coupling constant is now identical for all modes. According to the general property of this biquadratic equation that describes two coupled quantum oscillators [4] we can associate a coupling constant $2\Omega_{R\parallel}$ which evaluates the Rabi splitting between the polariton modes in the resonant case. By using Eq. (169) with $m = m'$ this coupling constant is

evaluated to be

$$4\Omega_{R\parallel}^2 = \omega_{P\parallel}^2 \sum_L Q_{mL}^2$$

$$= \omega_{P\parallel}^2 \frac{2}{3} \frac{L_{QW}}{L_{QW} + L_{\text{bar}}} = \omega_{P\text{cl}}^2, \quad (171)$$

$$\omega_{P\text{cl}}^2 = \frac{e^2 N_s}{m^* \epsilon_0 \epsilon (L_{QW} + L_{\text{bar}})}. \quad (172)$$

Here, we introduced the effective plasma frequency of the superlattice $\omega_{P\text{cl}}$ that corresponds to the bulk plasma frequency that would have been obtained if the same number of charges were homogeneously distributed in the whole volume of the waveguide. Therefore, for intrasubband excitations considered here, the Rabi splitting $2\Omega_{R\parallel}$ is exactly the equivalent 3D plasma frequency of the system.

In the present case, we obtain numerically a collective coupling strength $2\Omega_{R\parallel}/2\pi = \omega_{P\text{cl}}/2\pi = 3$ THz, which is now a significant fraction of the plasmon frequency $\omega_{P\parallel}/2\pi = 5$ THz. The corresponding dispersion is plotted in Fig. 7(b), where once again, for simplicity, we have neglected the phonon dispersion of the material. The intrasubband plasmon is coupled with each TE_m waveguide mode, which leads, according to Eq. (170), to two polariton solutions for each waveguide mode. These solutions have been indicated in Fig. 7(b) in continuous lines, while original uncoupled waveguide modes and cavity modes are indicated in dashed lines. Note that the coupling of a single plasmon mode with an infinity of high-order waveguide modes creates an infinity of lower polariton branches that accumulate around the frequency 4 THz. Similar phenomena were indicated by Zaluzny and Zietkowski in Ref. [30] for the case of intersubband plasmon polaritons. Note, however, from Eqs. (158) and (159) that the Hopfield coefficients for the lower polariton branch tend to zero as the detuning between the TE_m modes and the plasmon is increased as the index m increases. This would lead to low, yet observable, contribution of these high-order polariton modes in the absorption spectra of the system [30].

An interesting feature of the dispersion relation in Fig. 7(b) is the important red-shift of the lowest coupled modes for large wave vectors $\omega_{\mathbf{q}}^-$ that becomes constant beyond the light line of the waveguide, and that affects all modes. Indeed, even if one would expect that the effects of the coupling would vanish as the high-order TE_m modes are significantly detuned from the intrasubband plasmon, the lower polariton modes never recover the original plasmon frequency $\omega_{P\parallel}/2\pi = 5$ THz. This red-shift can be recovered from Eq. (170) taking the limit $\omega_{cm\mathbf{q}} \gg \omega$:

$$\omega_{\mathbf{q}}^-(|\mathbf{q}| \rightarrow \infty) = \sqrt{\omega_{P\parallel}^2 - \omega_{P\text{cl}}^2}. \quad (173)$$

From a quantum-mechanical point of view, the renormalization of the lowest plasmon-polariton branch can be seen as resulting from the repulsion of all cavity modes to lower frequencies owing to the light-matter coupling. Note that the full dispersion of the polaritons, including the region beyond the light line of the waveguide, can be observed in experiments with three-dimensional microcavities with quantized wave vector \mathbf{q} [6,42].

Since the coupling strength between the plasmon and the waveguide modes is now independent from the index m , we can associate to Eq. (170) a unique dispersion relation:

$$\epsilon_{\perp}(\omega_{\mathbf{q}}) \frac{\omega_{\mathbf{q}}^2}{c^2} = \mathbf{q}^2 + k_{zm}^2, \quad (174)$$

which now is expressed in terms of an effective nonlocal dielectric constant, that is valid for all TE_m waveguide modes:

$$\frac{\epsilon_{\perp}(\omega)}{\epsilon} = \left(1 + \frac{\omega_{P\text{cl}}^2}{\omega^2 - \omega_{P\parallel}^2} \right)^{-1}$$

$$= 1 - \frac{\omega_{P\text{cl}}^2}{\omega^2 - (\omega_{P\parallel}^2 - \omega_{P\text{cl}}^2)}. \quad (175)$$

We see that the effect of neglecting the off-diagonal terms of the matrix $\mathcal{M}_{mm'}^e(\omega)$ leads to a semiclassical nonlocal dielectric function of the system. This approximation is pertinent in the present case as the typical extension of the waveguide modes, that is, on the order of the light wavelength $\lambda = 2\pi c/\omega_{P\parallel}$, is much larger than the size of the quantum confinement, which allows averaging the off-diagonal terms to zero.

Equation (175) also allows us to understand the physical meaning of the asymptotic resonance from Eq. (173) from a semiclassical point of view. To this end, let us examine the form of the dielectric function in Eq. (175) in the limit where $L_{\text{bar}} \rightarrow 0$ and a large number of occupied subbands, as discussed in the end of Sec. III E. We showed in that section that in this limit, the intrasubband plasma frequency tends to the three-dimensional plasmon resonance described in Eq. (122), which in the present case writes $\omega_{P\parallel} \rightarrow \omega_{P\text{cl}}$. The dielectric constant $\epsilon_{\perp}(\omega)$ from Eq. (175) then becomes exactly a Drude dielectric constant with a vanishing pole $(\omega_{P\parallel}^2 - \omega_{P\text{cl}}^2) \rightarrow 0$. We showed in Ref. [3] that the presence of such zero-frequency solution corresponds to a perfect screening of the electromagnetic wave propagating in the medium by the field created by the oscillating electrons. In the case with quantum confinement, the electrons do not fill the whole medium, and such screening is impossible, which leads to the appearance of a nonvanishing low-frequency resonance from Eq. (173). This fact can be used as an experimental probe of the quantum confinement of the electronic system.

2. TM mixed plasmon polaritons

Let us consider, at present, the TM part of the light-matter coupling Hamiltonian:

$$\mathcal{H}_{\text{TM}} = \sum_{\mathbf{q}m} \hbar \omega_{cm\mathbf{q}} \left(a_{\mathbf{q}mh}^{\dagger} a_{\mathbf{q}mh} + \frac{1}{2} \right)$$

$$+ \sum_{\mathbf{q}K} \hbar \Omega_K P_{\mathbf{q}K}^{\dagger} P_{\mathbf{q}K} + \sum_{\mathbf{q}L} \hbar W_L \Pi_{\mathbf{q}L}^{\dagger} \Pi_{\mathbf{q}L}$$

$$+ i \sum_{\mathbf{q}K} \hbar \mathcal{V}_{\mathbf{q}mK}^z (P_{\mathbf{q}mK}^{\dagger} + P_{-\mathbf{q}K}) (a_{\mathbf{q}mh} - a_{-\mathbf{q}mh}^{\dagger})$$

$$- i \sum_{\mathbf{q}mL} \hbar \mathcal{V}_{\mathbf{q}mL}^{\parallel} (\Pi_{\mathbf{q}L}^{\dagger} + \Pi_{-\mathbf{q}L}) (a_{\mathbf{q}mh} - a_{-\mathbf{q}mh}^{\dagger}), \quad (176)$$

$$\mathcal{W}_{\mathbf{q}mK}^z = \frac{1}{2} R_{Km} \frac{qc/\sqrt{\varepsilon}}{\sqrt{\Omega_K \omega_{cmq}}}, \quad (177)$$

$$\mathcal{W}_{\mathbf{q}mL}^{\parallel} = \frac{1}{2} Q_{Lm} \frac{k_{mz}c}{\sqrt{\varepsilon}} \sqrt{\frac{W_L}{\omega_{cmq}}}. \quad (178)$$

In this Hamiltonian, the intrasubband and intersubband plasmons became coupled through the TM modes of the waveguide. The most general solution of the problem therefore is a mixed intrasubband-intersubband plasmon-polariton mode:

$$\begin{aligned} Y_{\mathbf{q}z\parallel} &= \sum_m (x_{qm} a_{qmh} + y_{qm} a_{-qmh}^\dagger) \\ &+ \sum_K (m_{\mathbf{q}K}^z P_{\mathbf{q}K} + h_{\mathbf{q}K}^z P_{-\mathbf{q}K}^\dagger) \\ &+ \sum_L (m_{\mathbf{q}L}^{\parallel} \Pi_{\mathbf{q}\parallel L} + h_{\mathbf{q}L}^{\parallel} \Pi_{-\mathbf{q}\parallel L}^\dagger). \end{aligned} \quad (179)$$

Using the Hopfield-Bogoliubov diagonalization method from the previous section, the commutator $[Y_{\mathbf{q}z\parallel}, \mathcal{H}_{\text{TM}}] = \hbar\omega_{\mathbf{q}} Y_{\mathbf{q}z\parallel}$ is computed in order to relate the Hopfield coefficients to the coupled-mode frequency $\omega_{\mathbf{q}}$. By eliminating the matter coefficients in favor of the photonic ones, we obtain the following eigenvalue equation:

$$\|\mathcal{M}_{mm'}^h(\omega_{\mathbf{q}})\| = 0, \quad (180)$$

$$\begin{aligned} \mathcal{M}_{mm'}^h(\omega) &= \delta_{mm'}(\omega^2 - \omega_{cmq}^2) \\ &- \sum_L \frac{4\omega_{cmq} W_L}{(\omega^2 - W_L^2)} \mathcal{W}_{\mathbf{q}mL}^{\parallel} \mathcal{W}_{\mathbf{q}m'L}^{\parallel} \\ &- \sum_K \frac{4\omega_{cmq} \Omega_K}{(\omega^2 - \Omega_K^2)} \mathcal{W}_{\mathbf{q}mK}^z \mathcal{W}_{\mathbf{q}m'K}^z. \end{aligned} \quad (181)$$

Let us consider the lowest-order truncation of the above eigenvalue problem, that corresponds to a single waveguide mode interacting with a single intersubband plasmon and a single intrasubband plasmon. The dispersion relation in this case becomes

$$\omega_{\mathbf{q}}^2 - \omega_{cmq}^2 = \frac{k_m^2 c^2}{\varepsilon} \frac{W_L^2 Q_{mL}^2}{\omega_{\mathbf{q}}^2 - W_L^2} + \frac{q^2 c^2}{\varepsilon} \frac{R_{mK}^2}{\omega_{\mathbf{q}}^2 - \Omega_K^2}. \quad (182)$$

We can easily show that this equation can be rewritten in the form

$$\frac{\omega_{\mathbf{q}}^2}{c^2} = \frac{k_m^2}{\varepsilon_{\parallel m L}(\omega_{\mathbf{q}})} + \frac{q^2}{\varepsilon_{zmK}(\omega_{\mathbf{q}})}. \quad (183)$$

This is a Helmholtz-type dispersion relation of an electromagnetic wave propagating in a birefringent media with two effective dielectric constants:

$$\frac{1}{\varepsilon_{\parallel m L}(\omega)} = \frac{1}{\varepsilon_{\perp m L}(\omega)} = \frac{1}{\varepsilon} \left(1 + \frac{W_L^2 Q_{mL}^2}{\omega^2 - W_L^2} \right), \quad (184)$$

$$\frac{1}{\varepsilon_{zmK}(\omega)} = \frac{1}{\varepsilon} \left(1 + \frac{R_{mK}^2}{\omega^2 - \Omega_K^2} \right). \quad (185)$$

The in-plane effective dielectric constant $\varepsilon_{\parallel m K}(\omega)$ is identical to the function $\varepsilon_{\perp m L}(\omega)$ from the previous section. In

particular, in the case where the cavity thickness is sufficiently small, so that only the TM₀ mode can be considered, the coupling with the intrasubband plasmon can be ignored, as in this case $k_{z0} = 0$. We therefore recover the intersubband plasmon-polariton mode that was discussed in Ref. [4].

We now examine the results from our formalism in the multimode case, for a waveguide filled with identical quantum wells, as discussed in the previous section. We consider the case of a single occupied subband. In order to evaluate the matrix elements of $\mathcal{M}_{mm'}^h(\omega)$, we need to compute the sums

$$\sum_L Q_{mL} Q_{m'L}, \quad \sum_K R_{mK} R_{m'K}. \quad (186)$$

The first sum was already computed from Eq. (169). To evaluate the second sum, we use the same technique that allows us to convert the sum over the quantum well positions z_j into integrals thanks to the long-wavelength approximation

$$\begin{aligned} &\sum_K R_{mK} R_{m'K} \\ &= \frac{1}{L} \sum_K \int \xi_K(z) u_m(z) dz \int \xi_K(z) u_{m'}(z) dz \\ &\approx \frac{1}{L} \frac{\omega_{P21}^2}{I_{21,21}} \left(\int \xi_{21}(z) dz \right)^2 \sum_{j=0}^{N_{\text{QW}}} u_{m'}(z_j) u_m(z_j) \\ &= \frac{e^2 N_s}{m^* \varepsilon \varepsilon_0 (L_{\text{QW}} + L_{\text{bar}})} \frac{\hbar^2}{2m^* \Delta\omega_{21}} \left(\int \xi_{21}(z) dz \right)^2 \\ &\quad \times \frac{1}{\pi} \int_0^\pi \cos(mx) \cos(m'x) dx \frac{2}{1 + \delta_{m0}} \\ &= \frac{e^2 N_s}{m^* \varepsilon \varepsilon_0 (L_{\text{QW}} + L_{\text{bar}})} f_{21} \delta_{mm'} = \omega_{P\text{cl}}^2 f_{21} \delta_{mm'}. \end{aligned} \quad (187)$$

Like before, the index K refers to the different spatial positions of the intersubband plasmons with identical frequency. To establish this result, we used the definitions from Eqs. (105), (151), and (172). Since the off-diagonal terms of the matrix average to zero, we obtain, similarly to the previous section, a unique dispersion relation that is valid for all TM_{*m*} waveguide modes:

$$\frac{\omega_{\mathbf{q}}^2}{c^2} = \frac{k_m^2}{\varepsilon_{\parallel}(\omega_{\mathbf{q}})} + \frac{q^2}{\varepsilon_z(\omega_{\mathbf{q}})}. \quad (188)$$

Here, we defined two global dielectric functions

$$\frac{1}{\varepsilon_{\parallel}(\omega)} = \frac{1}{\varepsilon_{\perp}(\omega)} = \frac{1}{\varepsilon} \left(1 + \frac{\omega_{P\text{cl}}^2}{\omega^2 - \omega_{P\parallel}^2} \right) \quad (189)$$

$$\frac{1}{\varepsilon_z(\omega)} = \frac{1}{\varepsilon} \left(1 + \frac{f_{21} \omega_{P\text{cl}}^2}{\omega^2 - \omega_{21}^2} \right). \quad (190)$$

This is the nonlocal semiclassical dielectric constant that corresponds to the TM-polarized waves. Clearly, this result can be combined with the results from the previous section, in order to define an anisotropic dielectric tensor of the

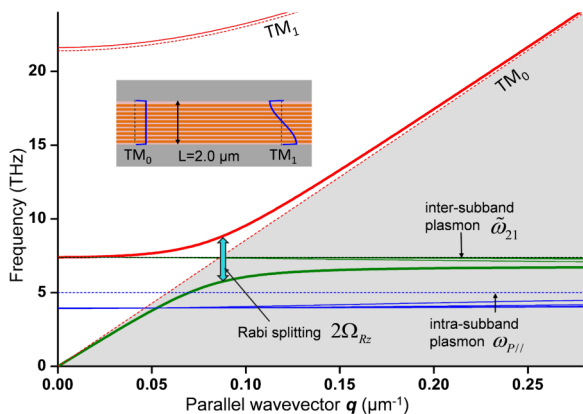


FIG. 8. (Color online) Confined plasmon-polariton modes arising from the coupling between the TM waveguide modes with the electronic collective excitations (intrasubband and intersubband plasmons) of the quantum wells, for the case of a $L = 2.2 \mu\text{m}$ thick waveguide. The uncoupled original modes are indicated in dashed lines, while the coupled polariton modes are indicated in continuous lines. Now, there are three polariton branches for each index m . However, only the polaritons that arise from the coupling between the TM_0 with the intersubband plasmon feature visible anticrossing behavior (thick lines). The coupling of the intersubband plasmon with the high-order modes gives rise to lower polariton branches that remain very close to the original frequency $\tilde{\omega}_{21}/2\pi = 7.4 \text{ THz}$. The intrasubband plasmon at $\omega_{p\parallel}/2\pi = 5 \text{ THz}$ does not couple to the TM_0 mode, yet there is a red-shift of all lower polariton branches due to the interaction of all higher-order $\text{TM}_{m>0}$ waveguide modes, that is identical to the interaction with the TE_m described in the previous section.

multi-quantum-well medium. Similar expressions were provided in Ref. [54]. Once again, the intensity of the light-matter coupling is provided by the effective 3D plasma frequency of the system, which is corrected by the oscillator strength of the transition in the case of the intersubband plasmon.

Examples of the resulting coupled polariton modes are provided in Figs. 8 and 9. We consider the case of the $L_{\text{QW}} = 23 \text{ nm}$ infinite square quantum well from the previous section, for which we have $f_{21} = 0.96$, $\tilde{\omega}_{21}/2\pi = 7.4 \text{ THz}$, and $\sqrt{0.96}\omega_{p\text{cl}} = 4.9 \text{ THz}$. The resulting polariton dispersion is plotted for two different values of waveguide thickness in Figs. 8 and 9. In Fig. 8, the waveguide thickness is chosen to be $L = 2.2 \mu\text{m}$, so that both the intersubband and intrasubband resonances appear well below the cutoff of the TM_1 mode. The coupling between each waveguide mode and the two plasmons now creates three plasmon-polariton branches for each waveguide index m . However, we observe only a splitting between the cutoff-less TM_0 mode and the intersubband plasmon, as discussed in Ref. [4]. The corresponding polariton branches have been highlighted with thick continuous lines in Fig. 8. The interaction of the intersubband plasmon with the higher-order TM_m modes creates branches that remain very close to the original intersubband plasmon frequency $\tilde{\omega}_{21}/2\pi = 7.4 \text{ THz}$, as also pointed out in Ref. [30]. As indicated in the aforementioned work, these branches cause a weak absorption peak around the uncoupled frequency $\tilde{\omega}_{21}$ in the polariton spectra, while the spectra are dominated by the lowest-order intersubband polariton branches [6].

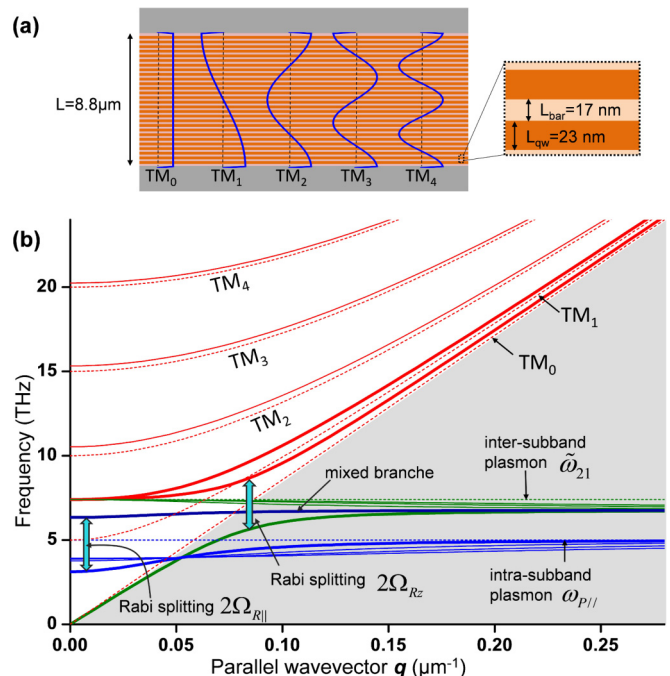


FIG. 9. (Color online) Confined plasmon polaritons from a $L = 8.8 \mu\text{m}$ thick waveguide. The thickness of the waveguide is set so that the TM_1 becomes resonant with the intrasubband plasmon at $|\mathbf{q}| = 0$. As in Fig. 8, the TM_0 is coupled only to the intersubband plasmon. At high wave vectors, the TM_1 couples to both intrasubband and intersubband plasmons, yielding the mixed branch indicated in the figure. These modes that arise from the resonant interaction with the plasmons are indicated with thick lines. The other plasmon-polariton modes are indicated in thin lines, while the original uncoupled modes are indicated in dashed lines.

The intrasubband plasmon at the frequency $\omega_{p\parallel}/2\pi = 5 \text{ THz}$ is not coupled in the TM_0 mode since this mode does not have a planar component of the electric field. Instead, its interaction with all higher-order TM_m modes is permitted, as these modes possess an in-plane component of the electric field. This interaction, that is formally identical to the coupling with the TE_m discussed in the previous section, induces global red-shift of all lower intrasubband polariton branches as described by Eq. (173). However, we expect that, for thin cavities as in the present case, these branches will have little influence on the absorption spectra. This is because the important detuning between the intrasubband plasmon and the TE_m gives very little weight to the Hopfield coefficients of these branches. The physics of the system will therefore be dominated essentially by the coupling between the intrasubband plasmon and the TM_0 mode, as described before [6,30].

The situation becomes more complex for a thick waveguide, as depicted in Fig. 9. In that case, the thickness is chosen at $L = 8.8 \mu\text{m}$ in order to render the TM_1 resonant with the intrasubband plasmon. Each waveguide mode, except the TM_0 , is then split into three branches, that arise from the interaction with the two kind of plasmons. In Fig. 9, we have indicated the Rabi splittings $2\Omega_{R\parallel} = \omega_{p\text{cl}}$ and $2\Omega_{Rz} = \sqrt{f_{21}}\omega_{p\text{cl}}$ that arise, respectively, from the resonant coupling between the TM_1 mode and the intrasubband plasmon and the TM_0 with

the intersubband plasmon. Note that the Rabi splitting $2\Omega_{R\parallel}$ is not affected by the intersubband plasmon, which does not couple with light at $|\mathbf{q}| = 0$. However, the TM_1 starts to interact with the intersubband plasmon as the planar wave vector \mathbf{q} is increased; this coupling yields, in particular, a mixed photon intrasubband-intersubband plasmon mode that has been indicated in Fig. 9.

Let us note that we can still recover the homogeneous electron plasma as a limiting case of Eqs. (189) and (190) for the case of multiple occupied subbands. This is already shown for intrasubband plasmons in the previous section, as $\varepsilon_{\perp}(\omega) = \varepsilon_{\parallel}(\omega)$. For intersubband plasmons of a square quantum well the demonstration is provided in Ref. [55], where it is shown that, as the number of occupied subbands increases, the oscillator strength of all intersubband excitations is concentrated in a single resonance with a frequency that tends to the equivalent bulk plasma resonance ω_{pcl} .

C. Inverse PZW transform

In this section, we will explore the image of our light-matter coupling Hamiltonian [Eq. (1)], describing the 2D electron gas, in the minimal-coupling representation. In Ref. [3], we performed a similar study with homogeneous three-dimensional systems. In the present case, we have two new constraints that were previously absent: on one hand, the electronic movement is quantized in the direction of quantum confinement, and on the other hand, the electromagnetic field is also subject to a photonic confinement within the metallic waveguide. In particular, our approach will reveal that the Coulomb potential of the system, that describes the particle-particle interactions, is modified not only by the quantum confinement, but also by the boundary conditions arising from the cavity walls.

In order to express correctly the unitary transformation relating the two representations, we must take into account all possible electronic transitions together with the full set of waveguide modes. For this purpose, we return to the general expressions of the polarization operator $\hat{\mathbf{P}}(\mathbf{r})$ in Eqs. (28) and (27) from Sec. II B. In that picture, the polarization operator is expressed in the \mathbf{k} -resolved single-particle electronic states, before the diagonalization of the matter part and the identification of the collective contributions. However, we still make use of the bosonization hypothesis which ensures the self-consistency of the polarization field operator. The coupling Hamiltonian spanned over the TE_m and TM_m modes is written as

$$\mathcal{H} = \mathcal{H}_{\text{ph}}^h + \mathcal{H}_{\text{ph}}^e + \mathcal{H}_e + \mathcal{H}_{\text{P2}} - \frac{1}{\varepsilon\epsilon_0} \int [\hat{P}_z \hat{D}_{hz} + \hat{\mathbf{P}}_{\parallel}(\hat{\mathbf{D}}_{h\parallel} + \hat{\mathbf{D}}_{e\perp})] d^3\mathbf{r}. \quad (191)$$

Here, we employed the initial expressions of the polarization field operator of the gas [Eqs. (28) and (27)]:

$$\hat{P}_z = -\frac{\hbar e}{2m^*S} \sum_{\mathbf{q}\alpha} \Pi_{z\alpha\mathbf{q}}^{\dagger} \xi_{\alpha}(z) e^{-i\mathbf{q}\mathbf{r}_{\parallel}}, \quad (192)$$

$$\hat{\mathbf{P}}_{\parallel} = -\frac{i\hbar e}{2m^*S} \sum_{\mathbf{q}\alpha} \Pi_{\parallel\alpha\mathbf{q}}^{\dagger} \eta_{\alpha}(z) e^{-i\mathbf{q}\mathbf{r}_{\parallel}}. \quad (193)$$

For convenience, the following operators are introduced:

$$\Pi_{z\alpha\mathbf{q}}^{\dagger} = \sum_{\mathbf{k}} \frac{c_{i\mathbf{k}+\mathbf{q}}^{\dagger} c_{j\mathbf{k}}}{\Delta\omega_{\mathbf{k}\mathbf{q}ij}}, \quad (194)$$

$$\Pi_{\parallel\alpha\mathbf{q}}^{\dagger} = \sum_{\mathbf{k}} \frac{c_{i\mathbf{k}+\mathbf{q}}^{\dagger} c_{j\mathbf{k}}}{\Delta\omega_{\mathbf{k}\mathbf{q}ij}} (2\mathbf{k} + \mathbf{q}). \quad (195)$$

As before, a single Greek index labels the subband index pair ij , however, now this labeling includes both intersubband $j \neq i$ and intrasubband $j = i$ transitions. The functions $\xi_{\alpha}(z)$ and $\eta_{\alpha}(z)$ are supposed to be real, implying a closed system. We should bear in mind that these definitions only make sense on the subspace spanned by the bosonized states defined in Sec. II A.

The unitary transformation that we use to obtain the minimal-coupling image of the Hamiltonian is

$$T = \exp\left(-\frac{i}{\hbar} \int \hat{\mathbf{A}}\hat{\mathbf{P}} d^3\mathbf{r}\right) = \exp\left\{-\frac{i}{\hbar} \int [\hat{P}_z \hat{A}_{hz} + \hat{\mathbf{P}}_{\parallel}(\hat{\mathbf{A}}_{h\parallel} + \hat{\mathbf{A}}_{e\perp})] d^3\mathbf{r}\right\}. \quad (196)$$

The explicit expression for this transformation can be inferred from the vector potential components provided in the previous section, and shall not be detailed here. Since we consider a subset of bosonized electronic excitations, we will benefit from the general properties of the inverse bosonic PZW transformation that were established in Ref. [3]. We split the total Hamiltonian \mathcal{H} in two parts in order to isolate the kinetic energy part \mathcal{H}_e from the rest:

$$T\mathcal{H}T^{\dagger} = T(\mathcal{H} - \mathcal{H}_e)T^{\dagger} + T\mathcal{H}_eT^{\dagger}. \quad (197)$$

Then, according to the results established in Ref. [3], the two parts of (191) are transformed under the operator T as follows:

$$T(\mathcal{H} - \mathcal{H}_e)T^{\dagger} = \mathcal{H}_{\text{ph}}^h + \mathcal{H}_{\text{ph}}^e + \mathcal{H}_{\text{P2}} - \mathcal{H}_{\text{IP2}} \quad (198)$$

$$T\mathcal{H}_eT^{\dagger} = \mathcal{H}_e + \int \hat{\mathbf{j}}\hat{\mathbf{A}} d^3r + \tilde{\mathcal{H}}_{\text{A2}}. \quad (199)$$

The transformation of the first contribution $\mathcal{H} - \mathcal{H}_e$ in Eq. (198) provides, apart from the free photon part $\mathcal{H}_{\text{ph}}^h + \mathcal{H}_{\text{ph}}^e$, the difference between the square-polarization term \mathcal{H}_{P2} and its transverse part \mathcal{H}_{IP2} . We recall that the transverse part \mathcal{H}_{IP2} can be obtained by projecting the operator $\hat{\mathbf{P}}$ onto the vector potential $\hat{\mathbf{A}}$ and using its expansion into normal modes. The difference appearing in Eq. (199) is the longitudinal part of the polarization self-energy, which plays the role of the Coulomb potential for our system:

$$\hat{V}_{\text{Coulomb}} = \mathcal{H}_{\text{P2}} - \mathcal{H}_{\text{IP2}}. \quad (200)$$

The transformation of the electronic part \mathcal{H}_e leads to the “ $\hat{\mathbf{j}}\hat{\mathbf{A}}$ ” linear interaction term, which mirrors the linear “ $\hat{\mathbf{P}}\hat{\mathbf{D}}$ ” interaction term of the PZW Hamiltonian. Furthermore, in Eq. (199) there is also a residual term that is square in the vector potential $\tilde{\mathcal{H}}_{\text{A2}}$. In the following, we discuss separately the terms \hat{V}_{Coulomb} and $\tilde{\mathcal{H}}_{\text{A2}}$.

1. Coulomb interaction

Let us analyze first the Coulomb interaction term \hat{V}_{Coulomb} that is derived from our PZW Hamiltonian. We spare the reader some lengthy, but straightforward, calculations, which make use of the Baker-Hausdorff expansion that is interrupted to second order thanks to the bosonic commutation rules imposed on the excitation operators [3]. At the end of the computation, the transverse part \mathcal{H}_{IP2} appears as a decomposition over all possible waveguide modes:

$$\begin{aligned} \mathcal{H}_{\text{IP2}} = & \frac{\hbar^2 e^2}{8m^* S \epsilon \epsilon_0 L} \sum_{\mathbf{q}, \alpha, \alpha', m} \frac{c^2}{\epsilon \omega_{cm\mathbf{q}}^2} \\ & \times \left\{ q^2 \int \xi_\alpha u_m dz \int \xi_{\alpha'} u_m dz \Pi_{z\alpha\mathbf{q}}^\dagger \Pi_{z\alpha'\mathbf{q}} \right. \\ & + k_{zm}^2 \int \eta_\alpha w_m dz \int \eta_{\alpha'} w_m dz (\mathbf{e}_\mathbf{q} \Pi_{\parallel\alpha\mathbf{q}}^\dagger) (\mathbf{e}_\mathbf{q} \Pi_{\parallel\alpha'\mathbf{q}}) \\ & - k_{zm} \int \xi_\alpha u_m dz \int \eta_{\alpha'} w_m dz \Pi_{z\alpha\mathbf{q}}^\dagger (\mathbf{q} \Pi_{\parallel\alpha'\mathbf{q}}) \\ & - k_{zm} \int \eta_\alpha w_m dz \int \xi_{\alpha'} u_m dz (\mathbf{q} \Pi_{\parallel\alpha\mathbf{q}}^\dagger) \Pi_{z\alpha'\mathbf{q}} \\ & + \frac{\epsilon \omega_{cm\mathbf{q}}^2}{c^2} \int \eta_\alpha w_m dz \int \eta_{\alpha'} w_m dz \\ & \left. \times (\mathbf{e}_\perp \Pi_{\parallel\alpha\mathbf{q}}^\dagger) (\mathbf{e}_\perp \Pi_{\parallel\alpha'\mathbf{q}}) \right\}. \quad (201) \end{aligned}$$

We now need to combine \mathcal{H}_{IP2} with \mathcal{H}_{IP1} in order to obtain explicitly the Coulomb potential. To this end, we expand \mathcal{H}_{IP2} into the basis of waveguide modes, taking advantage of the fact that the functions $u_m(z)$ and $w_m(z)$ form a Fourier basis with a period $2L$. Since the functions $\xi_\alpha(z)$ and $\eta_\alpha(z)$ are defined only on the bounded interval $[0, L]$, we may choose a convenient $2L$ -periodic extension of these functions on the entire z axis [40]. Equation (201) suggests that such extension must be symmetric for $\xi_\alpha(z)$ and antisymmetric for $\eta_\alpha(z)$ with respect to the origin. As shown in Appendix B, these periodic extensions lead to the integral expansions

$$\int \xi_\alpha \xi_{\alpha'} dz = \frac{1}{L} \sum_{m \geq 0} \int \xi_\alpha u_m dz \int \xi_{\alpha'} u_m dz, \quad (202)$$

$$\int \eta_\alpha \eta_{\alpha'} dz = \frac{1}{L} \sum_{m > 0} \int \eta_\alpha w_m dz \int \eta_{\alpha'} w_m dz. \quad (203)$$

For $m > 0$, we also have the following identity, which is easily shown by the use of Eq. (30) and integrating by parts:

$$\int \xi_\alpha u_m dz = \frac{2m^* \omega_\alpha}{\hbar k_{zm}} \int \eta_\alpha w_m dz. \quad (204)$$

To establish Eq. (204), we used the fact that all functions $w_m(z)$ vanish on the metal walls. The $m = 0$ term, which corresponds to the TM_0 mode, cancels identically in the difference $\mathcal{H}_{\text{IP2}} - \mathcal{H}_{\text{IP1}}$, therefore, the remaining expansion contains only $m > 0$ terms.

Another useful identity is the following formula for the excitation operators, stemming from the definitions (194) and (195):

$$D_{\alpha\mathbf{q}}^\dagger \equiv \omega_\alpha \Pi_{z\alpha\mathbf{q}}^\dagger + \frac{\hbar}{2m^*} (\mathbf{e}_\mathbf{q} \Pi_{\parallel\alpha\mathbf{q}}^\dagger) = \sum_{\mathbf{k}} c_{i\mathbf{k}+\mathbf{q}}^\dagger c_{j\mathbf{k}}. \quad (205)$$

Making use of these results, and after some lengthy algebra, we obtain the following expression for the longitudinal part of the polarization self-energy:

$$\begin{aligned} \mathcal{H}_{\text{IP2}} = \hat{V}_{\text{Coulomb}} = & \frac{e^2}{2S \epsilon \epsilon_0} \sum_{\mathbf{q}, \alpha, \alpha', m > 0} \int \eta_\alpha w_m dz \\ & \times \int \eta_{\alpha'} w_m dz \frac{D_{\alpha\mathbf{q}}^\dagger D_{\alpha'\mathbf{q}}}{k_{zm}^2 + q^2}. \quad (206) \end{aligned}$$

The sum over the waveguide modes can be computed by applying the Poisson summation formula [40] on the periodic extensions of $\eta_\alpha(z)$. The details are provided in Appendix B, and the result is

$$\begin{aligned} & \sum_{\mathbf{q}, \alpha, \alpha', m > 0} \int \eta_\alpha w_m dz \int \eta_{\alpha'} w_m dz \frac{1}{k_{zm}^2 + q^2} \\ & = \frac{L}{q} \int_0^L \int_0^L \eta_\alpha(z) \eta_{\alpha'}(z') \sum_{n \in \mathbb{Z}} e^{-q|z-z'+2nL|} dz dz'. \quad (207) \end{aligned}$$

Finally, replacing the density functions η_α with the products $\phi_i(z) \phi_j(z)$ we recognize a familiar expression for the Coulomb potential \hat{V}_{Coulomb} as a two-dimensional Fourier transform:

$$\begin{aligned} \hat{V}_{\text{Coulomb}} = & \frac{e^2}{2S \epsilon \epsilon_0} \sum_{\substack{\mathbf{q}, \mathbf{k}, \mathbf{k}' \\ i, j, j'}} \int_0^L \int_0^L \phi_i(z) \phi_j(z) \phi_{j'}(z') \phi_{i'}(z') \\ & \times \frac{e^{-q|z-z'|}}{q} \coth(qL) dz dz' c_{i\mathbf{k}+\mathbf{q}}^\dagger c_{j\mathbf{k}} c_{i'\mathbf{k}'-\mathbf{q}}^\dagger c_{j'\mathbf{k}'}. \quad (208) \end{aligned}$$

Here, the operator product can be rearranged in order to isolate divergent electron self-interaction terms [1,3]. Our expression of the particle-particle interaction from Eq. (208) takes into account explicitly the boundary conditions for the Coulomb potential, imposed by the metallic waveguide walls. These boundary conditions give rise to an infinite set of image charge contributions that appear explicitly through the weighting factor $\coth(qL)$:

$$\coth(qL) = \sum_{n \in \mathbb{Z}} e^{-2q|n|L}. \quad (209)$$

Note that in the limit of infinitely thick waveguide $L \rightarrow \infty$ we have $\coth(qL) \rightarrow 1$. In this limit, the image charges disappear, and we recover the well-known Fourier transform of the Coulomb potential for a quasi-two-dimensional electron gas [18]. Since Eq. (208) provides explicitly the longitudinal part of the square-polarization term \mathcal{H}_{IP2} , the collective longitudinal excitation of the confined geometry can be obtained by the diagonalization of $\mathcal{H}_e + \hat{V}_{\text{Coulomb}}$.

The advantage of our approach lies in the decomposition of the Coulomb potential from Eq. (200), which provides a

very convenient way to handle the boundary conditions of the problem. Indeed, the total polarization field $\hat{\mathbf{P}}$ and the corresponding self-energy \mathcal{H}_{p2} depend only on the confined wave functions, and are independent from the photonic constraints of the system. We can use a simplified version for the polarization density, by expressing it with the bozonized universal collective excitations described in Secs. II C and II E and that are obtained from the diagonalization of matter Hamiltonian $\mathcal{H}_c + \mathcal{H}_{\text{p2}}$. On the other hand, once the transverse photonic modes of the system are known, we can express the transverse part of the self-polarization \mathcal{H}_{p2} as a decomposition over the photonic modes that correspond to the confined geometry. However, we can approximate \mathcal{H}_{p2} with only a few modes that are resonant with the collective excitations; this in turn provides, with the help of Eq. (200), a simplified version of the particle-particle interactions, that can be used to obtain the longitudinal plasmon modes. For instance, in Ref. [4] we made use of a single $\text{TM}_{m=0}$ mode approximation. Such approach is certainly simpler than relying on the Coulomb potential from

Eq. (208), which would require us to sum over an infinite set of image contributions.

2. Square-vector potential contribution

Let us now consider the square-vector potential Hamiltonian $\tilde{\mathcal{H}}_{\text{A2}}$, obtained from Eq. (199). Unlike the Coulomb interaction for which we must consider all possible excitation wave vectors \mathbf{q} , we will discuss $\tilde{\mathcal{H}}_{\text{A2}}$ only in the long-wavelength limit (LWL). The LWL implies that (i) the typical electron wave vectors \mathbf{k} are large compared to the typical light wave vectors \mathbf{q} and (ii) the extensions of the confined wave functions are small as compared to the wavelength of light. Indeed, as we also showed in the numerical examples from the previous sections, the extension of the confining heterostructure potentials are on the order of tens of nanometers, while the light wavelengths are on the order of tens or hundreds of microns. The derivation of the vector potential Hamiltonian $\tilde{\mathcal{H}}_{\text{A2}}$ is outlined in Appendix C, and here we provide the final result

$$\begin{aligned} \tilde{\mathcal{H}}_{\text{A2}} = & \frac{\hbar e^2 c^3}{4\epsilon_0 \epsilon^2 m^* SL} \sum_{\mathbf{q}, m, m'} (\omega_{c\mathbf{q}m} \omega_{c\mathbf{q}m'})^{-3/2} \\ & \times \left\{ (q^2 \tilde{I}_{mm'} + k_{zm} k_{zm'} \tilde{J}_{mm'}) (a_{\mathbf{q}mh} + a_{-\mathbf{q}mh}^\dagger) (a_{-\mathbf{q}m'h} + a_{\mathbf{q}m'h}^\dagger) + \frac{\epsilon \omega_{c\mathbf{q}m} \omega_{c\mathbf{q}m'}}{c^2} \tilde{J}_{mm'} (a_{\mathbf{q}me} + a_{-\mathbf{q}me}^\dagger) (a_{-\mathbf{q}m'e} + a_{\mathbf{q}m'e}^\dagger) \right\}. \end{aligned} \quad (210)$$

The following quantities have been defined:

$$\tilde{I}_{mm'} = \sum_{\alpha} \frac{\hbar \Delta N_{\alpha}}{2m^* \Delta \omega_{\alpha}} \int \xi_{\alpha} u_m dz \int \xi_{\alpha} u_{m'} dz, \quad (211)$$

$$\tilde{J}_{mm'} = \sum_i N_i \int \eta_{ii} w_m dz \int \eta_{ii} w_{m'} dz. \quad (212)$$

This result must be compared with the square-vector potential term as derived from the standard minimal-coupling representation of the quantum electrodynamics:

$$\mathcal{H}_{\text{A2}} = \frac{e^2}{2m^*} \int \Psi^\dagger \Psi \hat{\mathbf{A}}^2 d^3 \mathbf{r}. \quad (213)$$

Note that the above expression is more general than $\tilde{\mathcal{H}}_{\text{A2}}$. Indeed, $\tilde{\mathcal{H}}_{\text{A2}}$ acts only on the photonic degrees of freedom, whereas now \mathcal{H}_{A2} acts also on the electronic degrees of freedom through the density operator term $\Psi^\dagger \Psi$. We are going to show that, just like for the case of the 3D electron gas, $\tilde{\mathcal{H}}_{\text{A2}}$ can be obtained as the ground-state average of the full Hamiltonian \mathcal{H}_{A2} , in the LWL. This is formally expressed by the following inequality:

$$\tilde{\mathcal{H}}_{\text{A2}} \leq \langle F | \mathcal{H}_{\text{A2}} | F \rangle |_{\text{LWL}}. \quad (214)$$

Here, the symbol \leq means that, as we are going to show, the matrix elements of $\tilde{\mathcal{H}}_{\text{A2}}$ are at best equal or smaller than those of the right-hand side. The square-vector potential Hamiltonian \mathcal{H}_{A2} is expressed from the formulas of the vector potential provided in the previous sections and the field operator from Eq. (22) :

$$\begin{aligned} \mathcal{H}_{\text{A2}} = & \frac{\hbar e^2 c^3}{4\epsilon_0 \epsilon^2 m^* SL} \sum_{\substack{\mathbf{q}, \mathbf{q}' \\ m, m'}} (\omega_{c\mathbf{q}m} \omega_{c\mathbf{q}'m'})^{-3/2} \\ & \times \left\{ (qq' \hat{I}_{mm'}^{\mathbf{q}\mathbf{q}'} + k_{zm} k_{zm'} \hat{J}_{mm'}^{\mathbf{q}\mathbf{q}'}) (a_{\mathbf{q}mh} + a_{-\mathbf{q}mh}^\dagger) (a_{-\mathbf{q}'m'h} + a_{\mathbf{q}'m'h}^\dagger) + \frac{\epsilon \omega_{c\mathbf{q}m} \omega_{c\mathbf{q}'m'}}{c^2} \hat{J}_{mm'}^{\mathbf{q}\mathbf{q}'} (a_{\mathbf{q}me} + a_{-\mathbf{q}me}^\dagger) (a_{-\mathbf{q}'m'e} + a_{\mathbf{q}'m'e}^\dagger) \right\}. \end{aligned} \quad (215)$$

Here, we defined the operators that act on the electronic degrees of freedom:

$$\hat{f}_{mm'}^{\mathbf{q}\mathbf{q}'} = \sum_{\mathbf{k}i\mathbf{j}} c_{i\mathbf{k}+\mathbf{q}-\mathbf{q}'}^\dagger c_{j\mathbf{k}} \int \eta_{ij} u_m u_{m'} dz, \quad (216)$$

$$\hat{f}_{mm'}^{\mathbf{q}\mathbf{q}'} = \sum_{\mathbf{k}i\mathbf{j}} c_{i\mathbf{k}+\mathbf{q}-\mathbf{q}'}^\dagger c_{j\mathbf{k}} \int \eta_{ij} w_m w_{m'} dz. \quad (217)$$

The average values of these operators over the electronic ground state $|F\rangle$, supposed to be the free-electron Fermi sphere, are

$$\langle F | \hat{f}_{mm'}^{\mathbf{q}\mathbf{q}'} | F \rangle = \delta_{\mathbf{q}\mathbf{q}'} \sum_i N_i \int \eta_{ii} u_m u_{m'} dz, \quad (218)$$

$$\langle F | \hat{f}_{mm'}^{\mathbf{q}\mathbf{q}'} | F \rangle = \delta_{\mathbf{q}\mathbf{q}'} \sum_i N_i \int \eta_{ii} w_m w_{m'} dz. \quad (219)$$

Clearly, we must compare these expressions with Eqs. (211) and (212). The comparison between Eqs. (219) and (212) is very straightforward. Indeed, we need to compare only the overlap integrals between the electronic wave functions $\eta_{ii}(z) = \phi_i^2(z)$ and the waveguide modes $w_m(z)$. Let z_i be the barycenter of the wave function $\phi_i(z)$. Since the variations of the modal functions $w_m(z)$ are very slow as compared to those of $\phi_i(z)$ in the LWL, we can express the overlap integrals in Eq. (219) as

$$\int \eta_{ii}(z) w_m(z) w_{m'}(z) dz \approx w_m(z_i) w_{m'}(z_i), \quad (220)$$

we used the fact that $\int \eta_{ii}(z) dz = 1$ owing to the normalization of the wave functions. Exactly the same result is obtained by applying the LWL in the overlap integrals in Eq. (212). This confirms the equivalence stated in Eq. (214) for the intrasubband part of the square-vector potential part of the Hamiltonian.

Let us now compare Eqs. (211) and (218). Without loss of generality, we will consider that there is only one quantum well situated at the position z_0 . The indexes α and i will therefore refer to the wave functions bound in this well. The overlap integrals in Eqs. (211) and (218) are then written in the LWL:

$$\sum_\alpha \frac{\hbar \Delta N_\alpha}{2m^* \Delta \omega_\alpha} \int \xi_\alpha u_m dz \int \xi_\alpha u_{m'} dz \approx \sum_\alpha \frac{\hbar \Delta N_\alpha}{2m^* \Delta \omega_\alpha} \left(\int \xi_\alpha dz \right)^2 u_m(z_0) u_{m'}(z_0), \quad (221)$$

$$\sum_i N_i \int \eta_{ii} u_m u_{m'} dz \approx \sum_i N_i u_m(z_0) u_{m'}(z_0). \quad (222)$$

From Eq. (151) we can recognize the oscillator strength of the intersubband transition α :

$$f_\alpha = \frac{\hbar}{2m^* \Delta \omega_\alpha} \left(\int \xi_\alpha dz \right)^2. \quad (223)$$

Then, Eq. (214) is satisfied because of the following inequality:

$$\sum_\alpha f_\alpha \Delta N_\alpha = \sum_{i < j} f_{ij} (N_i - N_j) \leq \sum_i N_i. \quad (224)$$

The sum runs over the occupied subbands. This inequality basically states that the total oscillator strength from all elec-

tronic transitions cannot exceed the total number of particles in the system. This inequality is always satisfied in intersubband systems, because of the Thomas-Reich-Kuhn sum rule [34,56]. According to the general results from Ref. [13], the inequality (214) therefore rules out the appearance of a quantum phase transition in our system, at least in the case of hard-wall boundary conditions for the wave functions discussed in Sec. II B. As discussed in Ref. [55], the case of equality in Eq. (214) is reached for a very high number of occupied subbands, which ensures the correct asymptotic limit of our model to the three-dimensional homogeneous plasma.

IV. CONCLUSION

In this work, we discussed a general quantum theory of the confined plasmons in a quasi-two-dimensional electron gas, including both intrasubband and intersubband excitations. In our theory, these modes can be directly expressed through the wave functions associated to the confining potential. With the current state of technology for the epitaxial growth of semiconductor heterostructures, a rich variety of potentials can be designed. As the confined plasmon modes have a significant impact of the optical properties of semiconductors in the infrared domain, our formalism allows for a direct engineering of the spectral response through the confining potential [8,55]. In previous works [8], the accent was put on intersubband plasmons, that correspond to electronic oscillations in the direction of the quantum confinement. Furthermore, only thin resonant structures were studied, where the physics is dominated by the light-matter coupling with the intersubband plasmons only [42]. This paper extends these studies by providing a model for the in-plane plasmons and their mutual couplings, and all possible waveguide modes are taken into account in the light-matter interaction problem. Our results include the previous studies as limiting cases, and, while the validity of the previous results is preserved in this more general treatment, we indicate several new features that can arise in thick resonators (Sec. III B 2) or asymmetric quantum wells (Sec. II C 3). We believe that this formalism also sets the basis for more advanced quantum optical applications in the solid state [36,57,58] implemented with quantum-confined electron gas. In that case, dissipation also must be included in the model, which can be achieved through several approaches [59,60].

Our formalism relies on the PZW representation of quantum electrodynamics, and it can be of particular convenience for a class of problems that involve a small number of electromagnetic modes that interact resonantly with the condensed matter system. Such situations arise, for instance, in the studies of the ultrastrong light-matter regime, where the quantum-confined plasmons are coupled with microresonators that provide very strong electromagnetic confinement [6,7,9,15–17,22,38]. In these systems, the boundary conditions of the electromagnetic field play a crucial role and the particle density is extremely high. Indeed, the Coulomb potential in a confined geometry generally appears as an infinite sum of image contributions, and involves a resummation over an infinite number electromagnetic modes and electronic transitions. This also holds for the quadratic vector potential part of the light-matter Hamiltonian [Eq. (215)] [61], that plays an important role for the regime of ultrastrong light-matter coupling [5]. In that

case, as we showed in this work, the PZW representation allows a more convenient and compact truncation of the Hilbert space of the system, both for the longitudinal and transverse interactions. Furthermore, the electronic degrees of freedom are also reduced to a few universal collective modes, that arise from a finite number of occupied subbands and are independent from the electromagnetic environment of the system.

Our method relies on the relation between the current density and the dynamical polarization of the system, expressed in Eq. (20). A key point of the theory is that, if we can neglect the effects of dynamic (time-varying) magnetic fields on the system, only the single-particle electronic Hamiltonian \mathcal{H}_e enters the commutator of Eq. (20). Since the current density operator $\hat{\mathbf{j}}$ can be obtained from the eigenfunctions of \mathcal{H}_e , the dynamical polarization field of the system can be constructed by solving an essentially single-particle problem. This approach can be applied for a number of electronic systems where \mathcal{H}_e is well known, such as the one-dimensional electron gas [18], an electron gas subject to a constant magnetic field [62], or the graphene [63]. In all those cases, the resulting polarization operator will provide not only the light-matter coupling, but also the particle-particle interactions to the dipole-dipole order of the Coulomb potential, and the corresponding collective states. Another generalization of the theory is to include several components in the system, each described with its own polarization field. Then, the square-polarization part of the PZW Hamiltonian will provide the interaction between these parts. For instance, the polarization field for phonons \mathbf{P}_{phon} can be obtained semiclassically [64]. By adding \mathbf{P}_{phon} to the polarization field of electrons and expanding the square-polarization term, we obtain the Fröhlich interaction [65]. A similar approach can be applied to obtain the coupling between a quantum-confined electron gas and the quasistatic electric field of circuitlike resonators [39].

APPENDIX A: CHARACTERISTIC TENSOR OF BOSON QUADRATIC FORMS

Let us consider the following bosonic quadratic form:

$$\mathcal{H} = \sum_{\alpha} \hbar\omega_{\alpha} b_{\alpha}^{\dagger} b_{\alpha} + \sum_{\alpha, \beta} \frac{\hbar \mathbf{D}_{\alpha} \mathbf{D}_{\beta}}{2} (b_{\alpha}^{\dagger} + b_{\alpha})(b_{\beta}^{\dagger} + b_{\beta}). \quad (\text{A1})$$

Here, \mathbf{D}_{α} can be, in general, n -dimensional vectors. Then, relying on the results from Ref. [3], we can associate to this Hamiltonian the following characteristic n -dimensional second-order tensor:

$$\zeta(\omega) = \mathbf{1}_n - \sum_{\alpha} \frac{2\omega_{\alpha}}{\omega^2 - \omega_{\alpha}^2} (\mathbf{D}_{\alpha} \otimes \mathbf{D}_{\alpha}). \quad (\text{A2})$$

Here, $\mathbf{1}_n$ is the n -dimensional unit tensor, and “ \otimes ” denotes a tensor product. As shown in Ref. [3], the main property of this characteristic tensor is that the zeros of its determinant provide the eigenvalues Ω_i of the Hamiltonian (A1):

$$\|\zeta(\Omega_i)\| = 0. \quad (\text{A3})$$

Furthermore, in the case of a three-dimensional system the characteristic function can be identified with the dielectric function of the medium described by the elementary bosonic excitations b_{α} [3].

In the case of quantum-confined plasmons, we often need to deal with a slightly different bosonic form

$$\mathcal{H}' = \sum_{\alpha} \hbar\omega_{\alpha} b_{\alpha}^{\dagger} b_{\alpha} + \sum_{\alpha \neq \beta} \frac{\hbar \mathbf{D}_{\alpha} \mathbf{D}_{\beta}}{2} (b_{\alpha}^{\dagger} + b_{\alpha})(b_{\beta}^{\dagger} + b_{\beta}). \quad (\text{A4})$$

The main difference with Eq. (A1) is that now the $\alpha = \beta$ terms are excluded from the interaction term. This is the case of interacting plasmons from different subbands. Nevertheless, we can use a unitary transform to recover a Hamiltonian in the form of Eq. (A1) from Eq. (A4). For this, we rewrite Eq. (A4) to make the $\alpha = \beta$ terms explicit:

$$\begin{aligned} \mathcal{H}' &= \sum_{\alpha} \hbar\omega_{\alpha} b_{\alpha}^{\dagger} b_{\alpha} - \sum_{\alpha} \frac{\hbar \mathbf{D}_{\alpha}^2}{2} (b_{\alpha}^{\dagger} + b_{\alpha})^2 \\ &\quad + \sum_{\alpha, \beta} \frac{\hbar \mathbf{D}_{\alpha} \mathbf{D}_{\beta}}{2} (b_{\alpha}^{\dagger} + b_{\alpha})(b_{\beta}^{\dagger} + b_{\beta}). \end{aligned} \quad (\text{A5})$$

We use a unitary transform to diagonalize the first line in Eq. (A5) with new operators f_{α} that satisfy [4]

$$f_{\alpha}^{\dagger} + f_{\alpha} = \sqrt{\frac{\bar{\omega}_{\alpha}}{\omega_{\alpha}}} (b_{\alpha}^{\dagger} + b_{\alpha}), \quad (\text{A6})$$

$$\bar{\omega}_{\alpha} = \sqrt{\omega_{\alpha}^2 - 2\omega_{\alpha} \mathbf{D}_{\alpha}^2}. \quad (\text{A7})$$

Here, $\bar{\omega}_{\alpha}$ are the new eigenfrequencies of self-interacting bosons in first line in Eq. (A5). Now, Eq. (A4) can be rewritten as

$$\begin{aligned} \mathcal{H}' &= \sum_{\alpha} \hbar\bar{\omega}_{\alpha} f_{\alpha}^{\dagger} f_{\alpha} \\ &\quad + \sum_{\alpha, \beta} \frac{\hbar \mathbf{D}_{\alpha} \mathbf{D}_{\beta}}{2} \sqrt{\frac{\omega_{\alpha} \omega_{\beta}}{\bar{\omega}_{\alpha} \bar{\omega}_{\beta}}} (f_{\alpha}^{\dagger} + f_{\alpha})(f_{\beta}^{\dagger} + f_{\beta}). \end{aligned} \quad (\text{A8})$$

We then use the previous result to obtain the characteristic tensor of Eq. (A4):

$$\zeta'(\omega) = \mathbf{1}_n - \sum_{\alpha} \frac{2\omega_{\alpha}}{\omega^2 - \omega_{\alpha}^2 + 2\omega_{\alpha} \mathbf{D}_{\alpha}^2} (\mathbf{D}_{\alpha} \otimes \mathbf{D}_{\alpha}). \quad (\text{A9})$$

For the case of intrasubband plasmons considered in the end of Sec. II E, the coefficients \mathbf{D}_{α} are scalars and we have $\omega_{\alpha} = \omega_{iP}^{\parallel}$ and $D_{\alpha} = \omega_{iP}^{\parallel} / \sqrt{3}$ which leads to the characteristic equation (121). However, in general the interacting term between quantum-confined plasmons can not be written as a scalar product, and numerical diagonalization must be performed [42].

APPENDIX B: PERIODIC EXTENSION OF η_{α}

In this Appendix, we describe the trigonometric resummation in Eq. (207). We start by rearranging the overlap integrals between the waveguide modes and the functions η_{α} :

$$\begin{aligned} &\int_0^L \eta_{\alpha}(z) w_m(z) dz \\ &= \frac{1}{i\sqrt{2}} \left[\int_0^L e^{\frac{i\pi m z}{L}} \eta_{\alpha}(z) dz + \int_{-L}^0 e^{\frac{i\pi m z}{L}} [-\eta_{\alpha}(-z)] dz \right]. \end{aligned} \quad (\text{B1})$$

Let us define a $2L$ -periodic function $\bar{\eta}_{\alpha}(z)$ that is equal to $\eta_{\alpha}(z)$ in the interval $[0, L]$ and to $-\eta_{\alpha}(-z)$ in the interval $[-L, 0]$. Then, Eq. (B1) defines the Fourier component $\tilde{\eta}_{\alpha m}$ of

the function $\tilde{\eta}_\alpha(z)$ in the interval $[-L, L]$:

$$\frac{1}{i\sqrt{2}} \int_{-L}^L e^{\frac{i2\pi mz}{2L}} \tilde{\eta}_\alpha(z) dz = \frac{1}{i\sqrt{2}} \tilde{\eta}_{\alpha m}. \quad (\text{B2})$$

We have the property $\tilde{\eta}_{\alpha m} = -\tilde{\eta}_{\alpha -m}$, and therefore $\tilde{\eta}_{\alpha 0} = 0$. With these definitions, we can now express the left-hand side of Eq. (207) as

$$\begin{aligned} & \frac{1}{4} \sum_{m=-\infty}^{+\infty} \frac{|\tilde{\eta}_{\alpha m}|^2}{q^2 + k_{zm}^2} \\ &= \frac{L^2}{4\pi^2} \int_{-L}^L \int_{-L}^L \tilde{\eta}_\alpha(z) \tilde{\eta}_\alpha(z') \sum_m \frac{e^{\frac{i2\pi m}{2L}(z-z')}}{m^2 + \frac{q^2 L^2}{\pi^2}} dz dz'. \end{aligned} \quad (\text{B3})$$

The summation has been extended to the $m = 0$ term which does not contribute anyway. To compute the right-hand side of this equation, we use the Poisson summation formula [40]

$$\sum_m \frac{e^{2i\pi mt}}{m^2 + b^2} = \frac{\pi}{b} \sum_n e^{-2\pi b|t-n|}. \quad (\text{B4})$$

Performing the sum over m and reducing the integrals into the interval $[0, L]$ we obtain Eq. (207). Furthermore, since $z, z' \in [0, L]$ we have $|z - z' - 2nL| = |z - z'| + 2|n|L$ which, with the help of Eq. (209), allows obtaining the final expression of the Coulomb potential (208).

APPENDIX C: DERIVATION OF $\tilde{\mathcal{H}}_{A2}$

To establish the result for the square-vector potential term $\tilde{\mathcal{H}}_{A2}$ we use Eq. (199), together with the bosonized expression of the electronic Hamiltonian (18). The unitary transform T in Sec. III C is expressed as

$$T = e^{-i\hat{B}}, \quad \hat{B} = \frac{1}{\hbar} \int \hat{\mathbf{A}} \hat{\mathbf{P}} d^3 \mathbf{r}. \quad (\text{C1})$$

For the polarization field, we use the expressions (37), (39), and (40) assuming that the wave functions are real. The unitary transform is computed with the Baker-Hausdor expansion

$$e^{i\hat{B}} \mathcal{H}_e e^{-i\hat{B}} = \mathcal{H}_e + i[\hat{B}, \mathcal{H}_e] + \frac{i^2}{2!} [\hat{B}, [\hat{B}, \mathcal{H}_e]]. \quad (\text{C2})$$

This expansion becomes exact at the second order as we imposed bosonicity of the electronic excitation operators. The square potential term is the second order of the expansion

$$\tilde{\mathcal{H}}_{A2} = \frac{i^2}{2!} [\hat{B}, [\hat{B}, \mathcal{H}_e]]. \quad (\text{C3})$$

Since the bosonized Hamiltonian (18) is split into inter-subband and intrasubband parts, then the transform (C2) will

respectively yield two parts from the Hamiltonian (C3):

$$\tilde{\mathcal{H}}_{A2} = \tilde{\mathcal{H}}_{A2|inter} + \tilde{\mathcal{H}}_{A2|intra}. \quad (\text{C4})$$

Let us consider first $\tilde{\mathcal{H}}_{A2|intra}$, which derives from the intra-subband part of \mathcal{H}_e . Using Eq. (40), the expressions for the vector potential Eqs. (129), (131), (135), and (C3), we obtain the following result:

$$\begin{aligned} \tilde{\mathcal{H}}_{A2|intra} &= \frac{e^2 c^2}{4\epsilon_0 \epsilon^2 S L} \sum_{\substack{\mathbf{qk} \\ mm'}} (\omega_{cqm} \omega_{cqm'})^{-3/2} \\ &\times \Delta\omega_{\mathbf{qk}} \int \eta_i w_m dz \int \eta_i w_{m'} dz C_{\mathbf{qkm}} C_{-\mathbf{qkm}'}, \end{aligned} \quad (\text{C5})$$

$$\begin{aligned} C_{\mathbf{qkm}} &= k_{zm} (\mathbf{e}_q \boldsymbol{\beta}_{\mathbf{qk}}) (a_{qmh} + a_{-qmh}^\dagger) \\ &\times \frac{\sqrt{\epsilon} \omega_{cqm}}{c} (\mathbf{e}_\perp \boldsymbol{\beta}_{\mathbf{qk}}) (a_{qme} + a_{-qme}^\dagger). \end{aligned} \quad (\text{C6})$$

We now develop the square in Eq. (C5) and perform the sum over the electronic wave vectors. We first notice that the cross-polarization terms vanish in the long-wavelength limit; indeed these terms are proportional to the factor

$$\sum_{\mathbf{k}} \Delta\omega_{\mathbf{qk}} (\mathbf{e}_q \boldsymbol{\beta}_{\mathbf{qk}}) (\mathbf{e}_\perp \boldsymbol{\beta}_{\mathbf{qk}}) \approx \frac{\hbar}{m^* q} \sum_{\mathbf{k}} \frac{2\mathbf{e}_\perp \mathbf{k}}{q\mathbf{k}} = 0. \quad (\text{C7})$$

This equality is easily proven transforming the sum over wave vectors into integral. The angular part of this expression appears as an integral between 0 and 2π of an odd angular function. The remaining square terms are proportional to

$$\begin{aligned} \sum_{\mathbf{k}} \Delta\omega_{\mathbf{qk}} (\mathbf{e}_\perp \boldsymbol{\beta}_{\mathbf{qk}})^2 &= \sum_{\mathbf{k}} \frac{\Delta\omega_{\mathbf{qk}}}{q^2} \\ &= \frac{\hbar}{2m^*} \frac{2\mathbf{qk} + q^2}{q^2} = \frac{\hbar}{m^*} N_i. \end{aligned} \quad (\text{C8})$$

In these equalities, we used the isotropy of the two-dimensional gas in the plane perpendicular to the quantum confinement, and in the last equality we used the twofold degeneracy of the electronic wave vectors due to the spin. The second and third terms of Eq. (210) are thus recovered.

The intersubband part is treated in the similar way. In this case, we use the fact that the in-plane intersubband polarization [Eq. (39)] does not contribute because of the long-wavelength approximation and the orthogonality of the wave functions. The remaining part [Eq. (37)] is coupled only to TM waves and leads to the first term of Eq. (210).

-
- [1] M. Babiker and R. Loudon, *Proc. R. Soc. London, Ser. A* **385**, 439 (1983).
 [2] C. Cohen-Tannoudji, J. Dupont-Roc, and G. Grynberg, *Photons et Atomes* (EDP Sciences/CNRS Editions, Paris, 2001).
 [3] Y. Todorov, *Phys. Rev. B* **89**, 075115 (2014).
 [4] Y. Todorov and C. Sirtori, *Phys. Rev. B* **85**, 045304 (2012).
 [5] C. Ciuti, G. Bastard, and I. Carusotto, *Phys. Rev. B* **72**, 115303 (2005).
 [6] Y. Todorov, A. M. Andrews, R. Colombelli, S. De Liberato, C. Ciuti, P. Klang, G. Strasser, and C. Sirtori, *Phys. Rev. Lett.* **105**, 196402 (2010).

- [7] M. Geiser, F. Castellano, G. Scalari, M. Beck, L. Nevou, and J. Faist, *Phys. Rev. Lett.* **108**, 106402 (2012).
 [8] G. Pegolotti, A. Vasanelli, Y. Todorov, and C. Sirtori, *Phys. Rev. B* **90**, 035305 (2014).
 [9] S. Campione, A. Benz, J. F. Klem, M. B. Sinclair, I. Brener, and F. Capolino, *Phys. Rev. B* **89**, 165133 (2014).
 [10] L. G. Suttorp and Martijn Wubs, *Phys. Rev. A* **70**, 013816 (2004).
 [11] L. G. Suttorp, *J. Phys. A: Math. Theor.* **40**, 3697 (2007).
 [12] J. Keeling, *J. Phys.: Condens. Matter* **19**, 295213 (2007).
 [13] P. Nataf and C. Ciuti, *Nat. Commun.* **1**, 1 (2010).

- [14] A. Vukics, T. Griebner, and P. Domokos, *Phys. Rev. Lett.* **112**, 073601 (2014).
- [15] A. Delteil, A. Vasanelli, Y. Todorov, C. Feuillet Palma, M. Renaudat St-Jean, G. Beaudoin, I. Sagnes, and C. Sirtori, *Phys. Rev. Lett.* **109**, 246808 (2012).
- [16] E. Strupiechonski, G. Xu, M. Brekenfeld, Y. Todorov, N. Isac, A. M. Andrews, P. Klang, C. Sirtori, G. Strasser, A. Degiron, and R. Colombelli, *Appl. Phys. Lett.* **109**, 131113 (2012).
- [17] A. Benz, S. Campione, S. Liu, I. Montano, J. F. Klem, A. Allerman, J. R. Wendt, M. B. Sinclair, F. Capolino, and I. Brener, *Nat. Commun.* **4**, 2882 (2013).
- [18] H. Haug and S. W. Koch, *Quantum Theory of the Optical and Electronic Properties of Semiconductors* (World Scientific, Singapore, 2004).
- [19] H. J. Lipkin, *Quantum Mechanics, New Approaches to Selected Topics* (Dover, New York, 1973).
- [20] D. Pines, *Elementary Excitations in Solids* (Perseus Books, Reading, MA, 1996).
- [21] L. Nguyen-thê, S. De Liberato, M. Bamba, and C. Ciuti, *Phys. Rev. B* **87**, 235322 (2013).
- [22] G. Scalari, C. Maissen, D. Turčinková, D. Hagenmüller, S. De Liberato, C. Ciuti, C. Reichl, D. Schuh, W. Wegscheider, M. Beck, and J. Faist, *Science* **335**, 1323 (2012).
- [23] G. Scalari, C. Maissen, S. Cibella, R. Leoni, P. Carelli, F. Valmorra, M. Beck, and J. Faist, *New J. Phys.* **16**, 033005 (2014).
- [24] Y. C. Jun, J. Reno, T. Ribaudo, E. Shaner, J.-J. Greffet, S. Vassant, F. Marquier, M. Sinclair, and I. Brener, *Nano Lett.* **13**, 5391 (2013).
- [25] T. N. Theis, J. P. Kotthaus, and P. J. Stiles, *Solid State Commun.* **26**, 603 (1978).
- [26] T. N. Theis, *Surf. Sci.* **98**, 515 (1980).
- [27] L. Wendler and E. Kändler, *Phys. Stat. Solidi B* **177**, 9 (1993).
- [28] M. Zaluzny and C. Nalewajko, *Phys. Rev. B* **59**, 13043 (1999).
- [29] A. Liu, *Phys. Rev. B* **55**, 7101 (1997).
- [30] M. Zaluzny and W. Zietkowski, *Phys. Rev. B* **80**, 245301 (2009).
- [31] M. Zaluzny and W. Zietkowski, *Phys. Rev. B* **88**, 195408 (2013).
- [32] F. Alpeggiani and L. C. Andreani, *Phys. Rev. B* **90**, 115311 (2014).
- [33] T. Ando, A. B. Fowler, and F. Stern, *Rev. Mod. Phys.* **54**, 437 (1982).
- [34] M. Helm, *Intersubband Transitions in Quantum Wells* (Academic Press, San Diego, 2000).
- [35] G. Bastard, *Wave Mechanics Applied to Semiconductor Heterostructures* (Les Editions de Physique, Paris, 1996).
- [36] S. De Liberato and C. Ciuti, *Phys. Rev. Lett.* **102**, 136403 (2009).
- [37] C. Cohen-Tannoudji, B. Diu, and F. Laloë, *Mécanique Quantique* (Hermann, Paris, 1977).
- [38] C. Maissen, G. Scalari, F. Valmorra, M. Beck, J. Faist, S. Cibella, R. Leoni, C. Reichl, C. Charpentier, and W. Wegscheider, *Phys. Rev. B* **90**, 205309 (2014).
- [39] Y. Todorov and C. Sirtori, *Phys. Rev. X* **4**, 041031 (2014).
- [40] C. Gasquet and P. Witomski, *Fourier Analysis and Applications* (Springer, New York, 1999).
- [41] G. Eliasson, P. Hawrylak, and J. J. Quinn, *Phys. Rev. B* **35**, 5569 (1987).
- [42] Y. Todorov, L. Toso, A. Delteil, A. Vasanelli, C. Sirtori, A. M. Andrews, and G. Strasser, *Phys. Rev. B* **86**, 125314 (2012).
- [43] L. Brey, N. F. Johnson, and B. I. Halperin, *Phys. Rev. B* **40**, 10647 (1989).
- [44] A. Wixforth, M. Sundaram, K. Ensslin, J. H. English, and A. C. Gossard, *Phys. Rev. B* **43**, 10000 (1991).
- [45] I. K. Marmorosk and S. Das Sarma, *Phys. Rev. B* **48**, 1544 (1993).
- [46] S. Haroche, *Fundamental Systems in Quantum Optics, Les Houches session LIII*, edited by J. Dalibard, J.-H. Raimond, and J. Zinn-Justin (North-Holland, Amsterdam, 1992).
- [47] K. Kakazu and Y. S. Kim, *Phys. Rev. A* **50**, 1830 (1994).
- [48] B. S. Williams, S. Kumar, H. Callebaut, Q. Hu, and J. L. Reno, *Appl. Phys. Lett.* **83**, 2124 (2003).
- [49] B. Huttner, J. J. Baumberg, and S. M. Barnett, *Europhys. Lett.* **16**, 177 (1991).
- [50] M. J. Adams, *An Introduction to Optical Waveguides* (Wiley, Chichester, 1981).
- [51] E. N. Economou, *Phys. Rev.* **182**, 539 (1969).
- [52] S. Collin, F. Pardo, and J.-L. Pelouard, *Opt. Express* **15**, 4310 (2007).
- [53] D. A. Dahl and L. J. Sham, *Phys. Rev. B* **16**, 651 (1977).
- [54] S. Zanotto, G. Biasiol, R. Degl'innocenti, L. Sorba, and A. Tredicucci, *Appl. Phys. Lett.* **97**, 231123 (2010).
- [55] B. Askenazi, A. Vasanelli, A. Delteil, Y. Todorov, L. C. Andreani, G. Beaudoin, I. Sagnes, and C. Sirtori, *New J. Phys.* **16**, 043029 (2014).
- [56] C. Sirtori, F. Capasso, J. Faist, and S. Scandolo, *Phys. Rev. B* **50**, 8663 (1994).
- [57] A. Delteil, A. Vasanelli, P. Jouy, D. Barate, J. C. Moreno, R. Teissier, A. N. Baranov, and C. Sirtori, *Phys. Rev. B* **83**, 081404 (2011).
- [58] M. Kira and S. W. Koch, *Semiconductor Quantum Optics* (Cambridge University Press, Cambridge, 2012).
- [59] M. Bamba and T. Ogawa, *Phys. Rev. A* **88**, 013814 (2013).
- [60] B. Huttner and S. M. Barnett, *Phys. Rev. A* **46**, 4306 (1992).
- [61] F. Bassani, J. J. Forney, and A. Quattropani, *Phys. Rev. Lett.* **39**, 1070 (1977).
- [62] D. Hagenmüller, S. De Liberato, and C. Ciuti, *Phys. Rev. B* **81**, 235303 (2010).
- [63] A. Altland and B. Simons, *Condensed Matter Field Theory* (Cambridge University Press, Cambridge, 2010).
- [64] F. Schwabl, *Advanced Quantum Mechanics* (Springer, Berlin, 2000).
- [65] C. Kittel, *Quantum Theory of Solids* (Wiley, New York, 1963).